GEORGIA INSTITUTE OF TECHNOLOGY
OFFICE OF CONTRACT ADMINISTRATION
SPONSORED PROJECT INITIATION

Date: October 20, 1978

Project Title: Excitation and Ionization of Ions by Electron Impact

Project No: E-21-642

Project Director: Dr. Robert K. Feeney

Sponsor: U. S. Department of Energy; Oak Ridge Operations

Agreement Period: From 9/1/78 Until 8/31/79 (Contract Period)

Type Agreement: Contract No. EY-76-S-05-3027, Modification No. A018

Amount:
$40,000 DOE
14,795 GIT (E-21-334)
$54,795 TOTAL

Reports Required: Publication Preprints; Publication Reprints; Annual Progress Report; Final Report

Sponsor Contact Person (s):

Technical Matters

Dr. Philip M. Stone
Experimental Plasma Research Branch
Applied Plasma Physics Program
Division of Magnetic Fusion Energy
U. S. Department of Energy
Washington, D. C. 20545

Contractual Matters
(thru OCA)

Mr. A. H. Frost, Jr., Chief
Research Contracts, Procedures & Reports Branch
Contract Division
U. S. Department of Energy
Oak Ridge Operations
P. O. Box E
Oak Ridge, TN 37830
(615) 483-8611, Ext. 34105
(Walker Love)

NOTE: CONTINUATION OF E-21-613

Defense Priority Rating: n/a

Assigned to: Electrical Engineering (School/Laboratory)

COPIES TO:

- Project Director
- Division Chief (EES)
- School/Laboratory Director
- Dean/Director–EES
- Accounting Office
- Procurement Office
- Security Coordinator (OCA)
- ✓ Reports Coordinator (OCA)
- Library, Technical Reports Section
- EES Information Office
- EES Reports & Procedures
- Project File (OCA)
- Project Code (GTRI)
- Other

GEORGIA INSTITUTE OF TECHNOLOGY
OFFICE OF CONTRACT ADMINISTRATION

SPONSORED PROJECT TERMINATION

Date: June 6, 1980

Project Title: Excitation and Ionization of Ions by Electron Impact

Project No: E-21-642

Project Director: Dr. Robert K. Feeney

Sponsor: U. S. Department of Energy; Oak Ridge Operations; Oak Ridge, TN 37830

Effective Termination Date: March 31, 1980

~~Clearance of Accounting Charges~~ March 11, 1980 (Final Report submitted)

Grant/Contract Closeout Actions Remaining:

Final Certified Statement of Costs

- [x] Final Invoice and Closing Documents
- [ ] Final Fiscal Report
- [x] Final Report of Inventions
- [x] Govt. Property Inventory & Related Certificate
- [ ] Classified Material Certificate
- [ ] Other _____

Assigned to: Electrical Engineering (School/Laboratory)

COPIES TO:

Project Director
Division Chief (EES)
School/Laboratory Director
Dean/Director–EES
Accounting Office
Procurement Office
Security Coordinator (OCA)
✓ Reports Coordinator (OCA)
Research Property Coordinator (OCA)
Library, Technical Reports Section
EES Information Office
Project File (OCA)
Project Code (GTRI)
Other _____

REPORT NO. ORO–3027–52
Technical Summary Report
Project No. E–21–642

ABSOLUTE EXPERIMENTAL CROSS SECTIONS FOR THE ELECTRON IMPACT IONIZATION OF RUBIDIUM

By:

D. W. Hughes
R. K. Feeney

Contract No. EY–76–S–05–3027

U. S. Department of Energy
Oak Ridge, Tennessee

31 March

GEORGIA INSTITUTE OF TECHNOLOGY
SCHOOL OF ELECTRICAL ENGINEERING
ATLANTA, GEORGIA 30332

1980

REPORT NO. ORO-3027-52

(TECHNICAL SUMMARY REPORT)

Category No. UC-34a

ABSOLUTE EXPERIMENTAL CROSS SECTIONS FOR THE ELECTRON IMPACT IONIZATION OF RUBIDIUM

by

D. W. Hughes

and

R. K. Feeney

Contract No. EY-76-S-05-3027

United States Department of Energy
Oak Ridge, Tennessee

March 31, 1980

PREFACE

This Technical Summary Report summarizes the apparatus assembled, techniques employed and results obtained in the course of studies conducted under Research Contract No. EY-76-S-05-3027 with the United States Department of Energy. Work completed on the electron impact multiple ionization of singly charged rubidium ions through March 31, 1980 is presented herein.

This report is identical in text to a thesis entitled "Absolute Experimental Cross Sections for the Electron Impact Ionization of Rubidium" which was submitted by D. W. Hughes to the faculty of the Division of Graduate Studies at the Georgia Institute of Technology in partial fulfillment of the requirements for the degree Doctor of Philosophy in the School of Electrical Engineering. Having completed all other requirements, Mr. Hughes was awarded this degree at the March 1980 commencement of the Georgia Institute of Technology.

TABLE OF CONTENTS

	Page
PREFACE	ii
LIST OF TABLES	v
LIST OF ILLUSTRATIONS	vii
ABSTRACT	viii
CHAPTER	
I. INTRODUCTION	1
Thesis Motivation	
Basic Ideas and Definitions	
Possible Experimental Approaches	
A Brief History of Crossed Beam Experiments	
Summary	
II. EXPERIMENTAL TECHNIQUE	10
Introduction	
Expression for the Ionization Cross Section in Terms of Experimentally Observable Quantities	
Critique of Crossed Beam Ionization Experiments	
Requirements for a Valid Crossed Beam Ionization Experiment	
III. EXPERIMENTAL APPARATUS	26
Introduction	
Vacuum System	
Ion Source	
Electron Source	
Interaction Region	
Charged Particle Analyzers	
Ion Collection and Measurement System	
Electron Collection and Measurement System	
Modes of Operation	
IV. EXPERIMENTAL PROCEDURES AND RESULTS	60
Introduction	
Measurement Procedures	

Page

Consistency Checks
Experimental Results
Discussion of Errors

V. COMPARISONS WITH AVAILABLE THEORY. 91

Introduction
A Brief Review of Electron Impact Ionization Models
Extension to Multiple Ionization of Ionic Targets
Comparison of Present Results with Available
Theoretical Estimates

VI. CONCLUSIONS. 105

APPENDIX A. DERIVATION OF σ_{1N} IN TERMS OF EXPERIMENTAL
PARAMETERS 107

APPENDIX B. TYPICAL EXPERIMENTAL PARAMETERS AND DATA 112

REFERENCES. 119

LIST OF TABLES

Table		Page
1.	Absolute Experimental Cross Sections for the Double Ionization of Rb^+ Ions by Electron Impact.	78
2.	Absolute Experimental Cross Sections for the Triple Ionization of Rb^+ Ions by Electron Impact.	81
3.	Absolute Experimental Cross Sections for the Quadruple Ionization of Rb^+ Ions by Electron Impact.	84
4.	Typical Experimental Operating Parameters.	113
5.	Typical Form Factor Data Sheet	114
6.	Typical DC Mode Measurement Data for σ_{13} Configuration . . .	116
7.	Typical Pulsed Mode Measurement Data for σ_{14} Configuration.	117
8.	Typical Pulsed Mode Measurement Data for σ_{15} Configuration.	118

LIST OF ILLUSTRATIONS

Figure		Page
1.	Schematic Diagram of the Crossed Beam Experiment	27
2.	Plan View Photograph of the Crossed Beam Experiment.	28
3.	Photograph of the Ion Gun Assembly	29
4.	Use of a Movable Slit Scanner to Determine Beam Current Density Profiles	31
5.	Overall View of the Crossed Beam Ionization Facility	33
6.	Photograph of the Completed Ion Emitter Assembly	37
7.	Photograph of the Pierce-Type Ion Gun.	39
8.	Typical Beam Current Density Distributions	41
9.	Typical Electron Beam Energy Distribution.	44
10.	Photograph of the Interaction Region as Seen from the Location Normally Occupied by the Electron Beam Faraday Cup.	46
11.	Typical Driving Pulses and their Resulting Beam Waveforms.	59
12.	Idealized Beam Pulse Current Waveforms	67
13.	Dependence of the Measured Cross Sections on Electron Current.	71
14.	Dependence of the Measured Cross Sections on Ion Current.	72
15.	Dependence of the Measured Cross Sections on the Form Factor	74
16.	Dependence of the Measured Cross Sections on Ion Energy.	75
17.	Absolute Experimental Cross Sections for the Double Ionization of Rb^+ Ions by Electron Impact.	80
18.	Absolute Experimental Cross Sections for the Triple Ionization of Rb^+ Ions by Electron Impact.	83

Figure Page

19. Absolute Experimental Cross Sections for the Quadruple Ionization of Rb^+ Ions by Electron Impact. 85

20. Absolute Experimental Cross Sections for the Double, Triple and Quadruple Ionization of Rb^+ Ions by Electron Impact 86

21. Cross Sections for the Double Ionization of Rb^+ Ions Calculated Using the Method of Gryzinski 103

22. Comparison of the Measured Double Ionization Cross Sections with Estimates Obtained Using the Method of Gryzinski. . . . 104

ABSTRACT

The absolute cross sections for the double, triple and quadruple ionization of Rb^+ ions by electron impact have been measured from below their respective thresholds to approximately 3000 eV. This determination has been accomplished using a crossed beam facility in which monoenergetic beams of ions and electrons are caused to intersect at right angles in a well-defined collision volume. Multiply charged, product ions born as a result of the electron impact are deflected into their respective detectors by cascaded electrostatic analyzers. The multiply charged beam current component is measured by means of a vibrating reed electrometer operating in the rate-of-charge mode.

The required singly charged rubidium ions are produced in a thermionic ion source and pass through a series of focusing, collimating and deflecting structures before entering the interaction region. A thermionically generated, rectangular electron beam intercepts the target ions in a spatially designated collision volume. Just prior to entering this interaction region the two beams can be made to pass through a movable slit scanner which determines their spatial profiles. The various charged particle currents, energies and beam current density distributions represent the experimental data from which the desired absolute cross sections have been determined. The results obtained with this technique are compared with available theoretical predictions of the appropriate cross sections.

CHAPTER I

INTRODUCTION

Thesis Motivation

This thesis reports a measurement of the absolute cross sections for the double, triple and quadruple ionization of Rb^+ ions by electron impact from below their respective thresholds to approximately 3000 eV. This determination has been accomplished using a crossed beam technique in which monoenergetic beams of ions and electrons are caused to intersect at right angles in a well-defined collision volume. The various charged particle currents, energies and beam current density distributions represent the experimental data from which the desired absolute cross sections have been determined.

This study was undertaken to provide the first reliable multiple ionization cross sections for a large alkali ion. The results contained herein are expected to complement advanced atomic collision theories presently under development by providing the initial data with which to check the attendant mathematical approximations. In addition, accurate multiple ionization cross sections for the particular case of singly charged rubidium targets are needed immediately for the calibration of ion beam probes presently performing measurements on thermonuclear research reactors.

Basic Ideas and Definitions

Interaction between electrons and ions is a fundamental process which has commanded the attention of physicists for well over half a century. When an energetic electron collides with an ion a number of microscopic events may take place. One possibility is for the target ion to lose one or more additional electrons as a result of this electronic collision. Such a process is called "electron impact ionization," and the relative likelihood of its occurrence is directly related to the electron impact ionization cross section, σ_{ij}.† The absolute magnitudes of these various cross sections are necessary for the understanding of both stellar atmospheres and thermonuclear plasmas and considerable effort has been devoted to their determination. Perhaps the earliest viable attempt was a theoretical procedure proposed by Thomson in 1912.[1] This pioneering calculation resulted in a simple, classical expression for the desired electron impact ionization cross section and provided considerable impetus for much subsequent theoretical modeling. Some idea of the extreme difficulties inherent in the development of a comprehensive ionization theory is emphasized by the multiplicity of possible electron impact ionization mechanisms. Equations (1), (2) and (3) summarize several of the possible processes.[2]

$$e^- + x^{n+} \longrightarrow e^- + x^{(n+m)+} + me^- \qquad (1)$$

---

†The cross section for the ionization from the initial state i to the final state j is conventionally denoted by the symbol, σ_{ij}.

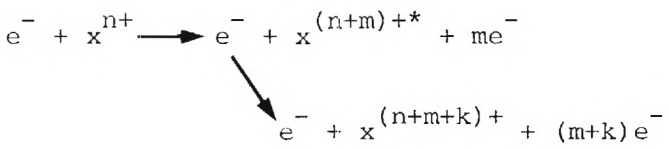

(2)

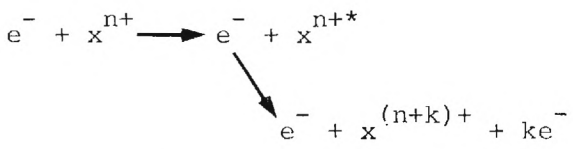

(3)

The mechanism enumerated in Equation (1) is a direct single or multiple ionization event and, in fact, the value of m indicates the order of the ionization process.† In contrast, Equation (2) considers the direct knock-out of inner shell electrons with subsequent Auger ejection of additional electrons. Finally, Equation (3) involves the excitation of the target particle to a state above one or more higher ionization continua and this is followed by autoionization.

In light of the complex physics involved, it is not surprising that rigorous quantum mechanical models are frequently characterized by some eminently intractable mathematics. Accordingly, the theorist generally concedes a number of approximations to facilitate the calculation of the desired cross section. This results in a hybrid model whose validity is assured only if the calculated cross section closely mimics an independent experimental result. At present however, many interesting comparisons are prevented by the lack of an adequately

---

†If, for instance, the target ion loses one additional electron, then the event is called "single ionization" regardless of the final charge state of the target. Thus, when in Equation (1), for example, n = 1 and m = 3, the process is described as "triple ionization of singly charged x."

comprehensive experimental data base. Furthermore, many of the predictions resulting from such theoretical models are either unreliable or not applicable to the higher order processes.[3-6] Even the popular Gryzinski method has been applied to only single and double ionization and no comprehensive theories have been developed for the interesting triple, quadruple or higher order ionization events.[7]

Complementing these theoretical calculations, much attention has been devoted to the experimental study of electron impact ionization. These experimental results have tested the validity of the computational assumptions inherent in the hybrid ionization models and have also yielded cross sections for which no theoretical predictions are yet available. Future experimental results are expected to contribute substantially to the catalog of reliable ionization cross sections and thereby help illuminate the path towards more accurate theoretical calculations. As a result of their extreme importance, it seems appropriate to discuss in detail some of the experimental procedures applicable to the measurement of selected atomic cross sections.

Possible Experimental Approaches

Historically, a considerable effort has been devoted to the development of techniques for the experimental investigation of collisions between interacting particles. Although quite diverse in their individual characteristics, nearly all of these procedures can be grouped into one of four general categories of experiments. Selected techniques from a particular category then allow either the direct

measurement or the indirect inference of the desired absolute atomic cross sections.

In the plasma afterglow experiments, for instance, a target gas is initially heated by means of a shock wave or an electrical discharge. Observation of the resulting afterglow then allows the experimenter to infer relative cross sections about the processes of interest.[8] Unfortunately, such a technique is not inherently absolute and thus it is necessary to calibrate the apparatus on a plasma whose characteristics have been independently determined.

An alternative approach attempts to deduce reaction rates from spectroscopic observations of plasmas with known characteristics.[9] This procedure suffers from a host of interpretive difficulties but appears to hold promise for the very highly charged ions whose cross sections are inaccessible by other methods.

The third technique involves trapping target particles by means of a static electric or magnetic field and subsequently bombarding them with projectiles of known energy.[10] This procedure has yielded relative atomic cross sections for several processes of interest but must be absolutely calibrated by comparison with events having independently determined cross sections.

Finally, the most frequently employed method, and the only technique which is inherently absolute, involves a direct collision between the two beams of particles. Subsequent measurement of the rate at which the resulting products are formed then allows the determination of the desired atomic cross sections. In principle, the two colliding

beams may intersect at any angle between zero and ninety degrees. In the particular case when the intersection angle is zero degrees, the technique is known as "merging beams." Formal suggestion of the merged beam concept has been in existence since at least 1959 when it was recognized that the interaction energy may be made arbitrarily small with this technique.[11,12] There is, in fact, little doubt that the merged beam procedure has allowed investigation of the previously inaccessible energy range from thermal energies to a few electron volts. Unfortunately, important difficulties with the method still exist and, in particular, it remains a formidable undertaking for experimentalists to determine the intersection geometry of the colliding particles with satisfactory accuracy in a merged beam configuration.[13,14]

In contrast, adjustment of the intersection angle to a value between zero and ninety degrees to conduct a "inclined beam" experiment was suggested in the 1960's.[15,16] This concept was introduced in an attempt to trade-off the low interaction energy inherent in the merged beam technique for a more accurate knowledge of the intersection geometry of the colliding beams. In principle, the most advantageous feature of inclined beams at different angles is the variety of interaction energies accessible. However, remaining difficulties with the collision geometry have encouraged manipulation of the intersection angle to the limiting value of ninety degrees. In fact, this special case of perpendicular intersection is of such importance that the term "crossed beams" has been reserved for its description.

A Brief History of Crossed Beam Experiments

Experimental realizations of the crossed beam concept have been in existence since the 1920's. Early measurements concentrated on the bombardment of neutral atoms with beams of electrons to infer ionizing potentials and, hence, binding energies for mercury, potassium and sodium.[17-20] These pioneering experiments demonstrated the fundamentals of the technique but frequently yielded excessive values for the resulting atomic cross sections. The universal difficulty with these early experiments involved the interaction of the atomic beam with the background gas. In particular, the target beam was often charged stripped on the residual gas in the system and, hence, gave rise to an erroneously high product collection rate. Shortcomings of this nature were largely circumvented in 1958 when experimentalists began using modulated beams and synchronous detection to separate legitimate signal from the charge stripping background.[21,22] Numerous measurements of electron impact ionization cross sections for neutral atoms soon followed and in the early 1960's the crossed beam technique was successfully applied to the study of charged particle - charged particle collisions. Of particular importance was the work performed at Culham Laboratory in England resulting in single ionization cross sections for He^+, Ne^+ and N^+ ions.[23-25]

Much of the subsequent activity has been motivated by the data needs of the Controlled Thermonuclear Research program. As a result, single ionization cross sections for Ba^+, Tl^+ and all the singly charged alkali ions have been determined.[26-34] Similarly, some effort has been devoted to the single ionization of multiply charged, atmospheric ions

in an attempt to extrapolate existing theory to more complex electronic structures.[3,35-38] Comparatively little attention has, however, been given to the interesting single collision, multiple ionization events. Scientists in the Netherlands have, however, attempted some relative abundance measurements for the production of multiply charged noble gases by electron impact.[39-41] Unfortunately, these experiments apparently suffer from metastable contamination of the primary beam and, in any event, the results do not agree with independent determinations of the relevant cross sections.[42,43] Similarly, the Georgia Tech group has recently done some preliminary work on the double ionization of alkali ions for use in ion beam probe calibration.[44-46] To date, however, Peart and Dolder's double ionization cross section for Li^+ is the only reliable multiple ionization measurement reported in the literature.[47]

Summary

Previous successful usage has demonstrated that the crossed beam technique is an appropriate tool for the determination of electron impact ionization cross sections. The various charged particle currents, energies and beam current density distributions represent the experimental data from which the desired absolute cross sections can be determined. This approach requires considerable technical sophistication but allows accurate manipulation of experimental parameters so that reliable results can be obtained. Many cross sections of interest have been determined using the crossed beam technique and much of the earlier work has been critically evaluated.[48-54] To date, however, most of the

studies have involved electron impact single ionization of either atoms or singly charged ions. The only double ionization measurements presented in the literature have been performed on singly charged lithium or on atomic noble gases. No reliable, higher order ionization studies have yet been reported. The present research is expected to contribute substantially to the higher order ionization data base by reporting the first successful measurement of the absolute cross sections for the electron impact double, triple and quadruple ionization of singly charged rubidium ions.

CHAPTER II

EXPERIMENTAL TECHNIQUE

Introduction

This research presents a measurement of the absolute cross sections for the double, triple and quadruple ionization of Rb^+ ions by electron impact from below their respective thresholds to approximately 3000 eV. The experimental technique utilizes a crossed beam apparatus in which monoenergetic beams of ions and electrons are caused to intersect at right angles in a well-defined collision volume. Multiply charged, product ions born as a result of the electron impact are separated from the singly charged, primary ion beam by electrostatic analysis. The incident electron current, the currents of the reacted and unreacted ions and the various charged particle energies and beam current density distributions represent the experimentally observed quantities from which the desired absolute cross sections can be determined. In order for this approach to yield valid results however, special precautions must be taken to properly assess the various potential errors inherent in this type of measurement. This chapter discusses the general principles of the crossed beam technique and enumerates a set of consistency criteria which must be rigorously enforced in order to ensure the validity of the resulting ionization data.

Expression for the Ionization Cross Section in Terms of Experimentally Observable Quantities

The crossed beam technique involves a perpendicular intersection between the beam of incident electrons and that of the target ions. Consider, for instance, a monoenergetic electron beam and a monoenergetic singly charged ion beam traveling parallel to the X and Y axes, respectively, of a Cartesian coordinate system. Let v_i and v_e be the ion and electron velocities. If both beams are sufficiently tenuous such that multiple collisions can be neglected, then it is easy to show that the cross section for the $(N-1)^{th}$ ionization of the singly charged ions is given by Equation (4),†

$$\sigma_{1N} = \frac{e\, v_i\, v_e}{N(v_i + v_e)^{\frac{1}{2}}} \cdot \frac{I_{SIG}^{N+}(I,J)}{\int_{-\infty}^{\infty} i(z)\, j(z)\, dz} \tag{4}$$

where $i(z)dz$ and $j(z)dz$ are the ion and electron currents passing through a region z to $z+dz$, $I_{SIG}^{N+}(I,J)$ is the total current of the N^{th} charged ions produced by electron impact and e is the electronic charge.[26] Normally, the electron velocity is much greater than the ion velocity and so it is very nearly correct and quite convenient to write Equation (4) in the following form:

$$\sigma_{1N} = \frac{e\, v_i}{N} \cdot \frac{I_{SIG}^{N+}(I,J)}{I\quad J} \cdot F \tag{5}$$

---

†Equation (4) is derived in Appendix A.

where

$$F \triangleq \frac{I \quad J}{\int_{-\infty}^{\infty} i(z)\ j(z)dz} \equiv \frac{\int_{-\infty}^{\infty} i(z)dz \int_{-\infty}^{\infty} j(z)dz}{\int_{-\infty}^{\infty} i(z)\ j(z)dz} \tag{6}$$

and I and J are the total target ion and total incident electron currents, respectively.

Note that with the exception of F, Equation (5) involves only known or directly measurable experimental quantities. The form factor, F, however, includes an overlap integral which depends upon the current density distributions of both the ion and electron beams. Fortunately, under certain conditions, an accurate numerical approximation for the form factor may be obtained by the use of a movable scanning apparatus as shown in Chapter III.

In the present experiment, the electron velocity is always very much greater than the ion velocity and hence the total collision energy in the center-of-mass reference frame is nearly equal to the laboratory energy of the incident electrons. Therefore, the measured cross sections should be a function of only the electron energy and are thus expected to be essentially constant with respect to variations in ion energy. Additionally, for a given electron energy, the cross sections should be independent of changes in the ion beam intensity, the electron beam intensity and the form factor. In fact, the invariance of the measured cross sections to systematic manipulation of these parameters provides a valuable means of diagnosing many aspects of the performance of the experimental apparatus.

Critique of Crossed Beam Ionization Experiments

Much previous work has demonstrated that the crossed beam experiment is an appropriate tool for the study of moderate energy, charged particle - charged particle collisions. Numerous cross sections of interest have been determined with this technique and many of the earlier measurements have been critically evaluated.[48-54] It is worth emphasizing that the crossed beam approach has the advantage of enabling absolute measurements to be performed even in the absence of calibration knowledge resulting from independently determined cross sections.[52] In return however, for these absolute cross sections, the experimentalist must take extensive precautions to ensure that each of the quantities in Equation (5) is being properly evaluated. Under normal circumstances, measurement of the parent beam currents is straightforward and most difficulties can be obviated with proper apparatus design and accurate instrumentation. In contrast however, problems associated with the determination of both the ionization signal and the form factor are considerably more subtle and special techniques are required to unambiguously determine their values. Accordingly, it is deemed appropriate to summarize some of the inherent characteristics of a crossed beam ionization experiment and examine the error mechanisms peculiar to this type of measurement.

Low Reaction Rates

Experiments involving collisions between two species of charged particles are handicapped by a space charge restriction on the maximum permissible particle number density in each of the parent beams. In

particular, the limited electron and ion densities allowable severely restricts the maximum product formation rate attainable. An example of the low reaction rates typical of a crossed beam experiment is furnished by the present research. If 16 nanoamperes of 1.5 keV ions collide with a 700 eV, 900 microampere electron beam, about two Rb^{+} ions in 10^{9} are converted to Rb^{5+} ions. Thus, the reacted beam emerging from the collision volume contains two current components differing in intensity by eight orders of magnitude. This huge intensity difference between the primary and signal beams requires that careful attention be given to the signal beam transport system so that stray particles and noisy backgrounds do not completely preclude the detection of the reaction ions.

Errors Caused by Collisions with Background Gases

The detection of reaction products in a crossed beam experiment is further complicated by the ratio of the parent beam particle density to that of the residual gas molecules in the vacuum enclosure. Typical target beam densities are so low that even in the ultra-high vacuum regime, the number of extraneous collisions between the targets and the air molecules in the system may be comparable to the number of desired collisions between the target ion and the incident electrons.[50] In such cases, the target beam is often charge stripped on the residual gas molecules and hence, gives rise to an erroneously high, product collection rate. In the present experiment, it was anticipated that the Rb^{+} targets might become charge stripped according to the following representative reactions:

$$Rb^+ + R \longrightarrow \begin{cases} Rb^{N+} + R + (N-1)\, e^- \\ Rb^{N+} + R^+ + Ne^- \end{cases} \qquad (7)$$

where R is a residual gas molecule. In N = 3, 4 or 5 respectively, the products of such reactions may result in spurious double, triple or quadruple ionization signal. Such charge stripped products are frequently born in the field-free region prior to the point of charge state separation and thus become superimposed on the desired multiply charged signal produced by electron impact. It is subsequently necessary to separate the legitimate ionization signal from the undesired stripping component and several procedures have been developed to effect this discrimination.

The first technique involves operating both the electron and Rb^+ beams in a DC mode while systematically measuring the individual backgrounds associated with each of these parent beams. In this manner, the contributions of the various background components to the measured signal frequently may be characterized and subsequently eliminated. Implicit in such a procedure is the assumption that the vacuum chamber pressure, and hence the magnitude of the charge stripped component, is unaffected by the presence or absence of the electron beam. It is therefore necessary to demonstrate that pressure modulation of the charge stripped background makes an insignificant contribution to the computation of the net electron impact ionization signal. Experimental verification of the absence of this undesired effect may be obtained by measurements of the cross sections below the respective thresholds for the onset of each of the ionization processes. Such measurements

should yield a result identically equal to zero for all collision energies below threshold. Note that a zero indicated cross section at only a single energy below threshold is not sufficient because competing background effects may accidentally cause the apparent ionization signal to vanish at a particular collision energy.

Alternatively, a pulsed beam technique may be employed to assess the effects of background on the experimentally observed cross sections. One such method involves pulsing both the electron and ion beams in either time coincidence or time anti-coincidence. This particular beam pulsing procedure is motivated by the desire to establish a steady-state pressure in the region surrounding the experiment. If the beams are pulsed at a rate several times faster than the characteristic frequency of the vacuum system, then a constant average pressure is maintained throughout the evacuated chamber. Under these conditions, pulsing the beams in time coincidence yields the algebraic sum of the electron impact ionization signal and the charge stripping background. In contrast, the time anti-coincidence mode of operation gives rise to only the stripping component. Simple subtraction then allows the unambiguous determination of the desired electron impact ionization signal. Dunn, however, cautions that localized electron beam induced outgassing occasionally invalidates the steady-state atmospheric assumptions inherent in such a beam pulsing scheme.[53] It appears however, that equality of DC and pulsed measurements along with a zero measured cross section below threshold constitutes an adequately comprehensive set of diagnostics to properly assess the effects of residual gas on the particle beam interactions.

Errors in the Determination of the Form Factor

Reduction of crossed beam ionization data to the desired absolute cross sections is critically dependent upon accurate knowledge of the current density distributions of the intersecting beams. Such a determination normally requires a movable slit scanner which is employed to spatially define corresponding current slices for each beam as discussed in Chapter III. The resulting incremental current samples are then used to calculate the desired form factor. Such a procedure however, yields only an approximation of the true form factor and the technique employed for its determination is subject to several inherent sources of error.

The first set of potential difficulties is a direct result of the constraints on the physical location of the slit scanner. In the usual experimental geometries, the form factor is determined near, but not in, the eventual region of beam overlap. As a result, beam misalignment and perturbation of the beam profiles between the scanner and the collision volume can yield an apparent result substantially removed from the actual form factor. Beam misalignment however, is circumvented by careful apparatus construction and, in any case, is rather easy to diagnose. If, for instance, electron impact ionization signal is detected with the slit scanner intercepting the beams then the maximum beam alignment error is evidently less than the height of the scanner slit.

In addition to beam alignment difficulties, space charge expansion of the parent beams occurring between the scanning apparatus and the interaction region leaves the form factor measurement subject

to error. In practice, ion beam expansion is usually negligible but electron space charge frequently causes the electron beam to diverge substantially between the scanner and the collision volume. Previous workers however, have observed that if the scanner is located reasonably close to the collision volume and if the ions are focused so that all of the electrons have the opportunity to pass through the ion beam, then this effect need not be troublesome.[52] A further degree of refinement is attained if the major axis of the electron beam is aligned parallel to the trajectories of the target ions. In this manner, an adequately large incident electron current can be obtained with the minimum possible electron density.[50,51] Furthermore, monitoring the electron current to a properly sized aperture located just beyond the collision volume provides a valuable check on electron beam divergence. If this aperture plate intercepts a miniscule fraction of the total electron current then it is reasonable to conclude that electron beam divergence is producing an insignificant error in the determination of the form factor. Finally, an additional assessment of this effect is obtained by recalling that the space charge expansion of the electron beam is proportional to the electron beam intensity. Thus, if the apparent cross sections at a fixed collision energy are independent of the incident electron current it is likely that the effect of beam divergence on the form factor determination is negligible.

Another, more subtle series of potential difficulties in the form factor measurement arises because the shuttering of the incident beams by the narrow slit in the scanner effectively eliminates the macroscopic space charge influence of one beam upon the other. In the

absence of the scanner it is possible that the ion trajectories are somewhat perturbed by the space charge of the incident electrons. Under such conditions, the ions will tend to migrate towards the densest portion of the electron beam and hence the presence of the electrons will deflect the ion trajectories. The magnitude of this deflection is expected to be systematic with ion beam intensity and should vary inversely with ion beam energy. Therefore, constancy of the measured cross sections as the ion energy is varied implies that deflection of the ion beam by the electron space charge is not significantly affecting the measured beam profiles.

In summary, experimental attempts at form factor estimation are subject to a variety of possible systematic errors. Most of these problems however, can be circumvented by strategic apparatus design and selection of reasonable beam currents. In addition to the diagnostic checks developed above, it is advantageous to examine the cross section for a particular electron energy as a function of the measured form factor. If the resulting cross sections are invariant with respect to changes in the ion energy, beam current intensities and beam current profiles then it is reasonable to assume that the form factor is being evaluated correctly.

Additional Errors Caused by Beam Space Charge

In addition to causing errors in the determination of the form factor, space charge effects associated with the colliding beams often confuse the detection of the ionization signal. Most such difficulties in crossed beam experiments stem from the electrostatic deflection of

ionic particles by electron space charge. Such deflection often causes loss of particles from the ion beam and can also modulate the magnitude of the ionic background.

Loss of Ions. In most crossed beam ionization experiments the product ions are detected at a location substantially removed from the collision region. As a result, small deflections of the ion trajectories as the target particles pass through the electron beam necessarily produce significant changes in the dimensions of the reacted ion beams at their collectors. If, for instance, the unperturbed beams are slightly larger than the entrance apertures of their respective collectors, then additional focusing resulting from electron space charge will increase the product collection efficiencies. In the extreme case, however, very high electron densities are likely to induce a crossover of ion beam trajectories. Such an eventuality yields a divergent beam at the ion detector with a consequent reduction in collection efficiency. In either event, the measured cross sections appear to vary systematically with the magnitude of the electron current.

In practice, a properly focused ion beam passing through adequately sized apertures will not experience a change in transport efficiency resulting from electron space charge focusing.[50] Furthermore, a diagnostic is provided by observing that the converging effect of the electron beam is dependent upon the electron number density. Thus, if the cross section measured at fixed electron energy is invariant to changes in the electron current, it is reasonable to assume that the above focusing effects are negligible. A further

check is obtained by examining the cross section as a function of ion energy at constant electron energy and current. Perturbing deflections of the ion beam should be inversely related to ion beam energy and hence, invariance of the measured cross sections to moderate changes in this parameter demonstrates that there are no significant deflection losses from the ion beam.

Modulation of Ionic Background. A significant source of error in the determination of the ionization signal can arise when the magnitude of the ion beam background component is modulated by space charge effects associated with the electron beam. Such background fluctuations are often comparable in magnitude to the electron impact ionization current and can thus preclude accurate measurement of the desired signal. Under normal conditions, most of the ionic background is the result of ions becoming charge stripped on slit edges or residual gas molecules. These stripping collisions can occur either before or after the ion has passed through the collision region. If, for instance, the stripping reaction occurs prior to the interaction region then some of the multiply charged particles are scattered relative to the parent ions and hence, the product beam is divergent. However, subsequent passage through the electron beam tends to refocus the perturbed trajectories and thus, an appreciable percentage of the charge stripped ions might be collected by the multiply charged signal detector. Consequently, a change in the electron beam current introduces a corresponding variation in the magnitude of the charge stripped background. Such an effect is eliminated in the present experiment however, by the inclusion of a set of primary beam steering plates prior to the interaction region. This

electrostatic deflection assembly removes any neutral particles or charge stripped ions from the target beam just before collision with the incident electrons.

Unfortunately, an analogous phenomenon occurs if the ions become stripped after passage through the collision volume. In this case, the presence of the electron beam will converge the ion trajectories and thus, modulate the stripping component of the total ionization current. Under these conditions, turning off the electron beam causes the stripping contribution to inflate and hence, the apparent electron impact component is less than the actual signal current.[50] Harrison has developed a simplistic model which predicts that the space charge effect of, say, the electron beam upon noise arising from ion beam background effects will vary directly as the electron current, inversely with the square root of the electron energy and inversely with the ion energy.[50] A truly accurate model however, would be extremely difficult to mathematically formulate. As a result, it is likely that the optimum compromise involves diagnostic explorations of the cross section dependence upon both electron current and ion energy. For instance, Feeney has observed that if stripping or energy loss on an aperture edge is present, the apparent cross sections usually tend to vary inversely with electron beam intensity.[55] However, if deflection losses from the ion beam are involved the cross sections depend directly on the electron current. Presumably, an accidental cancellation of competing effects is possible and, as a result, it is advisable to supplement these diagnostic checks with measurements below threshold. If the apparent cross section is zero below threshold and independent

of both electron current and ion beam energy, it is likely that the error introduced by ionic background modulation is negligible.

Excitation State of the Target Ion

In order to facilitate the determination of the desired cross sections from relevant experimental data it is imperative that the initial quantum state of the target ion be specified. If, for instance, the ion beam enters the collision volume in a multiplicity of excited states the measured cross sections will be an ambiguously weighted average of the ground state and excited state cross sections. However, in most experimental geometries, the time required for the target ion to traverse from the source to the interaction region is long compared to the lifetime of optically allowed transitions. Therefore, only metastably excited ions would be expected to significantly confuse the measured cross sections. Fortunately, all of the alkali ions can be generated thermionically and previous research has demonstrated that, for such electronic structures, the thermionic process precludes the emission of appreciable numbers of ions in excited states.[52]

An experimental check for metastable contamination is provided by measuring the cross section below the threshold for the ground state target but above the threshold for the metastably contaminated beam. If the measured cross section is identically zero over this range of electron energies and is independent of the ion beam energy, the electron beam intensity and the form factor, then one may be assured that there is no significant metastable contamination of the parent ion beam.

Requirements for a Valid Crossed Beam Ionization Experiment

The above discussion has summarized a number of the characteristics and corresponding error mechanisms peculiar to crossed beam ionization experiments. Most of these difficulties display a predictable dependence upon one or more of the parameters in Equation (5). The resulting functional dependence thus suggests techniques for diagnosing the presence of each of these errors. From these diagnostic procedures emerge a set of consistency checks which can be enforced to help ensure the validity of the resulting crossed beam ionization data. At a minimum, it seems reasonable to require that the cross sections measured at a given electron energy satisfy all of the conditions enumerated below.

(1) The measured cross sections should be independent of the electron beam intensity.

(2) The measured cross sections should be independent of the ion beam intensity.

(3) The measured cross sections should be independent of changes in the beam profiles.

(4) The measured cross sections should be independent of the ion beam energy.

(5) The measured cross sections should ideally be zero below the threshold energy for the onset of the ionization process being studied.

In summary, it is required that the measured cross sections depend solely upon the incident electron energy and hence, be independent of reasonable excursions in the other experimental quantities.

Typically, the required invariance will occur over only a finite range in the values of each parameter and it is incumbent upon the experimentalist to demonstrate an adequately broad operating plateau over which the crossed beam experiment yields self-consistent results. Unfortunately, few of the above consistency diagnostics are unambiguous and the inability to satisfy a particular check is occasionally symptomatic of several unrelated problems. By carefully enforcing all of the consistency criteria however, it is usually possible to operate the crossed beam apparatus in a manner that yields reliable, self-consistent ionization data.

CHAPTER III

EXPERIMENTAL APPARATUS

Introduction

The objective of the present research is a measurement of the absolute cross sections for the double, triple and quadruple ionization of Rb^+ ions by electron impact from below their respective thresholds to approximately 3000 eV. This determination has been accomplished by means of a crossed beam technique in which a beam of energetic electrons is perpendicularly incident upon an array of singly charged rubidium targets. Multiply charged, product ions born as a result of this electronic collision are separated from the primary ion beam by means of electrostatic analysis. The various charged particle currents, energies and beam current density distributions constitute the experimental data from which the desired absolute cross sections can be obtained.

A schematic diagram of the crossed beam ionization apparatus appears in Figure 1 and a plan view photograph is presented in Figure 2. Singly charged rubidium ions are thermionically generated in an aluminosilicate-molybdenum plug rigidly mounted behind a Pierce-type electrostatic gun as shown in Figure 3. This combination produces an intense, highly collimated beam of Rb^+ ions in the ionic ground state which subsequently receive additional collimation and focusing in the F_1 and F_2 structures. Just before entering the collision volume, C,

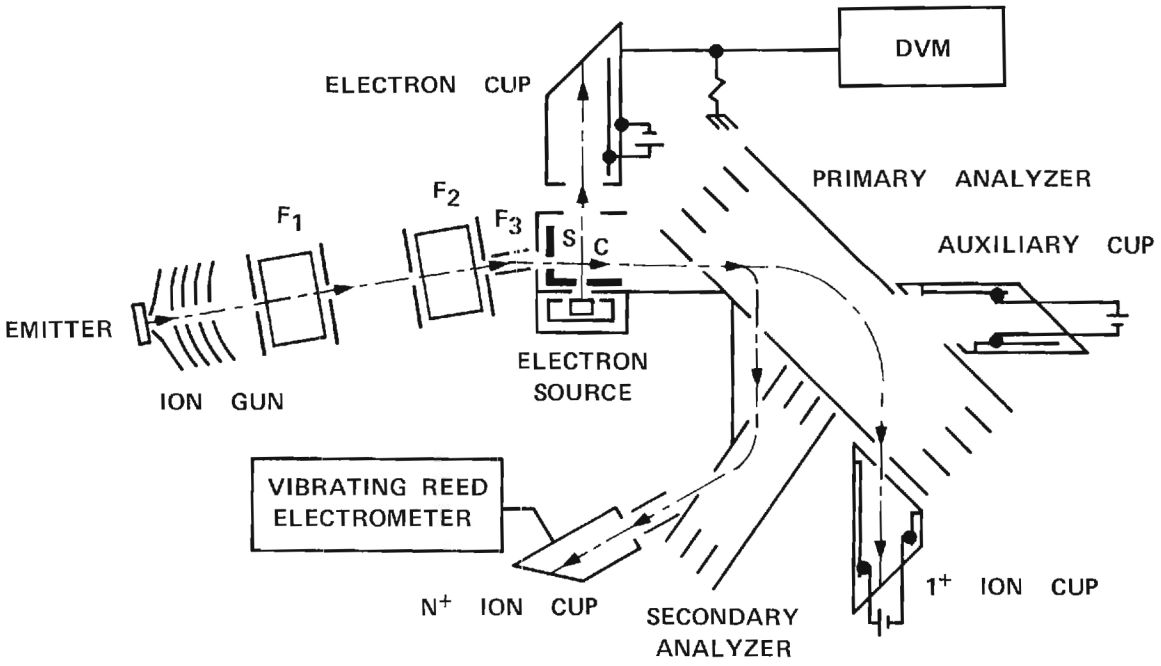

Figure 1. Schematic Diagram of the Crossed Beam Experiment.

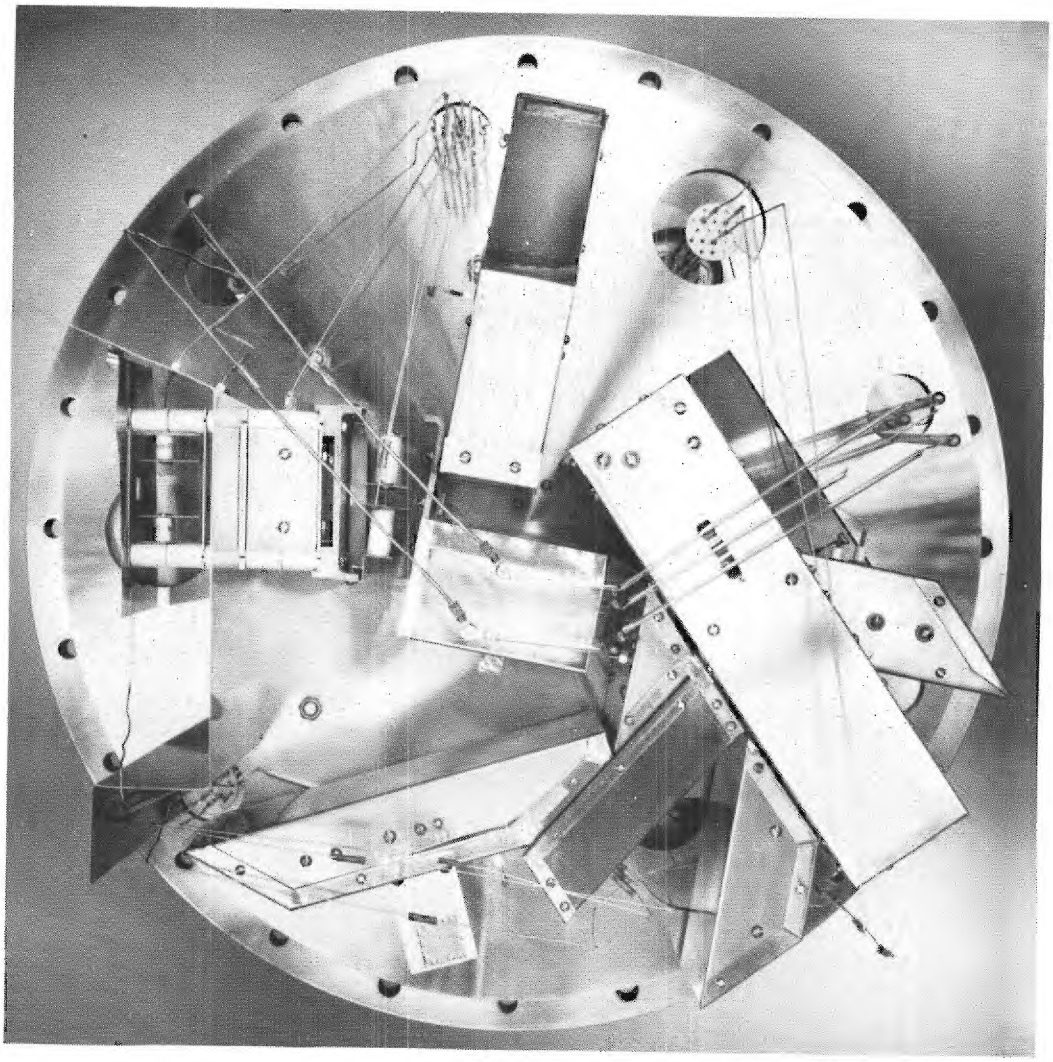

Figure 2. Plan View Photograph of the Crossed Beam Experiment.

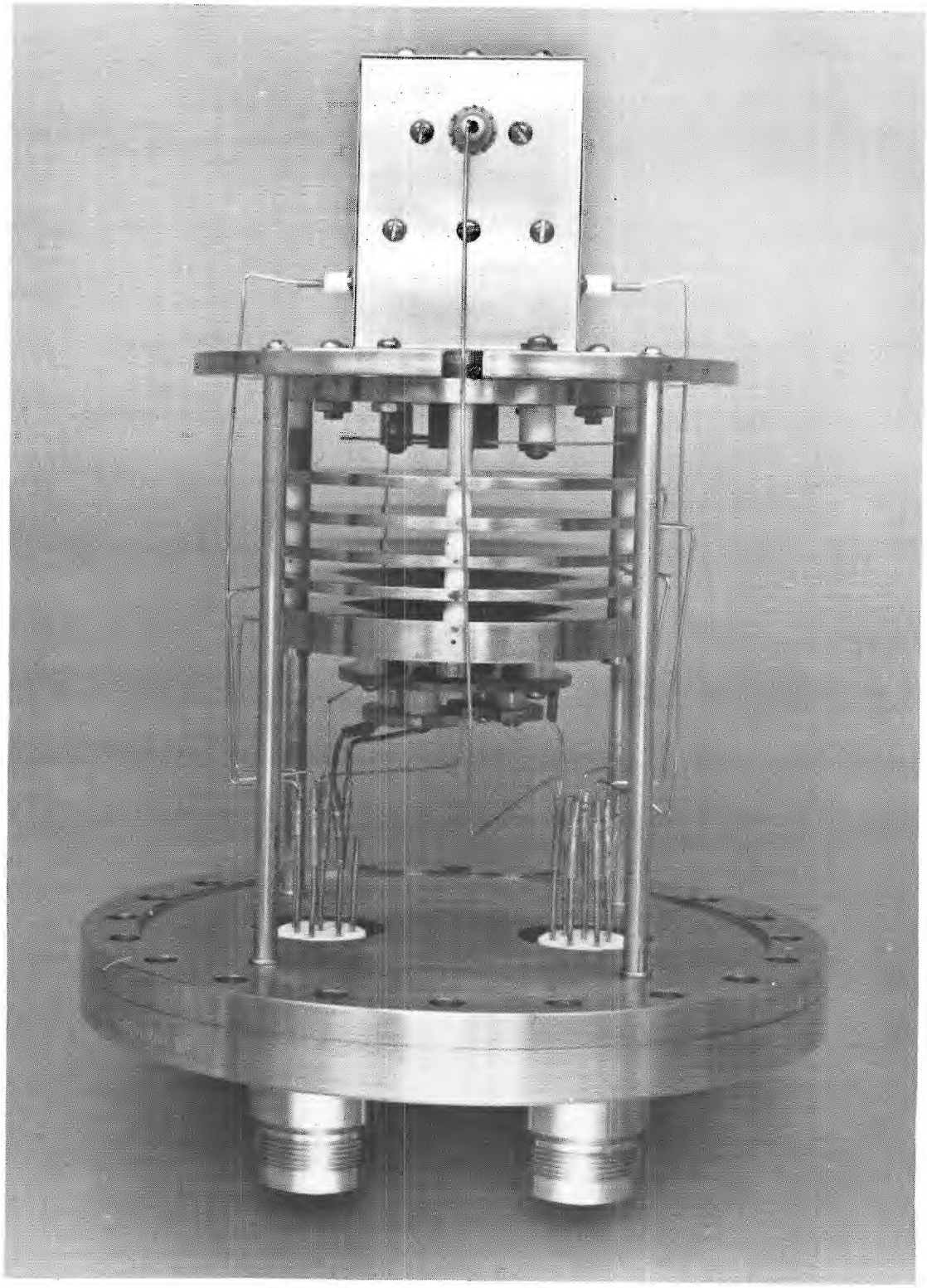

Figure 3. Photograph of the Ion Gun Assembly.

this primary beam is deflected through a slight angle by the F_3 stage in order to remove any neutrals or ions which have become multiply charged as a result of stripping on slit edges or residual gas molecules. A rectangular electron beam is produced by a 6L6 beam power tube and intersects the Rb^+ beam in the spatially designated collision volume, C. Just prior to traversing this interaction region the two beams can be made to pass through a movable slit scanner, S, which determines their respective current density profiles as shown in Figure 4.

After undergoing collision, the ion beam, which might now contain a number of charge state components, passes through the entrance aperture of the primary electrostatic analyzer. Note that the much greater mass of the Rb^+ ions makes it possible to ensure that any interaction with the electron beam results in small-angle scattering of the ions. Hence, those ions which have undergone interaction with the electrons emerge from the collision volume with essentially the same velocity as that of the unreacted ions, making the resulting beam amenable to electrostatic analysis. The multiply charged ions are subsequently deflected through the secondary electrostatic analyzer and thence into the N^+ Faraday cup. Note that when the Rb^+ beam is deflected into the 1^+ Faraday cup, the Rb^{3+} ion beam is incident upon the N^+ cup. Similarly, by simply scaling the analyzer potentials, it is possible to monitor either the Rb^{4+} or Rb^{5+} current in the N^+ cup while the Rb^+ beam is simultaneously being deflected into the auxiliary cup.

The Rb^+ current component is of the order of 10^{-8} amperes and is typically monitored with a conventional electrometer. The multiply charged current is frequently as small as 10^{-16} amperes and is measured

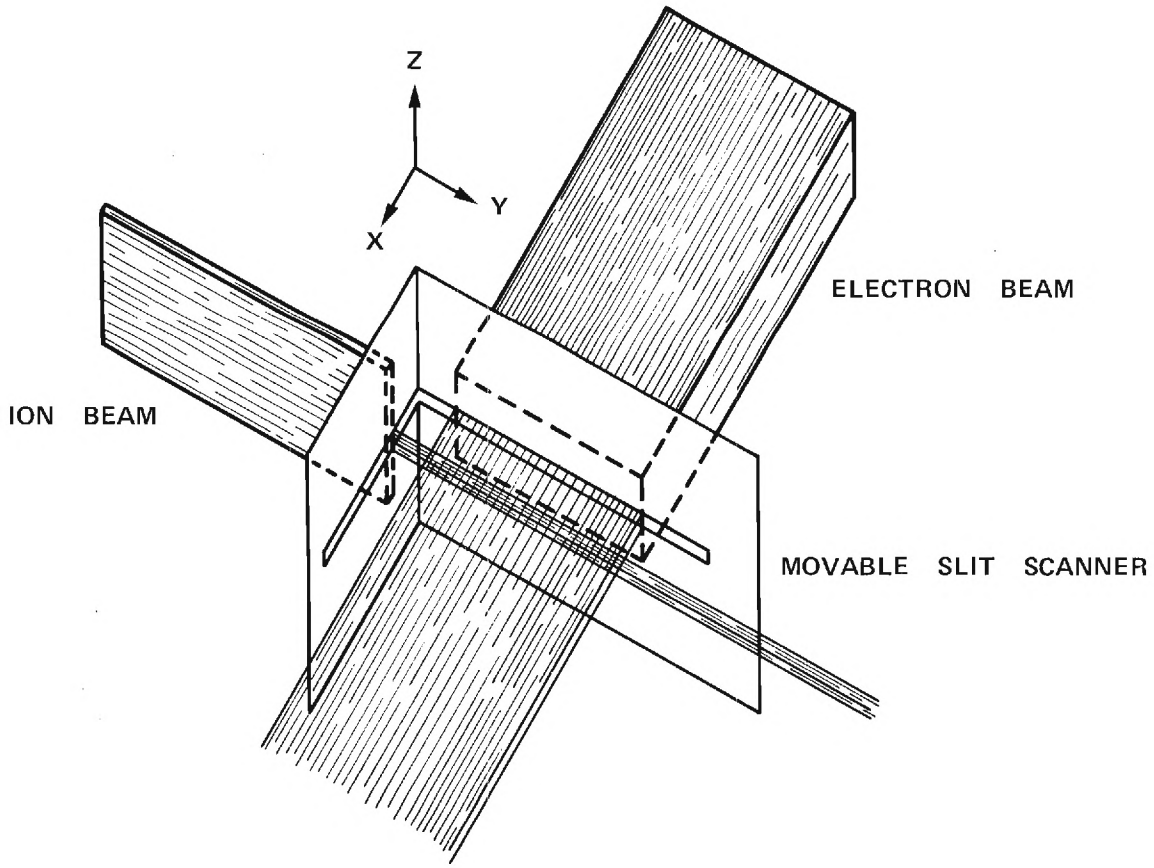

Figure 4. Use of a Movable Slit Scanner to Determine Beam Current Density Profiles.

with a Cary model 401 vibrating reed electrometer operating in the rate-of-charge mode. The electron current is of the order of 10^{-3} amperes and is easily measured with conventional techniques.

An overall view of the crossed beam ionization facility appears in Figure 5. The electronics to the right of the chamber support the vacuum system while the instrumentation on the left controls and monitors the actual experiment. The remainder of this chapter is devoted to a detailed description of the construction and operation of each of these major components of the experimental apparatus.

Vacuum System

The primary vacuum enclosure is an all stainless steel bakeable chamber 21.5 inches in diameter and 20 inches deep. The interior of this chamber is polished to a nominal eight microinch finish in order to reduce outgassing. Four Consolidated Vacuum Corporation four inch ports have been welded symmetrically around the periphery of the tank to house additional vacuum hardware. The ion gun assembly is mounted within an extension nipple bolted to one of these orfices. Adjacent orthogonal ports accommodate an ion gauge tube mounting flange and a water-cooled housing for a titanium sublimation pump. The remainder of the experiment is mounted on a one inch thick stainless steel plate which is then suspended from the top cover of the vacuum chamber.

Each of the components contained within the experimental vessel itself is constructed of metals or ceramics compatible with the ultra-high vacuum environment. All welds are inert gas welds, made on the interior of the chamber and machined. Gasketing is accomplished with

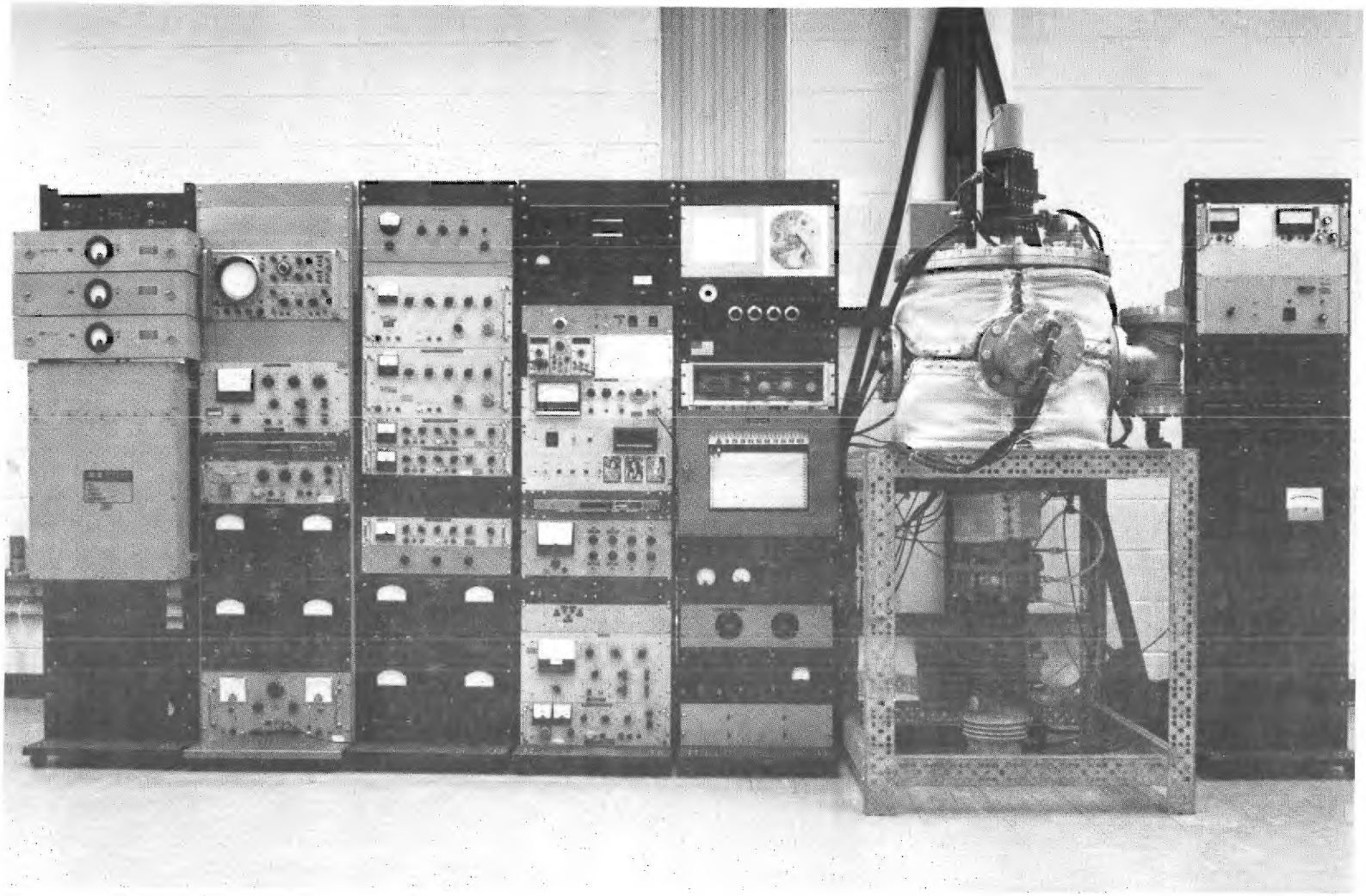

Figure 5. Overall View of the Crossed Beam Ionization Facility.

either copper annuli inside conflat assemblies or with compression type, metal o-rings fused from 0.086 inch diameter cold finished aluminum wire.

Pumping Apparatus

The pumping system consists of a Consolidated Vacuum Corporation type PMCU-6B six inch oil diffusion pump followed by a type BCRU-60 water-cooled chevron baffle and a type TSMU-60 zeolite molecular sieve trap. The diffusion pump is charged with 800 cubic centimeters of Dow Corning Corporation type DC-705 silicone diffusion pump fluid. Roughing is accomplished with a Welch model 1376 two stage, mechanical fore pump. In addition, a Varian model 922-0039 titanium sublimation pump is attached to the vacuum chamber via a water-cooled housing to act as a booster for the primary oil diffusion pump.

The oxide cathode in the electron source is very susceptible to hydrocarbon contamination and thus, provides a sensitive check on the backstreaming of diffusion pump fluid. In order to prevent such cathode contamination, it has been found advisable to replace the zeolite charge in the molecular sieve trap before every pumpdown.

Bakeout and Vacuum System Performance

The zeolite trap and the vacuum chamber walls are baked by means of heating mantles to approximately 300°C and 200°C, respectively for a period of 48 hours during the initial phase of a pumpdown. During this time the ion source is heated to its operating temperature and the electron source is subsequently activated. Immediately upon

reaching room temperature after termination of the bakeout, the indicated pressure with both beams operating is typically 5-8 x 10^{-8} torr. During the following several days of operation the pressure normally continues to decrease to a nominal 4-7 x 10^{-8} torr. No significant deterioration of this vacuum performance is evident over a period of at least 500 hours. With both the electron and ion sources cold, the base pressure in the chamber is approximately 2 x 10^{-9} torr.

Ion Source

The singly charged rubidium ions required in this experiment are thermionically generated in an aluminosilicate-molybdenum plug rigidly mounted behind a Pierce-type electrostatic gun. This combination produces an intense, highly collimated beam of Rb^+ ions in the ionic ground state which is subsequently shaped into the desired geometry by additional collimation, deflection and electrostatic focusing.

Ion Emitter Assembly

Several previous investigators have observed that the alkali aluminosilicates are the most copious thermionic-type ion emitters.[56] Such aluminosilicate materials may be produced by melting together stochiometric quantities of the carbonate of the desired ion with aluminum oxide and silicon dioxide. For the particular cases of rubidium emitters, the presumed reaction may be written as follows.[56]

$$Rb_2CO_3 + Al_2O_3 + 4SiO_2 \longrightarrow Rb_2O \cdot Al_2O_3 \cdot 4SiO_2 + CO_2\uparrow \qquad (8)$$

After firing at 1400°C in an alumina container, the resulting aluminosilicate is removed from the crucible and ground with a mortar and pestle until it will pass through a 200 mesh sieve. The composite is then mixed with molybdenum powder and pressed at 2000 psi into pellets 1/8 inch thick and 3/8 inches in diameter. Experience with this type of geometry has demonstrated the advisability of introducing an aluminosilicate concentration gradient throughout the thickness of the pellet. The optimal profile has about a 50 per cent by weight concentration of aluminosilicate on the surface and terminates in a base of 100 per cent molybdenum powder. The pellets are then sintered for 14 hours in a hydrogen-nitrogen atmosphere at 1400°C. Next, the electron impregnant is dissolved out of a 3/8 inch Semicon Associates dispenser cathode and the end of the cathode heater assembly is ground flat on a 180 grit silicon carbide lapping wheel. Finally, the emitter disc is molybdenum-nickel brazed onto the top of the modified dispenser cathode heater in a hydrogen-nitrogen atmosphere using a radio frequency induction furnace. A photograph of the completed ion emitter assembly appears in Figure 6.

Mass spectrographic analyses have been performed to evaluate the specific ion emission from such aluminosilicate sources. Upon initial heating to 1100°C, it was found that a substantial fraction of the emitted current consists of K^+ and Na^+ ions. However, after about one hour of operation the rubidium ions constitute more than 99.9 per cent of the total emission. The high purity of this emitted beam thus obviated the necessity of including mass analysis within

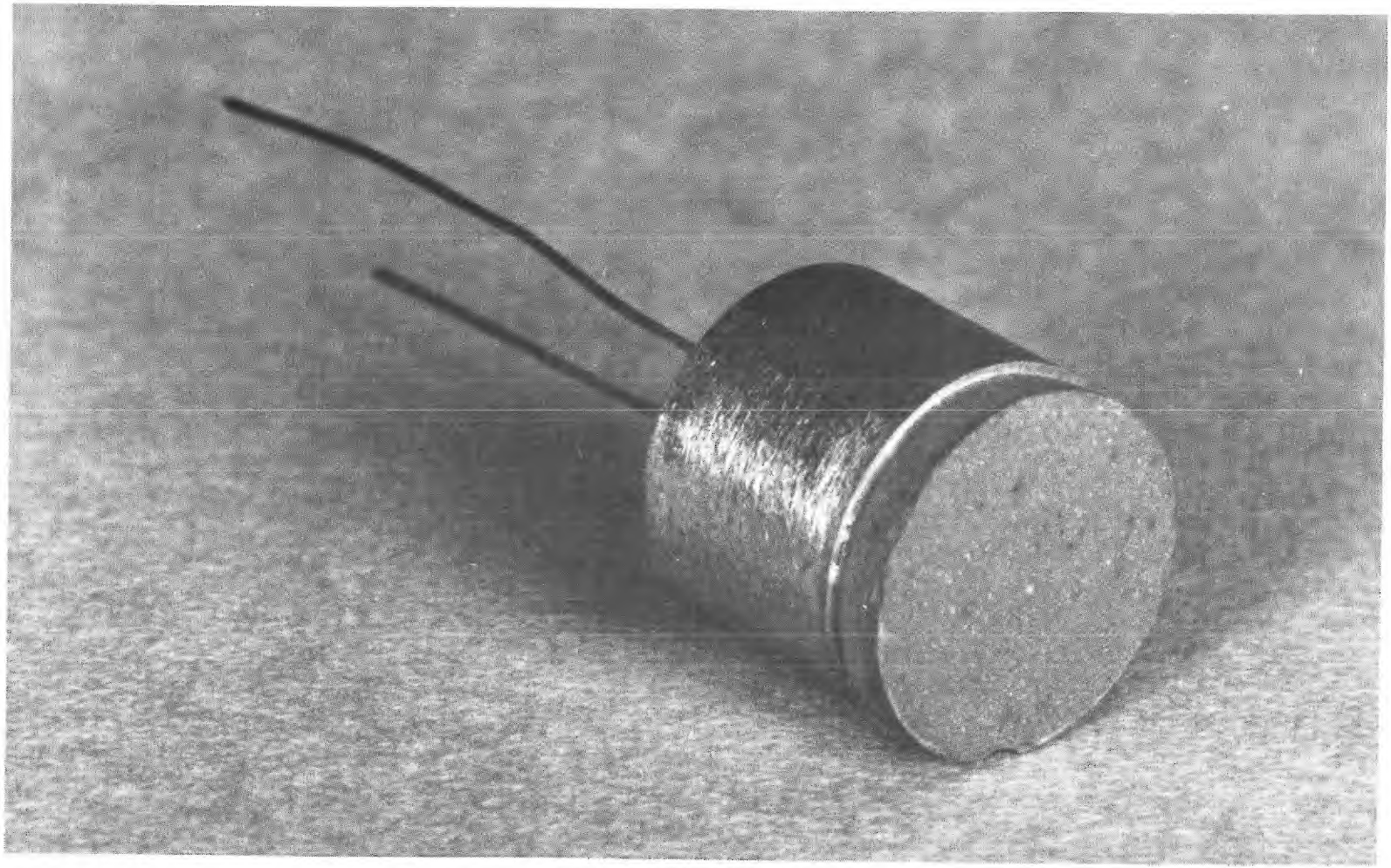

Figure 6. Photograph of the Completed Ion Emitter Assembly.

the experimental apparatus.

Ion Gun and Ion Beam Transport System

The ion gun employed in the present research consists of an aluminosilicate-molybdenum emitter assembly rigidly mounted behind a Pierce-type electrostatic focusing structure. The shape of the equipotential electrodes required for such a gun was obtained by J. R. Pierce in 1949 using an electrolytic tank.[57] Stainless steel electrodes displaying the desired geometry have been constructed by approximating Pierce's results with a combination of polynomial equations. These mathematical relations subsequently provided the input to a numerically-controlled milling machine which generated aluminum templates for the front and rear surfaces of each of the five Pierce elements. Next, a curve-following lathe was used to machine a set of stainless steel electrodes mimicking the geometry of the templates. Finally, telescoping alumina spacers and rods were employed to hold the completed Pierce elements in proper alignment. A photograph of the assembled Pierce gun appears in Figure 7.

Three additional focusing, steering and collimation structures have been cascaded with the Pierce gun to further define the geometry of the ion beam. These assemblies are designated in Figure 1 as the F_1, F_2 and F_3 stages respectively, and are employed to manipulate an appropriately shaped beam of ionic targets into the interaction region. Immediately upon exiting the final Pierce electrode, the ionic particles comprise a uniformly distributed, cylindrical beam 3/8 inches in diameter. During transit through the F_1 unit, the ions are

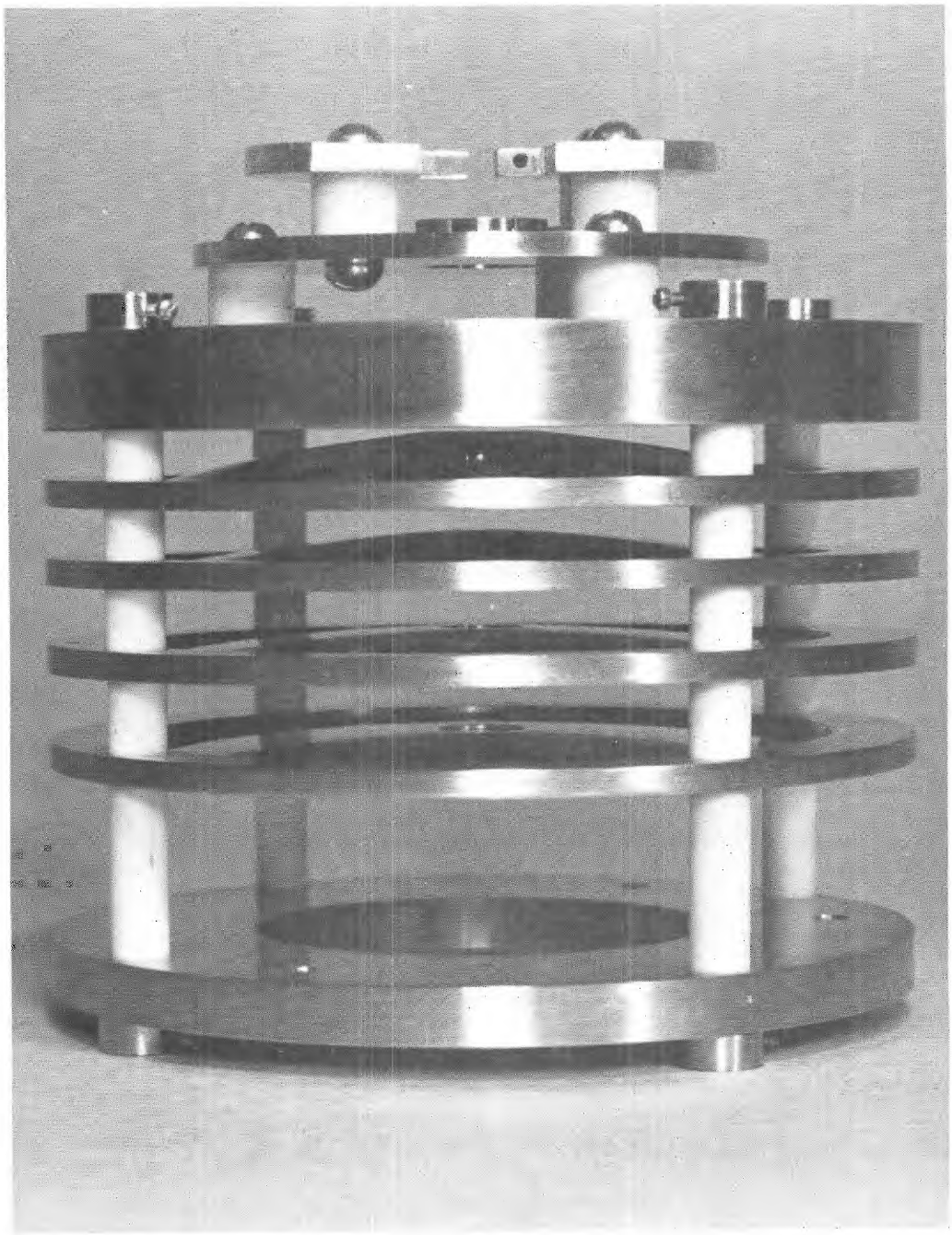

Figure 7. Photograph of the Pierce-Type Ion Gun.

collimated into a 1/2 inch by 0.050 inch rectangular beam and directed towards the F_2 region where they receive additional collimation and focusing. Just prior to entering the collision volume this primary beam is deflected through a slight angle by the F_3 stage in order to remove any neutral particles or ions which have become multiply charged as a result of stripping on slit edges or residual gas molecules. The total transit distance from the ion emitter assembly to the collision volume is approximately 30 inches. Calculations of beam divergence along this path length suggest that space charge expansion effects are negligible and measurements of beam size at numerous locations confirms this suspicion. This cascaded combination of focusing, deflection and collimation assemblies provides the crossed beam experiment with much diagnostic flexibility. For example, it is possible to make changes in the ion beam shape and location relative to the electron beam, so that the form factor can be systematically varied while all other experimental parameters are kept constant. A set of typical ion and electron beam current density distributions is presented in Figure 8.

In operation, the acceleration, focusing and deflection potentials are derived from a set of electronically regulated power supplies. The ion energy is determined by a John Fluke model 413C power supply and gaseous regulator tubes are employed to obtain the dual polarity outputs required for the deflection assemblies. The desired polarity for a given deflection plate is switch selected and its voltage is set by means of a 10-turn potentiometer. The deflectors

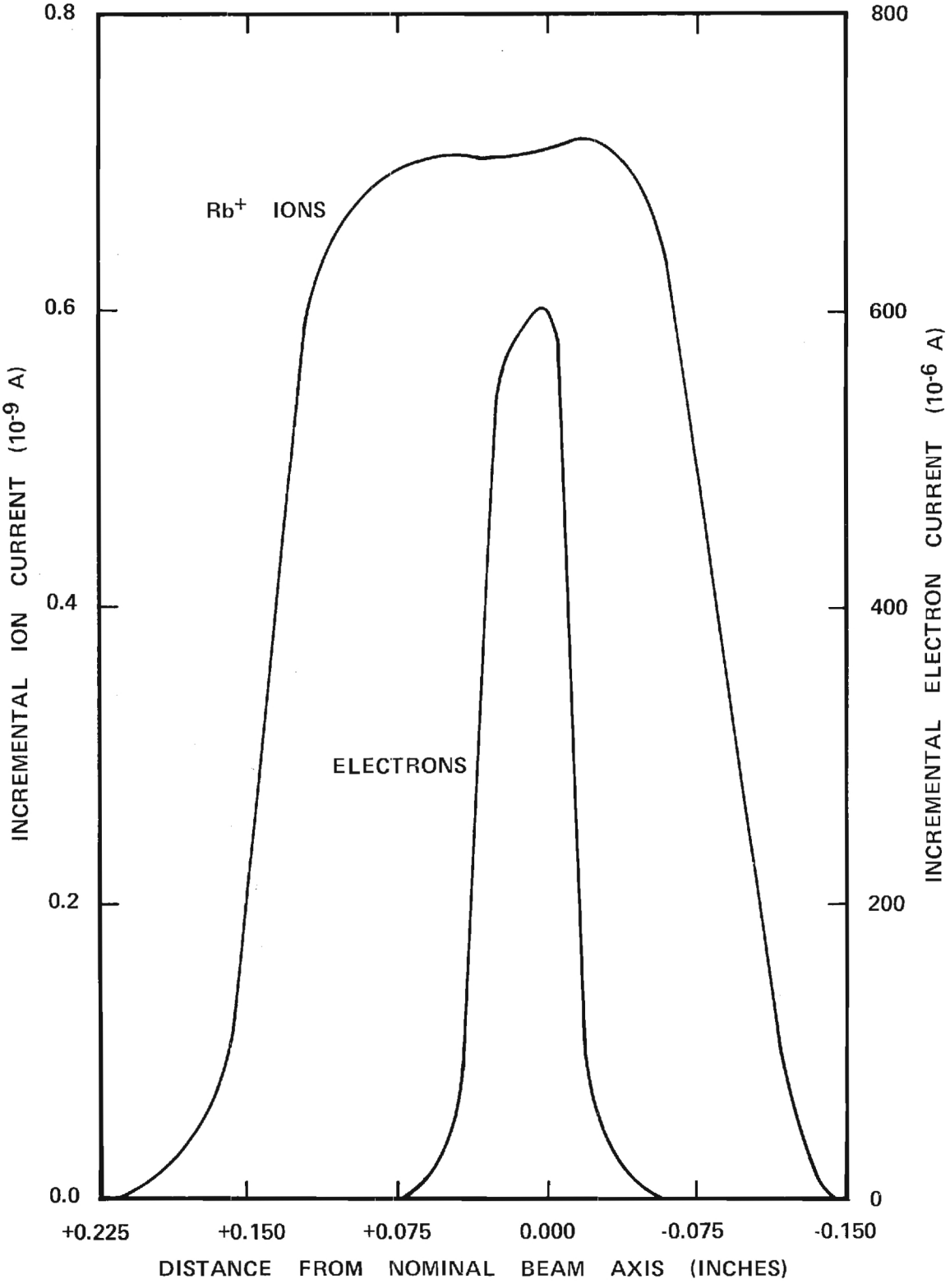

Figure 8. Typical Beam Current Density Distributions.

are then floated at arbitrary focus potentials which are generated by a set of Lambda Electronics Corporation model 50 power supplies. The output current density obtainable directly at the ion emitter assembly is typically 2-5 mA/cm^2. After collimation into a beam 1/4 inch high and 0.050 inches wide, currents of 60-150 nanoamperes can be transported to the interaction region. This thermionic ion source has provided a collimated beam current of greater than 30 nanoamperes for a continuous operating period of one month.

Electron Source

The electron source selected for the present research is a 6L6GC beam power tetrode modified for inclusion in the ionization experiment. First, the tube basing and the glass envelope are removed and the plate structure is cut back to expose the cathode and grids. Next, the remaining plate support strut is slotted into a mounting bracket and the entire assembly is properly positioned with respect to the ion beam.

It was found that arcing between the screen grid and the cathode for energies above approximately 1000 eV precluded the use of a single electron source configuration over the entire range of electron energies. For energies below this value, the metallic mounting bracket and screen grid may both be connected to experimental ground without any fear of electrical breakdown. In order to maintain electrical integrity for higher energies however, it was found advisable to isolate the tube mounting bracket on a set of 3/16 inch ceramic insulators and bias the bracket assembly and screen grid at no more than 700

volts above cathode potential. Additionally, for the higher energies, the cathode is typically canted a few degrees from its nominal horizontal position in order to maintain usable form factors. In practice, there is a range of energies from about 700 eV to 1500 eV where either assembly configuration can be used and measurements in this region serve as a useful transfer check on the performance of the electron source.

A typical electron beam energy distribution is shown in Figure 9. This determination was made by Bacon on a representative 6L6GC vacuum tube essentially identical to those used in the present series of measurements.[58] Note that the full width at half the maximum intensity is about 1.1 eV and observe that the mean electron energy is nearly two electron volts below that set on the electron acceleration power supply. Retarding potential measurements at several additional electron energies and verification of the theoretical thresholds for the onset of ionization in the present experiment appears to confirm the above electron energy distribution.

In operation, the electrons are accelerated from the negative cathode to experimental ground potential. The screen grid is normally operated at no more than 700 volts above cathode potential and the control grid is employed to adjust the electron beam intensity. The electron acceleration voltage is supplied by a John Fluke model 410B power supply and the control grid voltage is obtained from a 10-turn potentiometer connected across a gaseous regulator tube. The line voltage for these power supplies is stabilized with a Sola 2 kVA

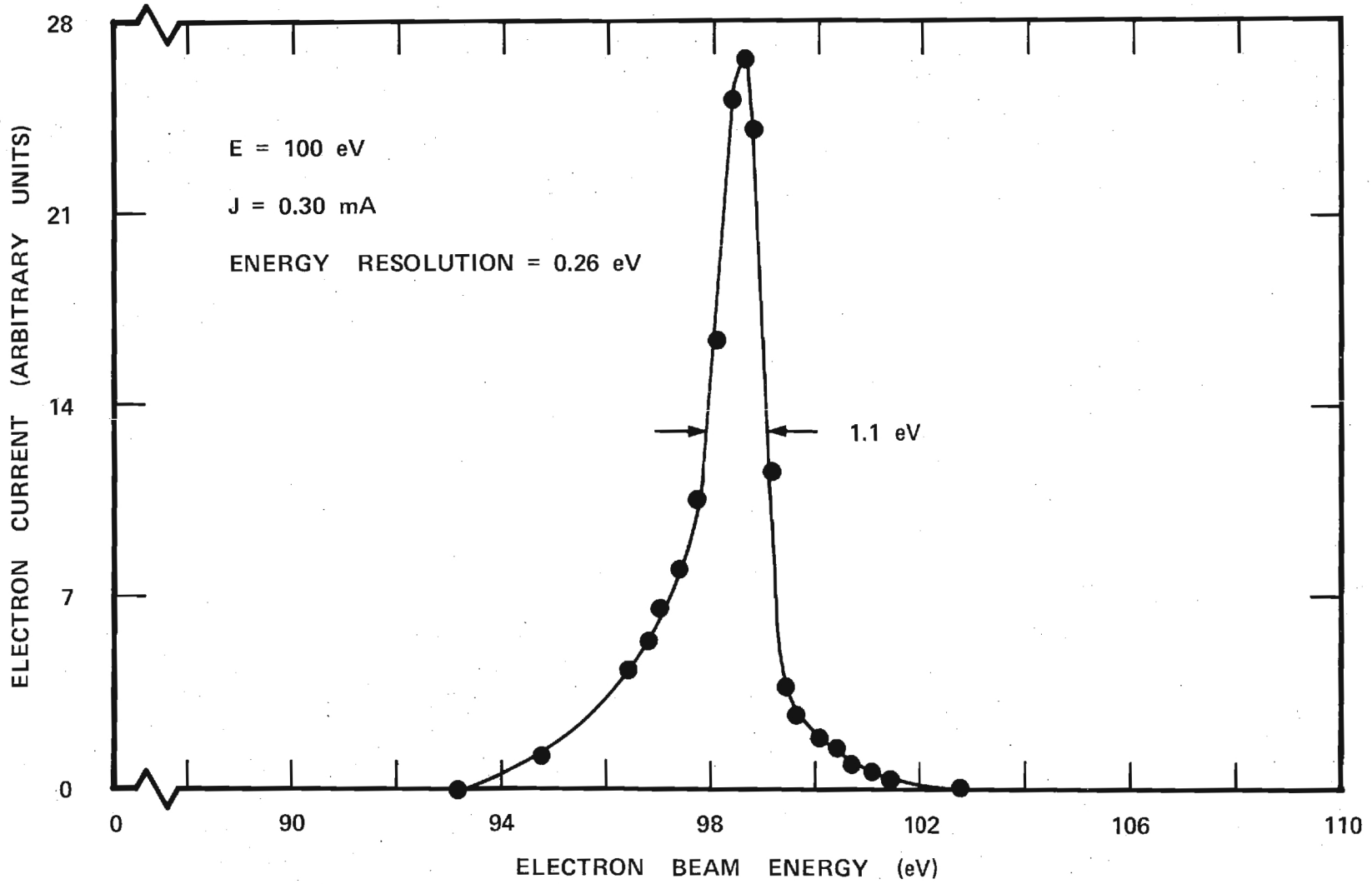

Figure 9. Typical Electron Beam Energy Distribution.

constant voltage transformer. Operating experience has demonstrated that this electron source can provide up to 1 milliampere of current at 150 eV and more than 10 milliamperes at 1500 eV.

Interaction Region

The interaction region is designed to provide a field-free volume for the intersection of the incident electrons and the target ions. This collision volume is spatially defined on two sides by the exit ports of both the ion and electron beam transport systems. The remaining surfaces are enclosed by stainless steel shields terminating near the entrance aperture of the primary analyzer. A photograph of the interaction region as seen from the location normally occupied by the electron beam Faraday cup appears in Figure 10.

Just prior to entering this interaction region, the two beams can be made to pass through a movable slit scanner which determines their respective current density profiles as shown in Figure 4. This scanner contains a set of 0.015 inch wide slits and is connected through the experimental chamber by means of vacuum feedthrough bellows. These bellows are driven by an external stepping motor coupled to the feedthrough with a gear train assembly. Inputs to the stepping motor are generated by a preset counter whose output is commensurate with the slit dimension on the scanner plate. The movable scanner position is remotely indicated on a four digit, seven segment display controlled by a 15-turn potentiometer.

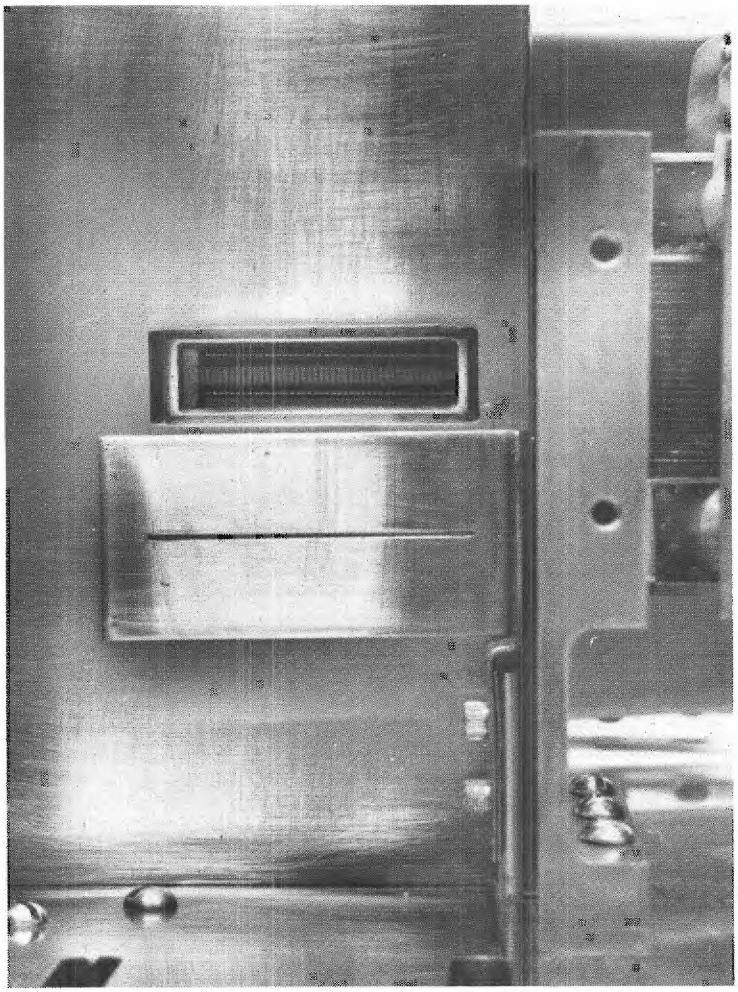

Figure 10. Photograph of the Interaction Region as Seen from the Location Normally Occupied by the Electron Beam Faraday Cup.

Charged Particle Analyzers

After undergoing collision with the electrons, the ion beam is generally composed of a number of equally energetic charge state components. In order to determine the desired cross sections from the various experimental parameters it is necessary to accurately measure the respective magnitudes of each of these currents. Unfortunately, the multiply charged signal is frequently eight orders of magnitude smaller than the singly charged beam current. This huge intensity difference between the primary and signal components necessitates complete discrimination of the requisite beams.

In the present experiment, the required charge state separation is accomplished by means of cascaded, parallel plate electrostatic analyzers as shown in Figure 1. Immediately upon passage through the collision volume, the reacted ion beam enters the primary analyzer at an angle of 45 degrees with respect to the electrostatic plates. The singly and multiply charged ionic species are separated by the electric field in the analyzer and traverse to their respective exit apertures. Subsequently, the multiply charged beam experiences additional isolation in the secondary analyzer and is finally incident upon the signal ion cup. Note that when the Rb^{+} beam is deflected into the 1^{+} Faraday cup, the Rb^{3+} ion beam is incident upon the N^{+} cup. Similarly, by simply scaling the analyzer potentials, it is possible to monitor either the Rb^{4+} or Rb^{5+} current in the N^{+} cup while the Rb^{+} beam is simultaneously being deflected into the auxiliary cup.

The primary electrostatic analyzer consists of a back plate biased at 2/N times the ion acceleration voltage and three guard plates

each held at the local equipotential. These stainless steel plates are separated by 0.500 inches and the entire assembly is enclosed in a shielded housing. Similarly, the secondary analyzer is composed of a back plate biased at 1/N times the ion acceleration voltage and two electrostatic guard plates. The adjacent stainless steel plates are each separated by 0.375 inches and the entire assembly resides in a shielded structure appended to the primary analyzer. Plate dimensions and aperture sizes have been selected so that field fringing effects are essentially absent in the region adjacent to the nominal ion trajectories.

Performance tests have demonstrated that both analyzers enjoy a broad plateau of operating voltage over which each component of the ion beam suffers negligible attenuation in traversing the cascaded analyzer assembly. Furthermore, illegitimate multiply charged ions born as a result of stripping on slit edges or background gas molecules rarely have the required velocity vector to traverse both the primary and secondary energy analyzers. Thus, it appears that the dual analyzer configuration represents a substantial improvement over the single stage analyzers used on earlier crossed beam experiments and it is likely that the present measurements would have been impossible without the enhanced noise rejection capability of the cascaded assembly.

Ion Collection and Measurement System

Careful monitoring of both the primary and signal beam currents is required if the crossed beam apparatus is to yield meaningful ionization data. The intensity of the primary beam current is selected

by the experimenter and is usually adjusted to be several tens of nanoamperes. The signal current however, is largely determined by the magnitude of the multiple ionization cross section and is frequently as small as 10^{-16} amperes. As a result of this huge intensity difference in the magnitudes of the primary and signal currents, widely differing techniques are required for the measurement of these two ion beam components.

Primary Ion Beam Collection and Measurement System

Two individual Faraday cups are employed in the present experiment to monitor the magnitude of the Rb^+ ion beam current. When, for instance, the analyzer voltages are adjusted to perform double ionization measurements, the resulting electrostatic potentials deflect the Rb^+ beam into the primary ion cup. This Faraday cup is geometrically deep and is constructed to maximize the retention of secondary electrons. In addition, a pair of sweep plates oriented parallel to the plane of the experiment plate enhance the secondary suppression characteristics of this cup. During normal operation, a sweep field of approximately 40 volts per centimeter is generated by these plates, although it has been demonstrated that the primary cup is essentially 100 per cent efficient even in the absence of this suppression potential.

Alternatively, if a triple or quadruple ionization event is under scrutiny, the resulting analyzer potentials cause the Rb^+ beam to be incident upon the auxiliary ion cup. Unfortunately, space constraints within the vacuum enclosure prevent the auxiliary cup from

having optimal geometry and hence, some internal sweep field is required for adequate suppression. Normally, an electrostatic field of approximately 60 volts per centimeter is applied and extensive testing has confirmed that the resulting assembly displays a suppression coefficient essentially equal to unity.

Regardless of which Rb^+ cup is in use, the primary ion beam current is monitored with a Keithley model 610CR electrometer driving a Tektronix model DM-501 digital voltmeter. This measurement and display instrumentation is frequently calibrated and it is estimated that the resulting accuracy of the Rb^+ current determination is better than ±2 per cent.

Signal Ion Beam Collection and Measurement System

The signal detector consists of a well shielded, Faraday cup assembly located adjacent to the exit aperture of the secondary analyzer. This stainless steel cup is geometrically deep and is designed to minimize the escape of secondary electrons. Additional electron suppression is provided by means of a negatively biased ion tunnel containing a pair of permanent magnets. This tunnel is located slightly in front of the signal cup but is shielded from the detector assembly by means of a grounded stainless steel aperture. The entire suppression structure is typically biased 150 volts negatively with respect to experimental ground and the resulting combination of magnetostatic and electrostatic fields effectively confines secondary electrons to the signal cup.

The ion tunnel also tends to isolate the N^+ cup from the signal degrading, background electrons. These slow electrons presumably originate from the electron gas permeating the vacuum enclosure when the electron source is operating. Further reduction of this electron background is achieved by carefully locating a permanent magnet external to the vacuum chamber. The resulting magnetic field is oriented perpendicular to the transport axis of the signal cup and hence, serves as a barrier to incident electrons. Properly located, this magnet produces a negligible field in the vicinity of either the electron beam or the interaction region. In addition, frequent checks are performed to demonstrate the invariance of the measured cross sections to both the orientation and proximity of this external magnet.

Although the multiply charged ion cup is completely isolated from stray charged particles, it is still possible for polarization currents generated by electrically charged insulators to couple into the N^+ Faraday cup. As a result, it is necessary to electrostatically shield all such insulators from the signal detection structure. Additional precautions include the use of sapphire pillars in the N^+ ion collection assembly and a coaxial shield for the vibration damped signal lead.

Finally, it should be noted that the Lorentz force acting on the multiply charged product ions is often considerable and extreme care must be exercised to ensure that the apertures in the beam transport system are adequately dimensioned to accommodate such perturbations. These apertures have considerable impact on the signal cup collection efficiency and several procedures have been developed to

evaluate this important parameter. The first technique involves a scaling of the electrostatic analyzer potentials in order to sequentially direct the Rb^+ beam into each of the three ion cups. Subsequent measurements of the primary beam intensity generally display no discernable difference in the currents indicated at each of the individual collection assemblies. This result, coupled with the invariance of the measured current with respect to changes in the ion tunnel suppressor potential, suggests that the N^+ cup collects the Rb^+ beam with an efficiency equal to unity. It is possible however, that the collection efficiency of the signal cup might be a function of the charge state of the incident particles. Accordingly, selected ionization cross sections at fixed electron energies have been measured as a function of the electrostatic analyzer potentials. There exists a moderate plateau of analyzer voltages and, hence, multiply charged beam collection geometries, over which the measured cross sections are constant. These observations lead to the conclusion that the multiply charged signal collection system is essentially 100 per cent efficient.

Multiply charged ion current collected by the signal cup is measured with a Cary model 401 vibrating reed electrometer operating in the rate-of-charge mode. The preamplifier for this unit mounts directly above the signal cup vacuum feedthrough and remains in thermal proximity to the remainder of the experimental enclosure. The output of the vibrating reed electrometer drives a 10 inch Honeywell electronik model 51 potentiometric chart recorder having an accuracy of ±0.25 per cent.

In the rate-of-charge mode, the electrometer indicates the instantaneous voltage developed across a precision capacitor by the unknown beam current. If both the capacitance and the beam current are constants, then

$$I = \frac{\Delta Q}{\Delta t} = \frac{\Delta V}{\Delta t} \cdot C \qquad (9)$$

where C is the value of the capacitor being charged by the unknown beam current I, and Δt is the time interval over which the voltage across the capacitor changes by ΔV volts.

The accuracy of the rate-of-charge method depends upon the accuracy with which both the time derivative of the voltage and the value of the input capacitor are known. Independent measurements of the precision capacitance used in the present experiment yield a value of 2.0167×10^{-11} farads. The accuracy with which the time derivative of the voltage can be determined from the resulting chart recorder output is typically about ±3 per cent. Therefore the overall error in the measurement of the multiply charged signal component is conservatively estimated to be ±5 per cent.

Electron Collection and Measurement System

A stainless steel Faraday cup located just beyond the interaction region is employed to monitor the magnitude of the electron current incident upon the target ions. This cup is geometrically deep and contains an internal suppressor plate to enhance the retention of secondary electrons. During normal operation, a sweep field of

approximately 15 volts per centimeter is generally applied although it has been demonstrated that the cup is essentially 100 per cent efficient even in the absence of this suppression potential.

The electron cup is electrostatically shielded from the interaction region by a stainless steel aperture plate located immediately beyond the collision volume. This shield can also be used to monitor the divergence of the electron beam in addition to serving as a diagnostic detector for scattered electrons. During data collection, the current to the aperture plate is always less than one per cent of the total current comprising the electron beam.

The magnitude of the electron beam current is determined by measuring the beam-induced voltage drop across a 1000 ohm, 0.1 per cent resistor. A Tektronix model DM-501 high impedance digital voltmeter is normally employed in this determination. The resulting estimated error in the measurement of the current incident upon the electron Faraday cup is taken to be ±1 per cent. Unfortunately, some of the incident current is the result of background electron gas which inflates the apparent electron beam current without making a legitimate contribution to the ionization signal. As a result, it is necessary that the electron current measurement circuit incorporate a small retarding potential which can be applied in series with the Faraday cup. This allows the determination of a parameter called the "slow electron correction" which is subsequently employed to adjust the value of the indicated electron beam current. The magnitude of the slow electron correction (SEC) is given by

$$SEC = \frac{J}{J'} \tag{10}$$

where J is the electron current measured in the absence of the retarding voltage and J' is the result indicated after sufficient bias has been applied to saturate the change in the electron current. In the present experiment, the required retarding potential is approximately nine volts and the resulting SEC is typically 1.01. Finally, the slow electron correction is introduced into Equation (5) to yield the following expression for the desired electron impact ionization cross section in terms of experimentally observable parameters.

$$\sigma_{1N} = \frac{e\, v_i}{N} \cdot \frac{I^{N+}_{SIG}\ (I,J)}{I \quad J} \cdot F \cdot SEC \tag{11}$$

Modes of Operation

In any experimental determination it is necessary that legitimate signal resulting from the process under study be discriminated from spurious signal produced by noisy backgrounds. These backgrounds frequently introduce systematic errors which can invalidate an otherwise well-executed measurement. In the present experiment, for instance, it is possible that the Rb^+ target beam may interact with the residual gas in the system and hence, give rise to charge stripped ions. These multiply charged particles might then result in spurious double, triple or quadruple ionization signal. Realistically, such undesirable multiple stripping processes are expected to have very small cross sections over the range of parameters applicable to the present measurement.

Furthermore, after such a collision with the background gas, it is doubtful that the resulting multiply charged ion has the required velocity vector to traverse both the primary and secondary electrostatic energy analyzers. Nevertheless, it is not appropriate to ignore even these potentially small backgrounds and both direct current (DC) and pulsed beam procedures have been developed to assess their effects.

DC Mode of Operation

The DC technique involves operating both the electron and Rb^+ beams in a continuous mode while systematically measuring the individual backgrounds associated with each of these parent beams. In this manner the contribution of the various background components to the measured signal frequently may be characterized and subsequently eliminated. Implicit in such a procedure is the assumption that the vacuum chamber pressure, and hence the magnitude of the charge stripped component, is unaffected by the presence of absence of the electron beam. It is therefore necessary to experimentally verify that electron beam modulation of the charge stripped background makes an insignificant contribution to the computation of the net electron impact ionization current. In the present determination, it has generally been possible to operate the experiment at a sufficiently high vacuum that the error introduced by pressure modulation is negligible. As a result, the larger average currents produced by DC operation frequently facilitated measurement of the desired cross sections in energy regimes where little ionization signal could be generated.

Pulsed Mode of Operation

As an independent check on the DC measurements, the electron and ion beams can be pulsed in either time coincidence or time anti-coincidence to assess the effects of background on the experimentally determined cross sections. This particular pulsing method is motivated by the desire to establish a constant average pressure in the region surrounding the experiment. If the beams are pulsed at a rate several times faster than the characteristic frequency of the vacuum system, then a steady-state pressure is maintained throughout the evacuated chamber.[53] Under these conditions, pulsing the beams in time coincidence yields the algebraic sum of the electron impact ionization signal and the various backgrounds. In contrast, the time anti-coincidence mode of operation gives rise to only the background components. Simple subtraction then allows the unambiguous determination of the desired electron impact ionization signal.

In the present experiment, pulses of arbitrary frequency are generated by integrated circuit logic and subsequently increased in magnitude using transistor pulse amplifiers. The duty cycle of the electron beam pulse is derived from a flip-flop and is, hence, precisely equal to 50 per cent. The duty cycle of the ion beam pulse is adjustable from 0 to 50 per cent and its phase delay can be varied with respect to the electron pulse. The system is changed from time coincidence to time anti-coincidence by switching the output digital state connection of the electron pulser flip-flop. The resulting electron beam pulse is applied by means of a clamping circuit to the control grid of the electron source while the ionic circuitry simply pulses

the extractor of the Pierce gun.

A number of investigations have been performed to evaluate the experimental integrity of this beam pulsing procedure. Selected cross sections measured at fixed electron energies have been shown to be constant over a significant range of pulse frequencies. Similarly, the indicated cross sections are independent of moderate changes in the ion beam duty cycle. Some representative driving pulses and their resulting beam waveforms appear in Figure 11. Note that the beam rise and fall times are such that the ion pulse is always completely contained within the electron pulse. Normally, the pulse frequency is set at 100 hertz and the ion and electron beam duty cycles are typically 42.5 and 50 per cent respectively. Approximately one half of the present experimental data were taken using the pulsed mode of operation.

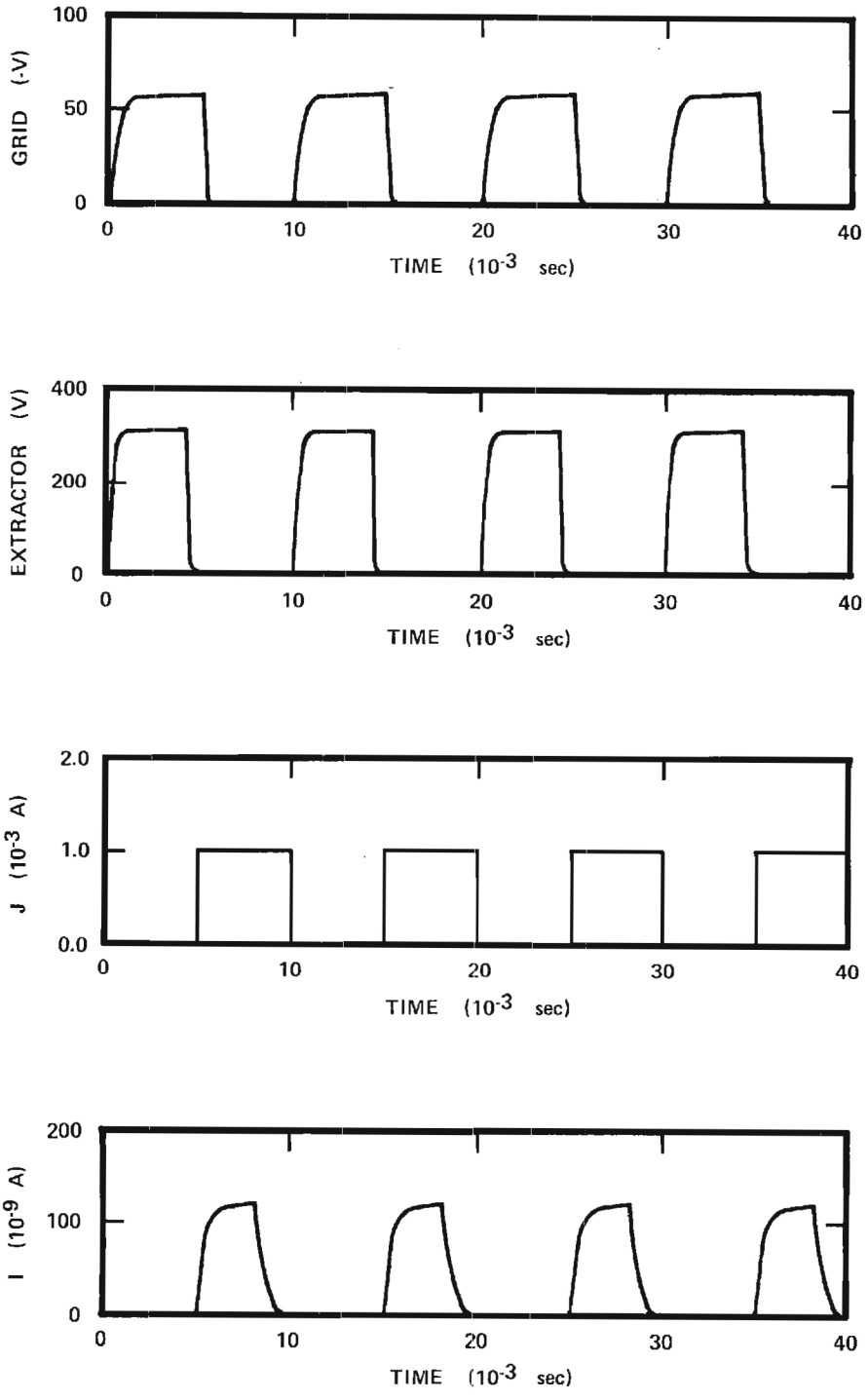

Figure 11. Typical Driving Pulses and their Resulting Beam Waveforms.

CHAPTER IV

EXPERIMENTAL PROCEDURES AND RESULTS

Introduction

The objective of the present research is a measurement of the absolute cross sections for the double, triple and quadruple ionization of Rb^+ ions by electron impact using the experimental apparatus described in Chapter III. In order to properly determine the desired cross sections it is necessary that all of the parameters in Equation (11) be unambiguously evaluated for a comprehensive set of collision conditions. This chapter describes the experimental procedures employed to accomplish this objective and presents the results for the multiple ionization of the singly charged rubidium targets. Adjacent sections in the text discuss these results in light of the consistency criteria enumerated earlier and evaluate the probable uncertainty in the resulting cross sections.

Measurement Procedures

Before a cross section measurement can be initiated, a number of preliminary adjustments must be made to the experimental apparatus. These adjustments prepare the equipment for data acquisition and serve to define the interaction parameters appropriate to the particular collision event under scrutiny. Subsequent adherence to proper experimental procedures then helps to ensure that the measured results will closely approximate the actual ionization cross sections.

Preliminary Adjustments

Upon termination of the vacuum chamber bakeout it is necessary to wait approximately 24 hours for the collision apparatus and the associated electronics to attain thermal equilibrium. During this period, the indicated background current produced by thermal gradients, contact potentials and stressed insulators decays to a nominally small value. Once this background has stabilized, a number of preliminary adjustments are made to prepare the apparatus for data acquisition. A synopsis of these adjustments, along with a discussion of their significance, is presented below.

First, the stray electron current to the N^+ detector is minimized by carefully positioning a small, permanent magnet near the periphery of the vacuum vessel. During this adjustment, it is advantageous to run at least a milliampere of electron current at the highest energy for which collision data is desired. Subsequent minimization of the stray electron current at this elevated energy then ensures a negligible electron background at lesser energies. Occasionally however, it is found that the electron background is prohibitively large for all orientations of the external magnet. This difficulty is usually symptomatic of a poorly activated cathode and typically necessitates disassembly of the apparatus with subsequent replacement of the electron source. In any event, it is imperative that the flux lines from this magnet remain confined to the region immediately surrounding the N^+ ion detector. As a result, frequent measurements with a variety of external magnet configurations are generally required to demonstrate

the invariance of the indicated cross sections to both the presence and the orientation of this magnet.

After an adequately small electron background has been attained, the driving voltages for the ion beam transport structures are optimized. Normally, this involves the selection of a set of potentials which centers both the singly and multiply charged rubidium ion beams on their respective detector apertures.

Thirdly, the Rb^+ ion beam is focused so as to minimize particle losses from the parent and product beams. During this phase of the procedure, the Rb^+ beam is sequentially deflected into the various ion cups by simply scaling the analyzer voltages. Comparison of the indicated beam currents in each of these detector cups then permits the final selection of the ion source focusing potentials.

Finally, the vertical profile of the Rb^+ ion beam is adjusted to yield a satisfactory form factor commensurate with an adequately small, beam transport loss. Fortunately, it is generally possible to adjust the apparatus to yield an arbitrarily small, particle beam loss for a reasonably comprehensive set of intersection geometries.

It should be noted that many of these adjustments are interrelated and some iteration is normally required for their mutual satisfaction. Under certain circumstances however, it may be impossible to satisfy all of these requirements simultaneously. For example, unusual focusing conditions occasionally preclude the generation of a satisfactory form factor without introducing unacceptable losses from the ion beam. This difficulty typically indicates a poorly activated

or improperly positioned cathode and hence, necessitates disassembly of the apparatus with subsequent replacement of the electron source.

In general, these preliminary adjustments are repeated before the performance of each individual cross section measurement. It has been observed however, that the external magnet need be relocated only when changing the order of the ionization process presently under study.

Determination of the Electron Impact Ionization Signal

The total current indicated at the N^+ ion detector includes, in general, a multiplicity of background components superimposed on the desired electron impact ionization signal. Both DC and pulsed beam procedures have been employed in the present research to assess the effects of these backgrounds and hence, extract the legitimate ionization component from the various currents measured at the N^+ detector.

DC Procedure. The DC technique involves operating both the electron and Rb^+ beams in a continuous mode while systematically measuring the individual backgrounds associated with each of these parent beams. If the experiment is free from the troublesome focusing effects discussed earlier, then the electron impact ionization signal can be extracted from the various beam current components. The following definitions will be employed to simplify the subsequent discussion.

(1) $I^{N+}(I,J)$ is the total current measured at the N^+ detector when an Rb^+ beam of I amperes and an electron beam of J amperes are simultaneously present in the interaction region.

(2) $I^{N+}(I,O)$ is the current measured at the N^+ detector with

only an Rb^+ beam of I amperes present.

(3) I^{N+} (O,J) is the current measured at the N^+ detector with only an electron beam of J amperes present.

(4) I^{N+} (O,O) is the current measured at the N^+ detector with neither of the parent beams present.

(5) I^{N+}_{SIG} (I,J) is the electron impact ionization current produced when an Rb^+ beam of I amperes and an electron beam of J amperes are simultaneously present in the interaction region.

Note that the desired I^{N+}_{SIG} (I,J) signal is not directly observable at the N^+ detector because it is only one of several components comprising the I^{N+} (I,J) current. However, under certain conditions, it is possible to extract this electron impact ionization signal by noting that the indicated I^{N+} (I,J) current is the algebraic sum of the following components.

(1) The legitimate electron impact ionization signal, I^{N+}_{SIG} (I,J).

(2) A background noise component, I^{N+} (O,O), whose magnitude is assumed to be independent of the presence or absence of the parent beams.

(3) An ion beam noise component, $[I^{N+}(I,O) - I^{N+}(O,O)]$, whose magnitude is assumed to be independent of the presence or absence of the electron beam.

(4) An electron beam noise component, $[I^{N+}(O,J) - I^{N+}(O,O)]$, whose magnitude is assumed to be independent of the presence or absence of the ion beam.

Then, by summing the above components, it is possible to obtain an expression for the indicated, $I^{N+}(I,J)$ current as shown in Equation (12).

$$I^{N+}(I,J) = I^{N+}_{SIG}(I,J) + I^{N+}(O,O) + [I^{N+}(I,O) - I^{N+}(O,O)] + [I^{N+}(O,J) - I^{N+}(O,O)] \quad (12)$$

This relation, upon simplification, yields the following equation for the desired electron impact ionization signal in terms of the currents observable at the N^+ ion detector.

$$I^{N+}_{SIG}(I,J) = [I^{N+}(I,J) - I^{N+}(I,O)] - [I^{N+}(O,J) - I^{N+}(O,O)] \quad (13)$$

Note that the assumptions inherent in the determination of the components appearing in Equation (13) are merely manifestations of the crossed beam validity criteria developed in Chapter II. Under these conditions, the experiment yields a correct result for $I^{N+}_{SIG}(I,J)$ which, when coupled with accurate knowledge of the other parameters in Equation (11), allows the subsequent determination of the desired electron impact ionization cross section.

Pulsed Procedure. An alternative technique for extracting the desired ionization signal from the noisy backgrounds involves pulsing both the electron and ion beams. In the present research, the ion beam is pulsed with a 42.5 per cent duty cycle while the electron pulse displays a 50 per cent duty cycle. The pulsing frequency of each beam is approximately 100 hertz and is sufficiently high to ensure a steady, average pressure throughout the vacuum vessel. In addition, the phase

of the electron beam pulse is adjustable with respect to that of the ion beam. This capability gives rise to both the time coincidence and time anti-coincidence modes of operation as shown in Figure 12. In the time coincidence mode, the electron beam crosses the interaction region only when the target ions are present. Therefore, the resulting I_C^{N+} current contains both the electron impact ionization signal and the background noise current components. Alternatively, in the time anti-coincidence mode, the primary ion current flows only when the electrons are absent. Thus, the I_A^{N+} current consists entirely of the various noise components. The algebraic difference between the mean current levels in these two modes of operation then gives a measure of the electron impact ionization signal. Recalling that the mean current levels are a function of the beam pulse duty cycles, the desired ionization signal is given by Equation (14).

$$I_{SIG}^{N+}(I,J) = \frac{I_C^{N+} - I_A^{N+}}{2} \tag{14}$$

Numerous such pulsed data runs have been compared with similar measurements made in the DC mode of operation. The numerical equivalence of the resulting cross sections strongly suggests that the experimental procedures employed in the present research yield a valid result for the electron impact ionization signal.

Cross Section Measurements

A mathematical relationship defining the electron impact ionization cross section in terms of experimentally observable quantities

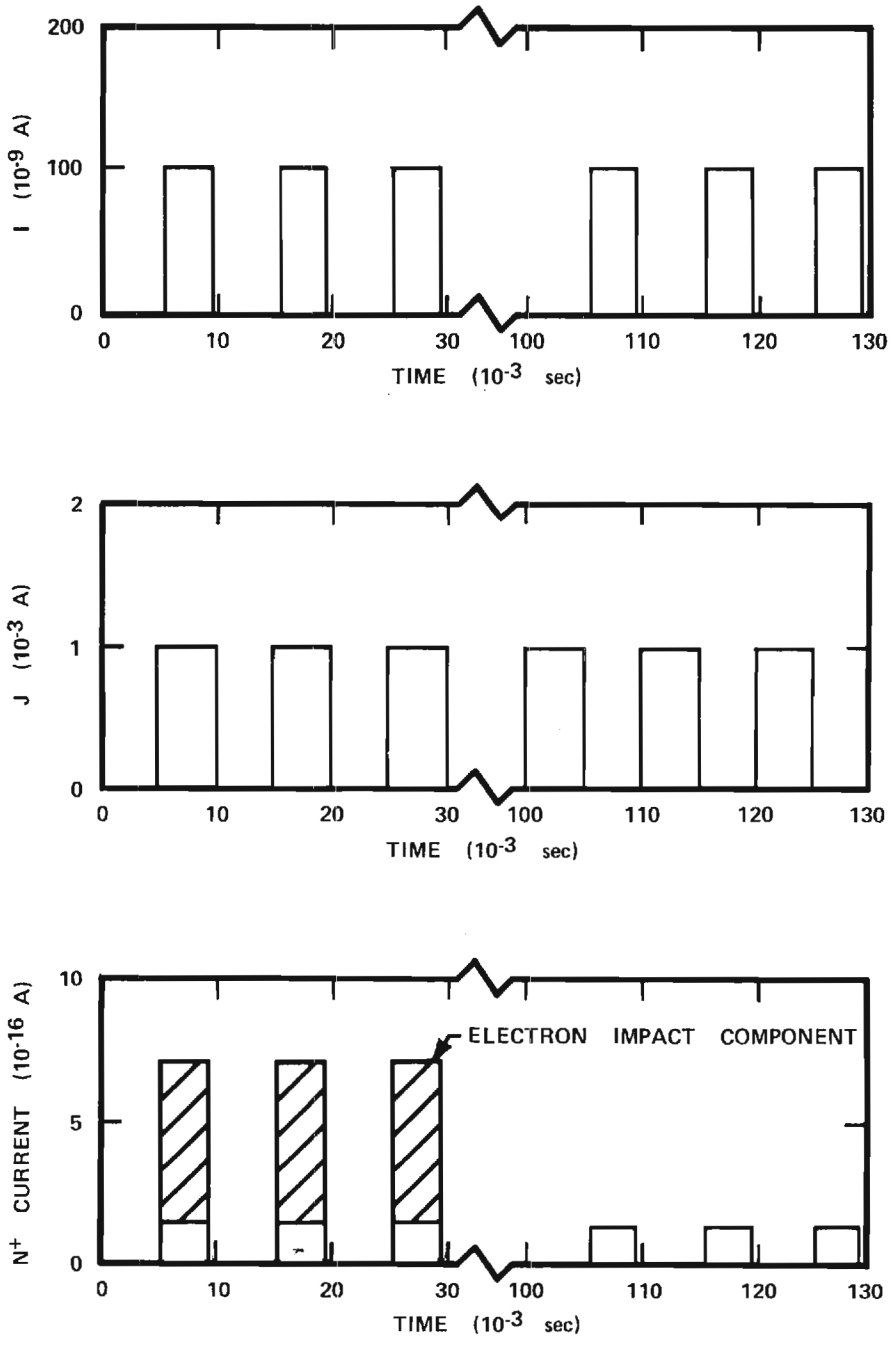

Figure 12. Idealized Beam Pulse Current Waveforms.

appears in Equation (11). It is therefore necessary to unambiguously evaluate all of the parameters entering into this expression for a large number of incident electron energies in order to comprehensively determine the desired ionization cross sections. A step-by-step procedure for obtaining a value for the cross section at a particular electron energy is summarized below.

(1) The incident electron energy, the target ion energy and the electron and ion beam intensities are selected.

(2) The preliminary adjustments discussed earlier are completed.

(3) The movable slit scanner is lowered across the parent beams to provide data for the calculation of the form factor.

(4) The slow electron correction is measured.

(5) A DC technique or a pulsed beam procedure is employed to determine the electron impact ionization signal. In either event, each of the requisite current components is measured at least three times in a random sequence. These current measurements are typically performed with the vibrating reed electrometer operating in the rate-of-charge mode. Normally, the length of time occupied by each individual determination is approximately 60 seconds. Subsequently, an average value for the ionization signal is calculated using Equation (13) for the DC mode or Equation (14) for pulsed operation.

(6) A value for the desired electron impact ionization cross section at the preselected electron energy is determined by substituting the experimentally observed quantities into Equation (11).

Representative data generated using the above procedure and example calculations of the resulting cross sections are presented in

Appendix B. Typically, the electron and ion beam intensities and beam current density distributions are randomly selected before every data run in order to demonstrate that the measured cross sections are independent of these parameters. Furthermore, several electron energies are designated as check points and are frequently remeasured under widely varying experimental conditions in order to help evaluate the consistency of the resulting data. The electron energies normally chosen as check points are two values below threshold and an energy near the peak of each of the respective cross sections. Approximately one out of every five data runs is a measurement at one of these check points. Failure for a particular measurement to yield a satisfactory result makes all data taken since the previous check suspect and these runs are subsequently eliminated from the final data compilation.

Consistency Checks

In general, consistency checks constitute a set of diagnostic tests which can help establish whether or not a particular apparatus is yielding valid experimental results. The consistency criteria appropriate to crossed beam ionization studies require that the measured cross sections depend solely upon the incident electron energy and hence, be independent of reasonable excursions in the other experimental parameters. It is important to emphasize that data for all electron energies must be conscientiously evaluated in light of these criteria. Representative plots displaying the required consistency invariance for each of the three ionization cross sections measured in the present

research are presented and discussed below. Similar graphics for all other electron energies comprehensively demonstrate an adequately broad operating plateau over which the ionization apparatus yields self-consistent results.

Dependence of the Cross Sections upon Electron Current

The dependence of the measured cross sections on electron current for the double, triple and quadruple ionization events is given in Figure 13. The variation of the cross section with electron current is well within the random scatter of the data and displays no systematic dependence upon the test variable. It is apparent from the figure that this consistency check is satisfied over an operating plateau in electron current extending from a few tens of microamperes to approximately 1.7 milliamperes. All final experimental results have thus employed a mean electron beam intensity constrained by these extreme values.

Dependence of the Cross Sections upon Ion Current

The dependence of the measured cross sections on ion current is presented in Figure 14. No systematic variation is evident over an operating plateau in ion beam intensity extending from approximately 15 to 70 nanoamperes.

Dependence of the Cross Sections upon the Form Factor

It is also required that the measured cross sections be independent of reasonable variations in the parent beam profiles. These profile changes manifest themselves in the magnitude of the form factor,

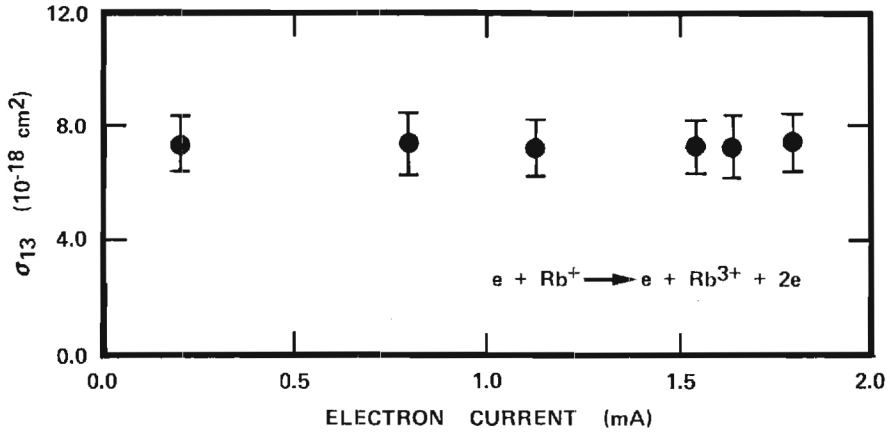

a. Dependence of σ_{13} on electron current for 298 eV electrons.

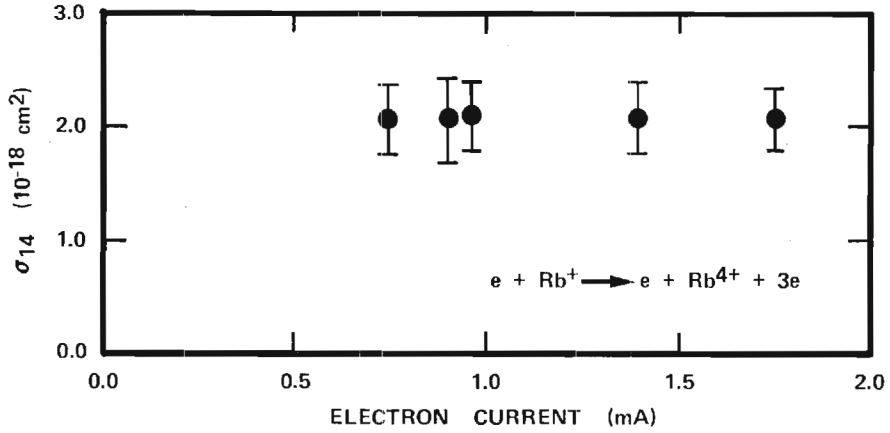

b. Dependence of σ_{14} on electron current for 598 eV electrons.

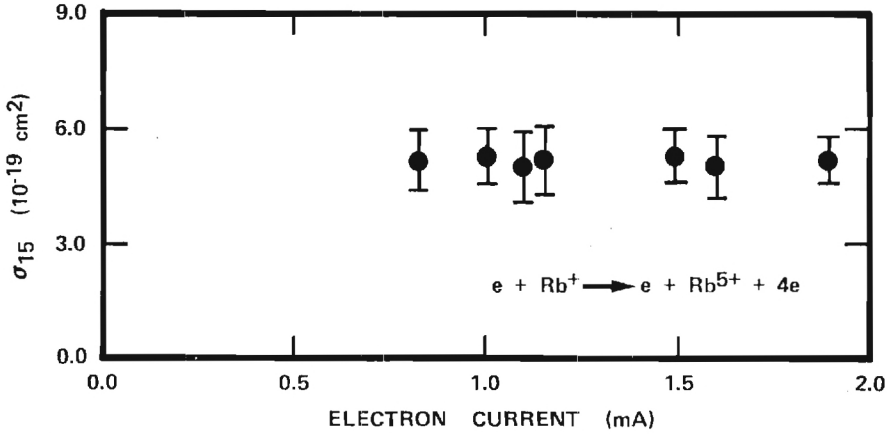

c. Dependence of σ_{15} on electron current for 798 eV electrons.

Figure 13. Dependence of the Measured Cross Sections on Electron Current.

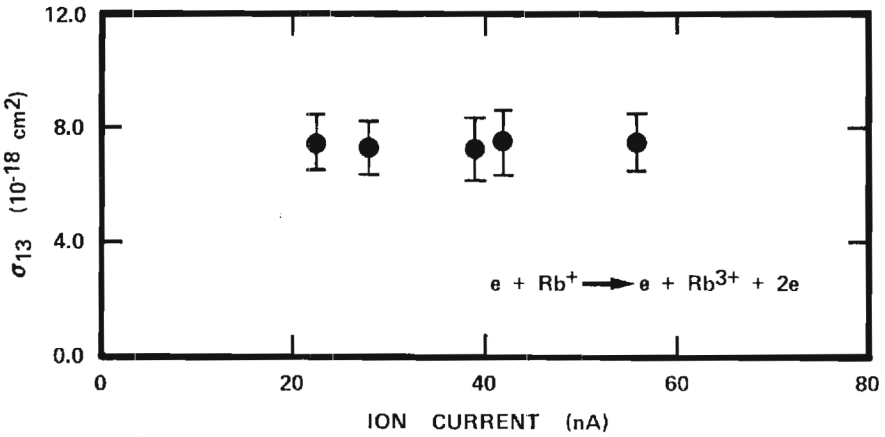

a. Dependence of σ_{13} on ion current for 298 eV electrons.

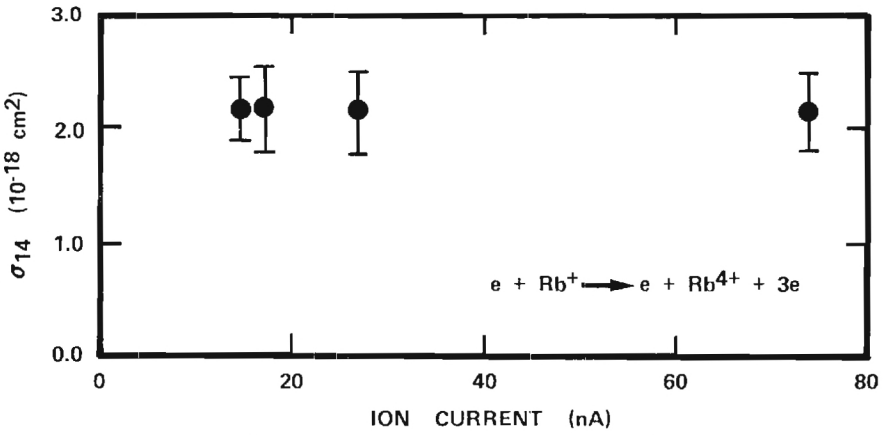

b. Dependence of σ_{14} on ion current for 598 eV electrons.

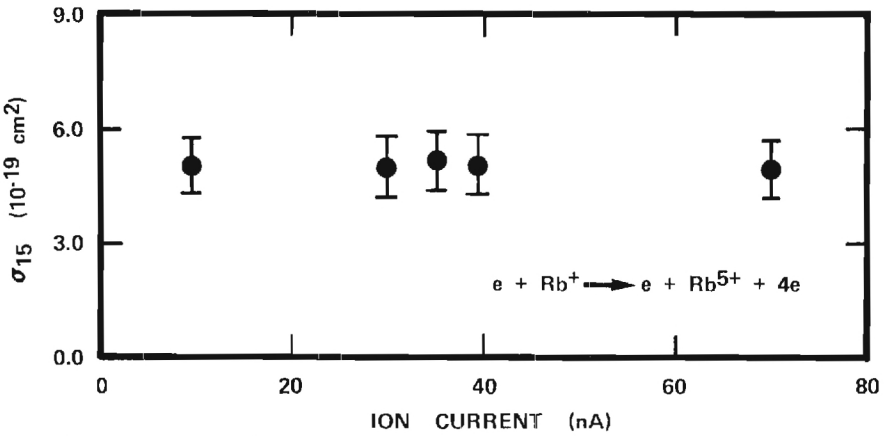

c. Dependence of σ_{15} on ion current for 798 eV electrons.

Figure 14. Dependence of the Measured Cross Sections on Ion Current.

thus defining a test variable for this series of consistency checks. Previous crossed beam research has demonstrated a systematic cross section dependence upon beam profiles for form factors less than 0.470 or greater than 0.700.[26,31] Physically, this phenomenon apparently arises from the ion beam becoming incapable of accommodating all of the particles comprising the electron beam. Therefore, loss of signal is inevitable and the measured cross sections are found to vary systematically with the electron beam intensity. As a result, all data taken during the present series of measurements have employed form factors between these two extreme values. Figure 15 shows that the measured cross sections are independent of the parent beam profiles over this operating plateau in the magnitudes of the corresponding form factors.

Dependence of the Cross Sections upon Ion Energy

Figure 16 illustrates the dependence of the measured cross sections on ion beam energy for each of the three ionization processes of interest. Note that there is no systematic variation in the cross sections for these representative energies. Therefore, perturbation of the ion trajectories by the electron beam space charge is evidentally negligible. This important observation, coupled with the invariance of the measured cross sections to changes in the beam profiles and the electron current then leads to the conclusion that no serious errors are present in the determination of the form factor.

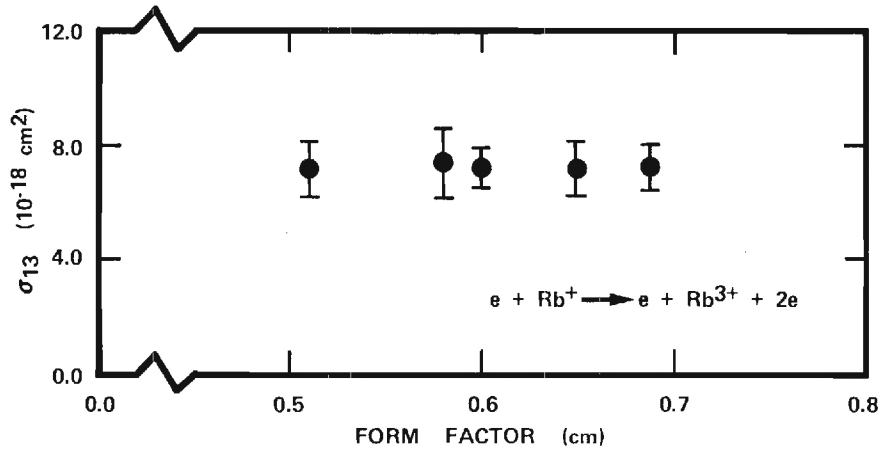

a. Dependence of σ_{13} on form factor for 298 eV electrons.

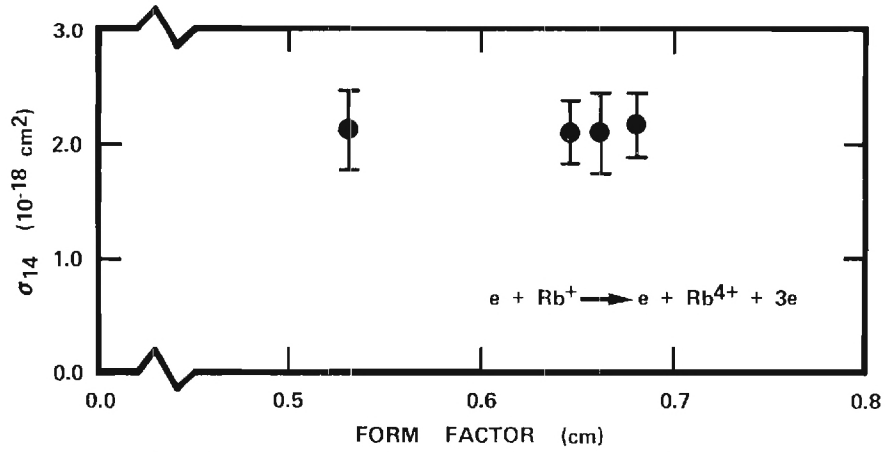

b. Dependence of σ_{14} on form factor for 598 eV electrons.

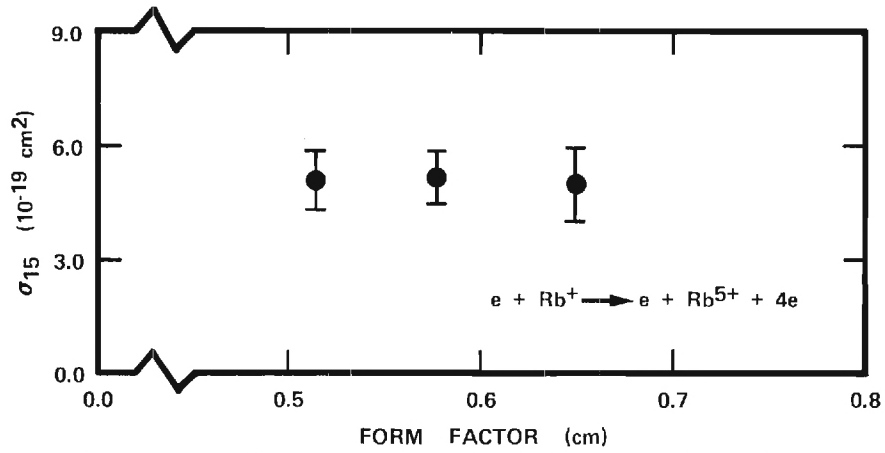

c. Dependence of σ_{15} on form factor for 798 eV electrons.

Figure 15. Dependence of the Measured Cross Sections on the Form Factor.

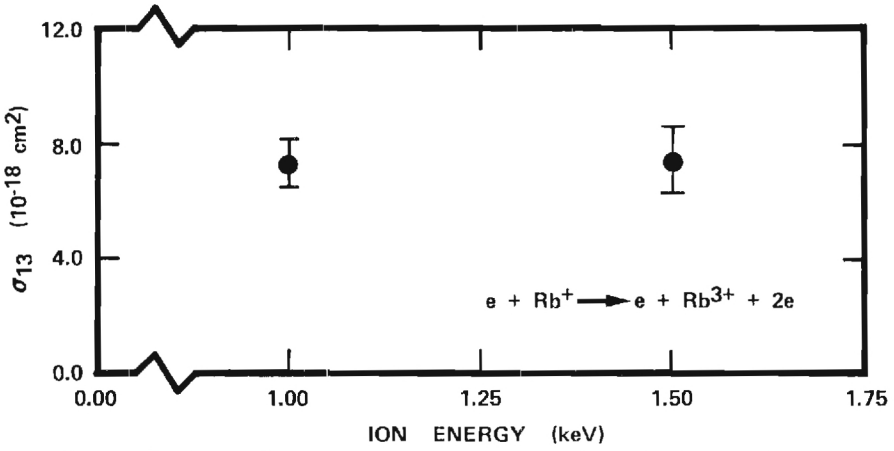

a. Dependence of σ_{13} on ion energy for 298 eV electrons.

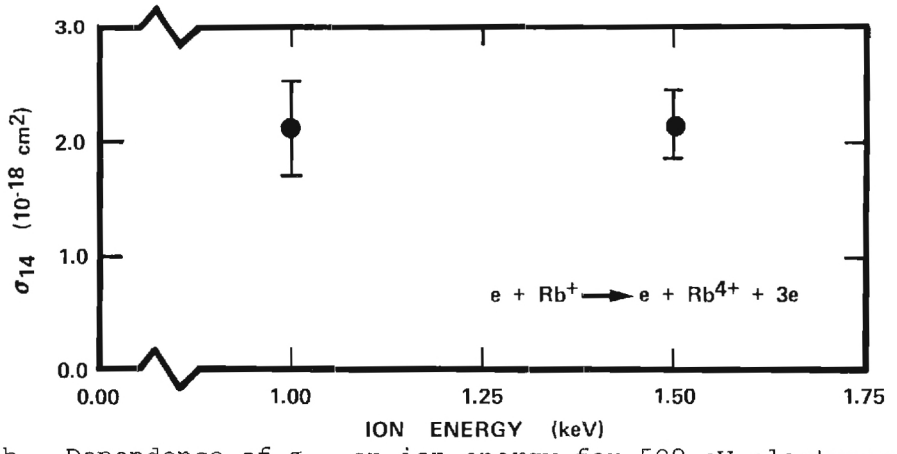

b. Dependence of σ_{14} on ion energy for 598 eV electrons.

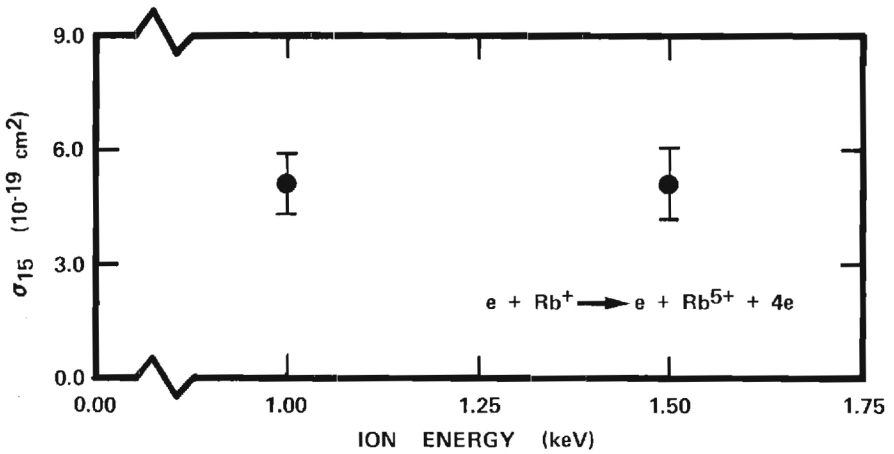

c. Dependence of σ_{15} on ion energy for 798 eV electrons.

Figure 16. Dependence of the Measured Cross Sections on Ion Energy.

Cross Sections Below Threshold

The cross sections measured below threshold are zero to within ±1 per cent of the maximum values displayed by each of their respective processes. Most of the random variation above and below the nominal zero value is presumed to result from the small signal-to-noise ratio inherent in all measurements below threshold. Moreover, the indicated cross sections at several points below threshold have been found to be independent of electron current, ion current, ion energy, form factor and the magnitude of the electron background. This suggests that the troublesome space charge focusing and background modulation effects occasionally occurring in crossed beam experiments are notably absent in the present determination. Furthermore, the vanishing of the measured cross sections below threshold also demonstrates that there is no appreciable metastable contamination of the primary ion beam.

In summary, a cross section is not derived from a single observation but is evaluated statistically by performing a large number of measurements over widely varying experimental conditions. Numerous electron energies must be selected so that the cross sections are comprehensively sampled as a function of this collision defining variable. In addition, the required invariance of the ionization cross sections to the other experimental parameters must be conclusively demonstrated. Finally, many measurements must be performed at identical electron energies to enable prediction of the resulting cross sections with adequate statistical regularity.

Measurements comprising the results presented herein have been taken over a period of 17 months and have occupied 14 successful pumpdowns of the apparatus. After each individual pumpdown, both the electron source and the ion emitter assembly were replaced. This precaution has helped to ensure that characteristics peculiar to a particular source had minimal statistical effect on the final results. More than 800 individual measurements have been performed with approximately equal balance between DC and pulsed determinations. All of the ionization data were subjected to the consistency checks discussed earlier and any suspected results have been eliminated from the final compilation. Approximately 500 of the data runs performed are deemed satisfactory and these measurements constitute the final experimental results.

Experimental Results

Absolute cross sections for the double, triple and quadruple ionization of Rb^+ ions by electron impact have been measured for electron energies from below their respective thresholds to approximately 3000 eV. The results of these measurements are summarized in Tables 1 through 3 and presented graphically in Figures 17 through 19, respectively. Figure 20 reproduces all three of the cross sections on a single plot in order to facilitate comparison of the characteristic structure peculiar to each ionization process. In all cases, only the actual, measured values are presented and no assumptions have been made about the magnitudes of the cross sections intermediate to the sampled electron energies. The maximum probable uncertainties in

TABLE 1. Absolute Experimental Cross Sections for the Double Ionization of Rb^+ Ions by Electron Impact

Indicated Electron Energy, eV	Actual Electron Energy, eV	Cross Section Units of 10^{-18} cm^2	90 Per Cent Confidence Limits, Per Cent	Total Systematic Error, Per Cent	Total Probable Error, Per Cent
50	48 ± 1	0.0	-	-	-
60	58 ± 1	0.0	-	-	-
70	68 ± 1	0.32	± 59	± 8	± 67
80	78 ± 1	1.95	± 11	± 8	± 19
90	88 ± 1	4.34	± 10	± 8	± 18
100	98 ± 1	6.37	± 6	± 8	± 14
120	118 ± 1	8.39	± 6	± 8	± 14
140	138 ± 1	8.77	± 4	± 8	± 12
170	168 ± 1	9.20	± 4	± 8	± 12
190	188 ± 2	8.93	± 4	± 8	± 12
250	248 ± 2	7.79	± 3	± 8	± 11
300	298 ± 2	7.35	± 3	± 8	± 11
400	398 ± 2	6.72	± 6	± 8	± 14
500	498 ± 2	6.53	± 4	± 8	± 12

TABLE 1. Absolute Experimental Cross Sections for the Double Ionization of Rb^+ Ions by Electron Impact (Continued)

Indicated Electron Energy, eV	Actual Electron Energy, eV	Cross Section Units of 10^{-18} cm^2	90 Per Cent Confidence Limits, Per Cent	Total Systematic Error, Per Cent	Total Probable Error, Per Cent
600	598 ± 3	6.22	± 2	± 8	± 10
700	698 ± 3	5.85	± 6	± 8	± 14
800	798 ± 3	5.60	± 3	± 8	± 11
900	898 ± 3	5.34	± 3	± 8	± 11
1000	998 ± 4	5.06	± 4	± 8	± 12
1250	1248 ± 5	4.69	± 3	± 8	± 11
1500	1498 ± 5	4.40	± 5	± 8	± 13
2000	1998 ± 6	3.83	± 3	± 8	± 11
3000	2998 ± 9	3.04	± 4	± 8	± 12

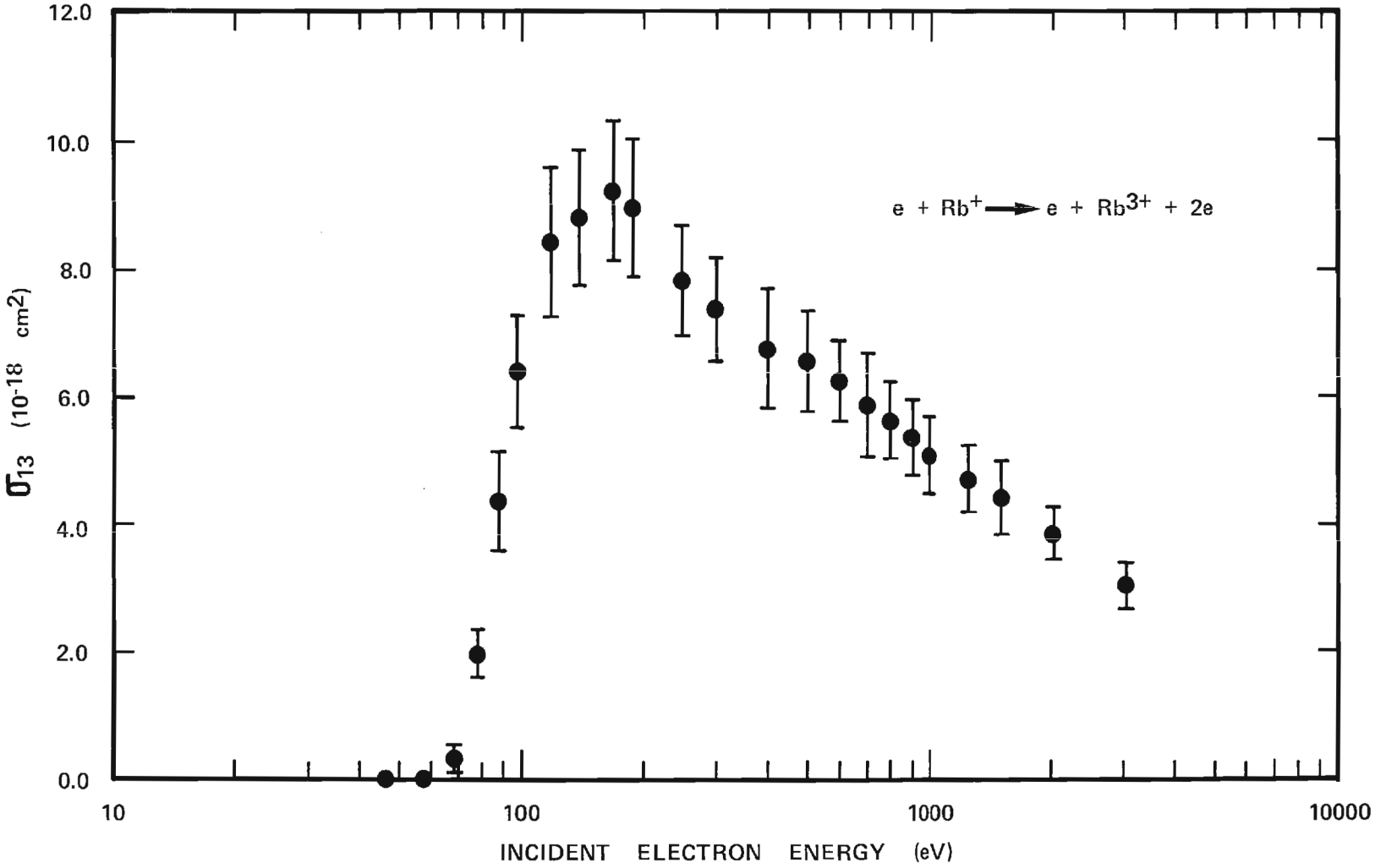

Figure 17. Absolute Experimental Cross Sections for the Double Ionization of Rb^+ Ions by Electron Impact.

TABLE 2. Absolute Experimental Cross Sections for the Triple Ionization of Rb^+ Ions by Electron Impact

Indicated Electron Energy, eV	Actual Electron Energy, eV	Cross Section Units of 10^{-18} cm^2	90 Per Cent Confidence Limits, Per Cent	Total Systematic Error, Per Cent	Total Probable Error, Per Cent
100	98 ± 1	0.0	-	-	-
120	118 ± 1	0.0	-	-	-
140	138 ± 1	0.10	± 32	± 8	± 40
170	168 ± 1	0.26	± 16	± 8	± 24
190	188 ± 2	0.527	± 7	± 8	± 15
250	248 ± 2	1.01	± 10	± 8	± 18
300	298 ± 2	1.33	± 8	± 8	± 16
400	398 ± 2	1.72	± 5	± 8	± 13
500	498 ± 2	2.00	± 4	± 8	± 12
600	598 ± 3	2.14	± 7	± 8	± 15
700	698 ± 3	2.09	± 4	± 8	± 12
800	798 ± 3	2.06	± 4	± 8	± 12
900	898 ± 3	2.03	± 6	± 8	± 14
1000	998 ± 4	1.97	± 4	± 8	± 12

TABLE 2. Absolute Experimental Cross Sections for the Triple Ionization of Rb^+ Ions by Electron Impact (Continued)

Indicated Electron Energy, eV	Actual Electron Energy, eV	Cross Section Units of 10^{-18} cm^2	90 Per Cent Confidence Limits, Per Cent	Total Systematic Error, Per Cent	Total Probable Error, Per Cent
1250	1248 ± 5	1.85	± 5	± 8	± 13
1500	1498 ± 5	1.71	± 6	± 8	± 14
2000	1998 ± 6	1.57	± 4	± 8	± 12
3000	2998 ± 9	1.19	± 4	± 8	± 12

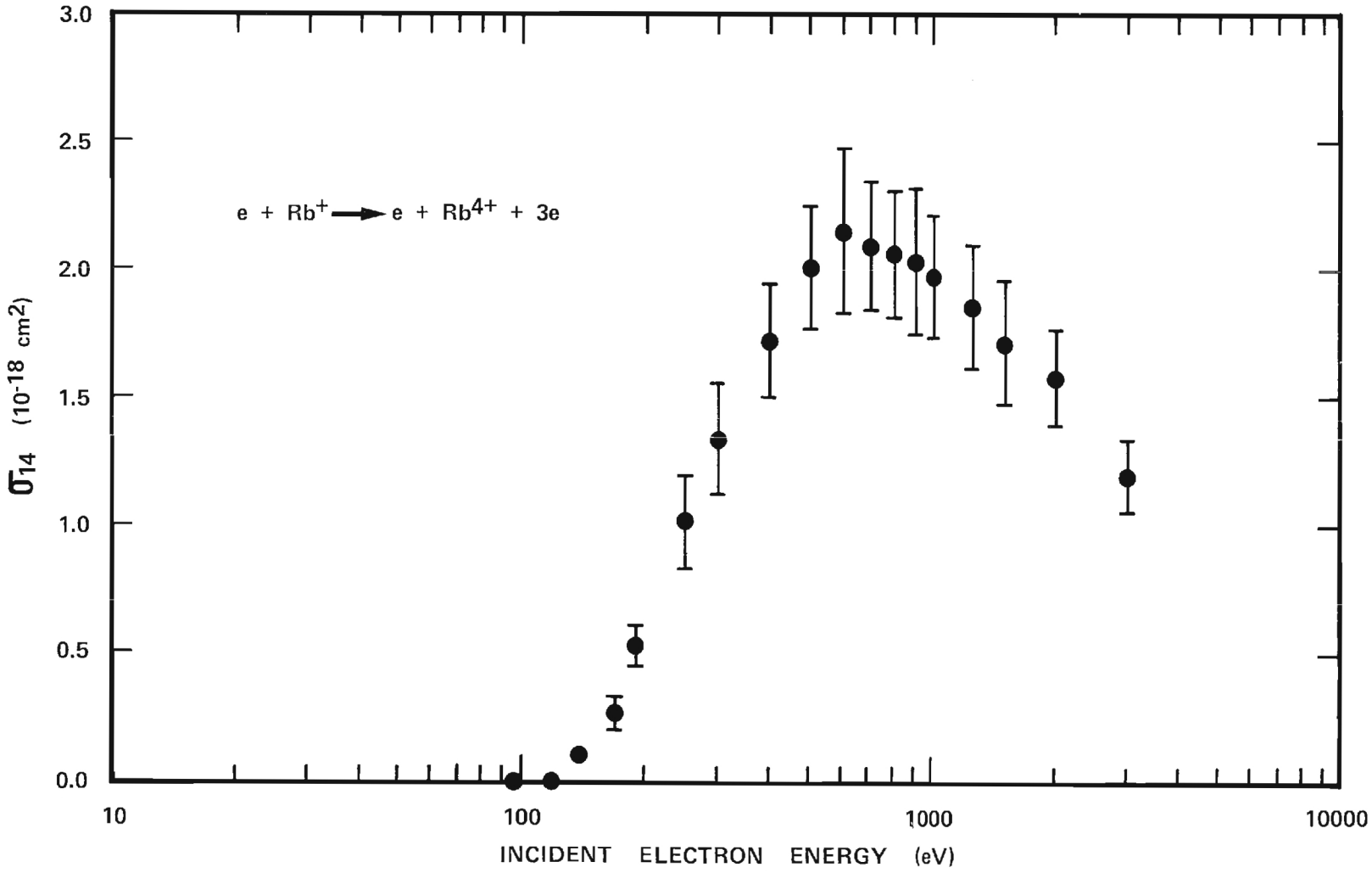

Figure 18. Absolute Experimental Cross Sections for the Triple Ionization of Rb^+ Ions by Electron Impact.

TABLE 3. Absolute Experimental Cross Sections for the Quadruple Ionization of Rb^+ Ions by Electron Impact

Indicated Electron Energy, eV	Actual Electron Energy, eV	Cross Section Units of 10^{-19} cm^2	90 Per Cent Confidence Limits, Per Cent	Total Systematic Error, Per Cent	Total Probable Error, Per Cent
160	158 ± 1	0.0	-	-	-
190	188 ± 2	0.0	-	-	-
250	248 ± 2	0.35	± 45	± 8	± 53
300	298 ± 2	0.73	± 16	± 8	± 24
400	398 ± 2	2.41	± 7	± 8	± 15
500	498 ± 2	3.69	± 6	± 8	± 14
600	598 ± 3	4.18	± 9	± 8	± 17
700	698 ± 3	4.73	± 10	± 8	± 18
800	798 ± 3	5.11	± 3	± 8	± 11
900	898 ± 3	5.01	± 6	± 8	± 14
1000	998 ± 4	4.98	± 4	± 8	± 12
1250	1248 ± 5	4.63	± 4	± 8	± 12
1500	1498 ± 5	4.32	± 7	± 8	± 15
2000	1998 ± 6	3.88	± 3	± 8	± 11
3000	2998 ± 9	2.76	± 6	± 8	± 14

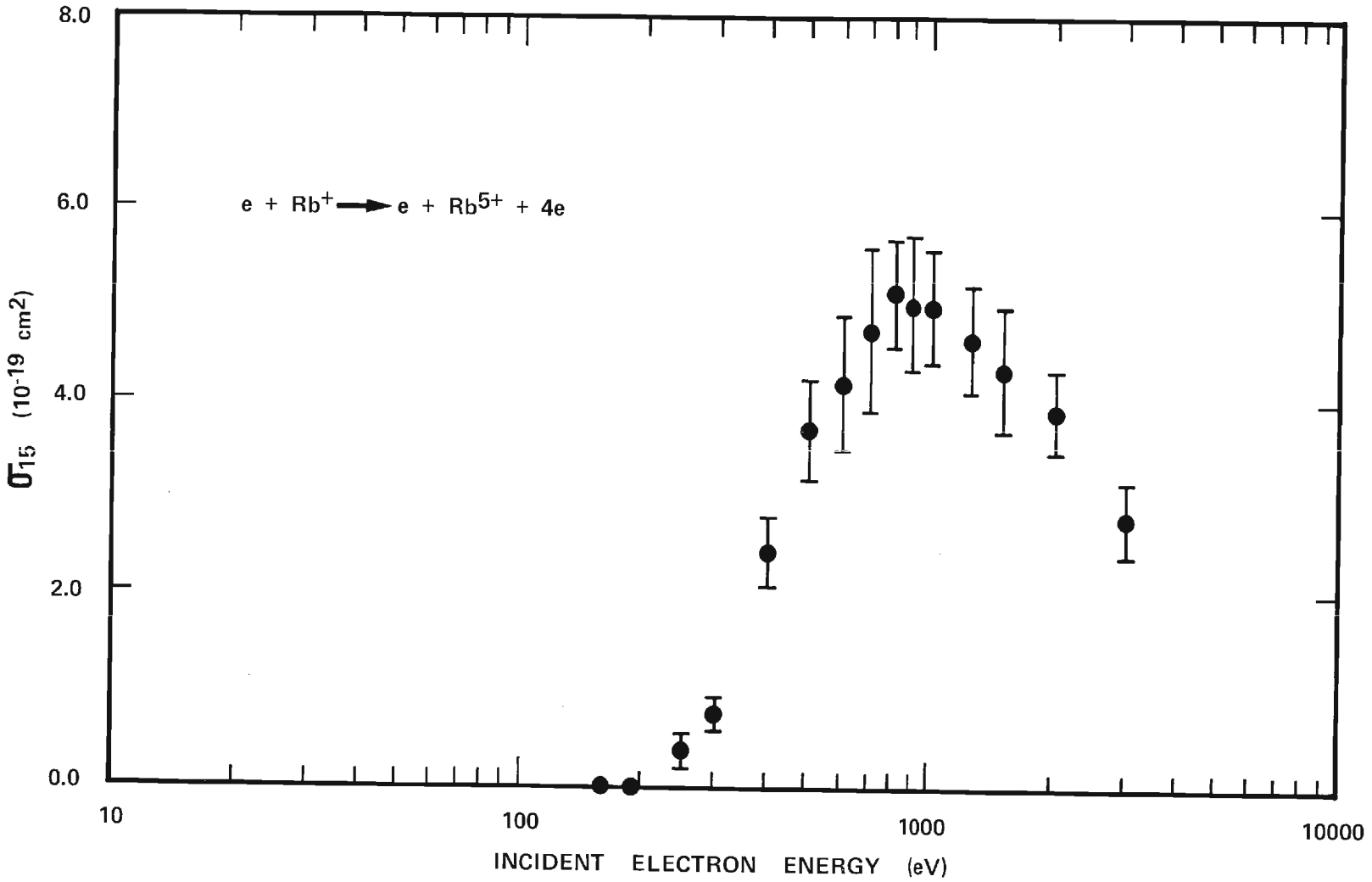

Figure 19. Absolute Experimental Cross Sections for the Quadruple Ionization of Rb^+ Ions by Electron Impact.

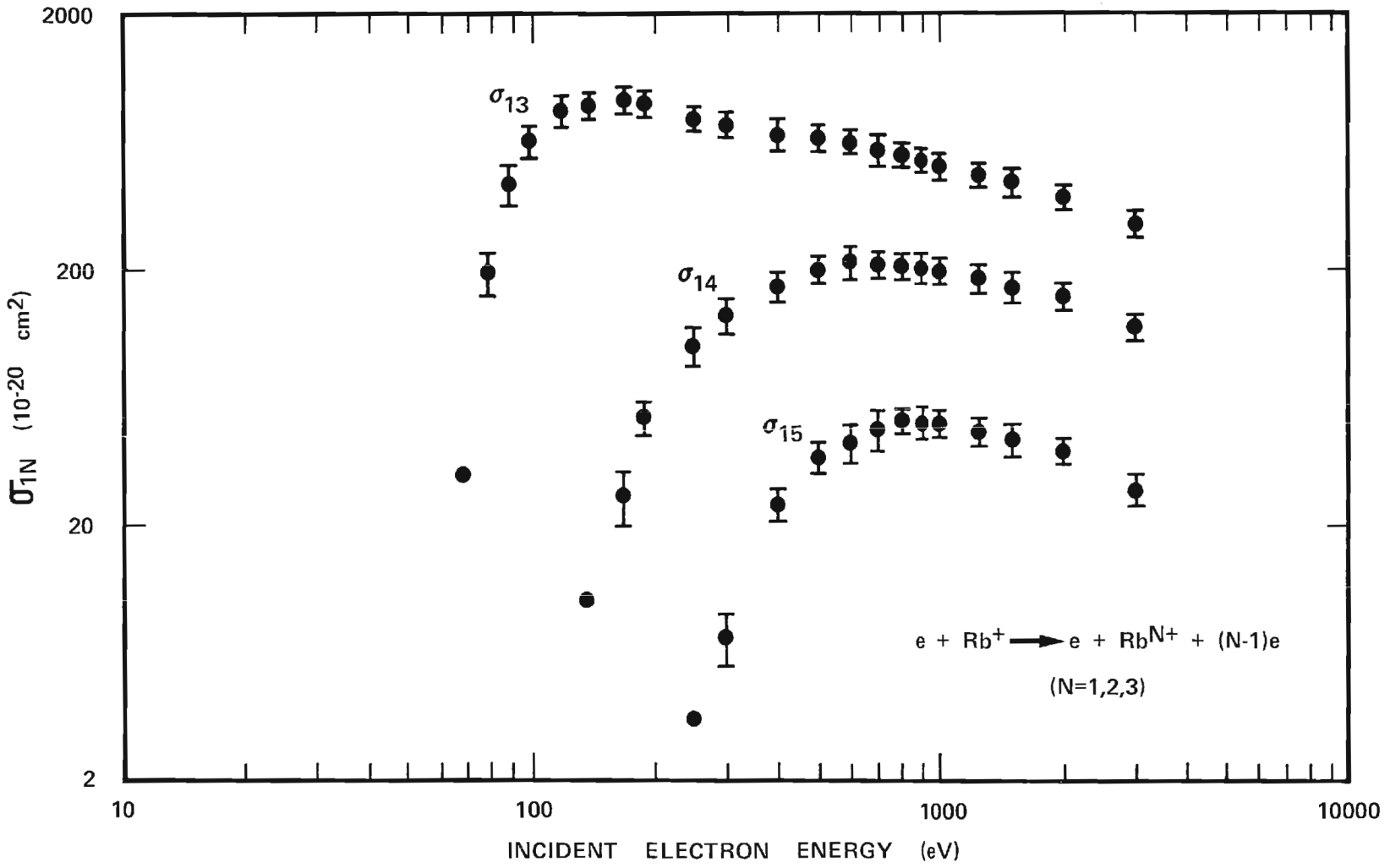

Figure 20. Absolute Experimental Cross Sections for the Double, Triple and Quadruple Ionization of Rb^+ Ions by Electron Impact.

the resulting cross sections are indicated in both the tables and the figures and the error analysis employed to evaluate their extent is discussed below.

Discussion of Errors

The errors inherent in any experimental determination result from a combination of both systematic effects and random variations. Systematic phenomena generate those errors which cause all the measured values to be uncertain by a similar amount. In the present experiment, these errors arise principally from uncertainties in the parent beam energies and the calibration constraints on the associated instrumentation. Rigid enforcement of the consistency criteria however, ensures that none of the experimentally observed quantities display a definite functional dependence upon any of these systematic effects.

In contrast, random errors arise because seemingly equivalent data runs rarely yield identical cross sections. Presumably, such errors are generated by small, apparently random fluctuations in some experimental condition. Such random errors never display a functional dependence upon diagnostic test variables and are evidentally uncorrelated with any observable parameter. The total probable error in the final experimental result is taken to be equal to the sum of the systematic error and the random error assigned to that particular measurement.

Systematic Errors

The systematic errors characteristic of the present experiment arise from uncertainties in the electron and ion beam energies and

from calibration constraints on the measuring instruments. Each of these effects is discussed separately in the following sections and their cumulative impact is employed to assess the magnitude of the systematic error inherent in the resulting cross sections.

Electron Beam Energy Error. A typical electron beam energy distribution characteristic of the oxide cathodes employed in the present research appears in Figure 9. Note that the curve displays a full width at half maximum equal to approximately 1.1 electron volts. Similarly, the mean electron energy is nearly two electron volts less than the indicated acceleration voltage. As a result, it is deemed appropriate to simply subtract two volts from each preselected acceleration potential in order to obtain the corresponding actual electron energy. Subsequent consideration of the representative energy distribution, combined with calibration knowledge of the acceleration power supply, then facilitates estimation of the uncertainty in the electron beam energy. The resulting worst-case bounds on this important collision parameter appear in Tables 1 through 3. However, because of the nonlinear nature of the absicssas in Figures 17 through 20, the electron beam energy error is not reflected in these graphical displays of the measured cross sections.

Ion Beam Energy Error. The total systematic uncertainty in the ion beam energy is presumed to be the result of the calibration error in the ion acceleration supply and the voltage drop across the ion emitter assembly. The resulting uncertainty in the ion beam energy is taken to be ±1 per cent. However, it has been shown that the equation for

the ionization cross section involves the ion velocity and is hence, dependent upon the square root of the ion energy. Therefore, the systematic error in the measured cross sections resulting from uncertainties in the ion beam energy is conservatively estimated to be ±0.5 per cent.

Instrumentation Error. The calibration errors characteristic of the instruments used in the present experiment have been combined to yield an estimate of the overall instrumentation accuracy. The resulting systematic uncertainty arising from instrumentation errors is taken to be ±7 per cent.

In conclusion, an overall systematic error is generated by uncertainties in the parent beam energies and calibration constraints on the associated instrumentation. These various effects have been combined to yield a worst-case approximation of the uncertainty arising from all such phenomena. The resulting total systematic error in the measured cross sections is thus estimated to be ±8 per cent.

Random Errors

The magnitudes of the random errors inherent in the present experimental results have been estimated from the 90 per cent confidence limits of the mean.[59] This component of the overall experimental uncertainty arises because seemingly equivalent measurements generally yield slightly different cross sections. For instance, similar data runs made over a short period of time typically display a random variation of perhaps several per cent. Cross sections resulting from measurements performed over longer periods however, tend to fluctuate

on the order of five to seven per cent about the eventual sample mean. These larger variations are presumed to arise from electron source peculiarities characteristic of the cathode used during that particular pumpdown of the apparatus. Accordingly, numerous pumpdowns and hence, electron sources, have been employed in order to comprehensively assess the statistical importance of these random variations.

The resulting estimate of the random error has been added to the previously discussed systematic error in order to obtain the corresponding total probable error. These total errors are then appended to the final experimental results and thus, appear in both the tabular and graphical presentations of the measured cross sections. It should be remarked that the indicated bounds on the total experimental uncertainty are felt to be conservative, but their magnitudes seem commensurate with the statistics of the crossed beam measurement process.

CHAPTER V

COMPARISONS WITH AVAILABLE THEORY

Introduction

Much previous work has been devoted to the theoretical calculation of electron impact ionization cross sections from a variety of atomic collision models. These approaches range from exact quantum mechanical formulations to heuristic empirical arguments requiring considerable a priori data. Several procedures in particular have been found to provide reasonably accurate cross section estimates with a tolerable amount of mathematical labor. This chapter summarizes selected theoretical approaches that have been advanced to date and compares available theoretical predictions with the present experimental results.

A Brief Review of Electron Impact Ionization Models

A number of mathematical models have been developed to theoretically calculate selected electron impact ionization cross sections. Several simple cases have been formulated with quantum mechanical rigor but numerous assumptions are generally required to facilitate the final computation. As a result of the extreme mathematical difficulties inherent in a complete quantal treatment, classical and empirical techniques are widely employed to deduce the desired cross sections.

Selected Quantum Mechanical Formulations

A comprehensive quantum mechanical treatment of electron impact ionization is an example of a many-body problem whose solution requires a total wave function description of the target, the incident electron and any ejected electrons. The usual procedure attempts to determine an asymptotic form of this total wave function by an expansion in terms of the unperturbed wave functions of the target.[60] Next, boundary conditions are imposed to define the particular collision event under consideration, thus allowing the generation of an integral or variational expression for the scattering amplitude. Finally, it is required to express the ionization cross section in terms of the various components of the scattering amplitude. Of course, the series expansions inherent in the above procedure generate an infinite number of equations and hence, some mathematical concessions are generally required to facilitate the final calculation. These simplifications constitute a number of approximate quantal techniques which aim to retain the essential features of the rigorous treatment while allowing reasonably accurate cross sections to emerge with a tolerable amount of mathematical labor. Of all the quantal simplifications, the Born approximation and its major variations have proven to be the most significant.

Born Approximation. One of the most widely used quantual simplifications is the Born approximation. This technique assumes a plane wave description for the incident electron and writes the initial and final state wave functions as the product of the unperturbed wave functions of the target state in question.[60,61] Thus, for example, the total wave function before the collision is the product of a plane

wave representing the incident electron and a bound state wave function describing the individual target electrons. It is further required that the collision be a binary encounter and hence, the ejected electron is assumed to completely screen the scattered electron from the nucleus.[61] This latter assumption may be very nearly correct at high collision energies but is, however, likely to produce questionable results for energies near threshold.[60]

Coulomb-Born Approximation. The Coulomb-Born technique is a variation of the Born approximation particularly applicable to ionic targets. In this formulation, a Coulomb wave description is used for both the incident and ejected electrons. This modification tends to compensate for the Coulombic perturbation on the trajectory of the incident electron by the ion. Such a refinement however, introduces an additional level of mathematical difficulty.

Bethe-Born Approximation. The Bethe-Born approximation includes some additional mathematical simplifications in order to more easily calculate the desired ionization cross sections. Unfortunately, the assumptions inherent in this procedure tend to obscure the functional form of the cross section near threshold. In most cases however, the predictions of the Bethe-Born technique converge to the more precise Born results at very high collision energies.[60,61]

Born-Oppenheimer Approximation. The Born-Oppenheimer procedure modifies the Born approximation by anti-symmetrizing the free electrons and hence, includes the quantum mechanical effect of exchange. The predictions of this technique are normally in error for neutrals but generally improve for ionic targets.[60] In both cases however, the

results calculated by the Born-Oppenheimer approximation tend to be larger than independent determinations of similar cross sections.[61]

Selected Classical Formulations

Classical procedures for the analysis of electron impact ionization date from the pioneering calculations of Thomson in 1912.[1] Even today, the unparalleled ease of application and surprisingly accurate predictive capability characteristic of these classical techniques ensures their continued role in the regime of atomic collision physics. Inherent in all such calculations is the requirement that a classical description be found for the initial state of the target electrons. It is also assumed that the collision event can be completely described in terms of the Newtonian laws of classical mechanics. Finally, it is usual to presume that the collision takes the form of a binary encounter in order to reduce the many-body problem to the simpler two-body analog.

Several refined theories have been advanced which attempt to introduce the quantal effect of exchange into these classical treatments.[60] Nevertheless, the more elementary models of Thomson and of Gryzinski seem adequately comprehensive for a significant number of ionization calculations.

The Method of Thomson. Thomson's analysis requires that the collision be regarded as a binary encounter between the incident electron and one of the atomic electrons. It is further assumed that the target electron is at rest prior to its interaction with the projectile particle. Under these conditions, the electron impact ionization cross section for a target having N electrons with binding energy

I is given by

$$\sigma(x) = 4\pi a_o^2 \, N\left(\frac{I_H}{I}\right)^2 \frac{x-1}{x^2} \tag{15}$$

where I_H is the hydrogen ionization potential, a_o is the Bohr radius and x is a reduced ionization energy equal to the collision energy, E divided by the binding energy, I.[1] Thomson's equation is particularly significant because it introduces the concept of a reduced ionization cross section as defined by Equation (16).

$$\sigma_R(x) = \frac{1}{N}\left(\frac{I}{I_H}\right)^2 \sigma(x) \tag{16}$$

Subsequent substitution of Equation (15) into Equation (16) then makes it clear that the reduced cross section is a function of only the reduced ionization energy, x. This observation led Thomson to suggest that $\sigma_R(x)$ is a universal function which should thus, yield similar results for all elements in all stages of ionization.[1,62] Therefore, a classical scaling procedure can be developed which converts a known cross section to that appropriate for a different atomic system. In particular, if one knows $\sigma_1(x)$, then classical scaling predicts that the desired, unknown cross section, $\sigma_2(x)$ can be calculated from

$$\sigma_2(x) = \left(\frac{I_1}{I_2}\right)^2 \frac{N_2}{N_1} \sigma_1(x) \tag{17}$$

where I_1 and N_1 are respectively, the ionization energy and the number

of electrons having that energy in the known system; I_2 and N_2 are similarly defined for the unknown structure.[55] A further simplification results when the two atomic systems are members of an isoelectronic sequence. In this case, $N_1 = N_2$ and hence, $\sigma_1(x)$ is scaled by only the square of the ratio of the ionization potentials.

For all its simplistic elegance, the Thomson formulation unfortunately fails to generate the proper functional form of the cross section for high collision energies. Persual of Equation (15) suggests that the cross section will vary as $1/x$ at high energies in contrast to the more accurate Born result which predicts the experimentally observed $\ln(x)/x$ dependence.

The Method of Gryzinski. The classical binary encounter theory of Gryzinski is, without question, the most comprehensive atomic collision model developed to date. Gryzinski's method is founded upon the premise that the effect of the energetic electron on the target can be completely described by the Coulombic interaction between the incident particle and the atomic electrons.[7,63-65] This technique also assumes that the projectile electron interacts with only one atomic electron at a time and it is further required that the mutual interaction between the nucleus and the atomic electrons be disregarded during the collision.[66] Gryzinski then assigns a particular velocity distribution to the atomic electrons and assumes that the resulting kinetic energy of each electron is equal to its ionization potential. This subsequently results in an expression for the ionization cross section of each electronic shell. Finally, the total cross section is obtained by summing all of the contributions from each of the individual

shells.

It is interesting to note that the assumed velocity distribution for the atomic electrons is physically incorrect but its inclusion yields the proper $\ln(x)/x$ dependence of the cross section at high electron energies.[55] In addition, the relative mathematical ease of this technique has encouraged its application to a wide variety of atomic collision problems. In nearly all cases, the Gryzinski predictions agree to within about a factor of two with independent determinations of the relevant cross sections.[60,61,66]

Selected Empirical Formulations

In addition to the theoretically motivated calculations presented above, a number of empirical formulations have also been developed. These relations are generally contrived to fit previously determined results and are subsequently used to predict variations in the cross sections for particular members of the same isoelectronic sequence. Several such representative empirical schemes are the procedures suggested by Elwert and Drawin.

The Elwert Formula. The Elwert approach uses the previously discussed concept of a reduced ionization energy and attempts to fit the cross section curve over the energy range, $1 \leq x \leq 2$. Elwert apparently plotted all the reduced ionization results available at that time and developed a formula which seemed to fit all data to within about a factor of two.[67] The Elwert formula, in terms of the reduced ionization energy, is presented in Equation (18).[67,68]

$$\sigma_R(x) = 2\left(\frac{x - 1}{x^2}\right)[1 + 0.3(x - 1)]\pi a_o^2 \qquad (18)$$

This empirical relation has since been applied to evaluate a number of independently determined cross sections. Measurements by Lineberger, for instance, have demonstrated that the Elwert equation accurately predicts the cross sections for the single ionization of Li^+ ions for collision energies near threshold.[68]

The Drawin Formula. Drawin has also proposed an empirical formula for the calculation of electron impact single ionization cross sections. The Drawin relation predicts a linear behavior near threshold and the correct $\ln(x)/x$ dependence at higher energies as seen by Equation (19).[27,60,69,70]

$$\sigma_R(x) = 2.66\ f_1\left(\frac{x - 1}{x^2}\right)\ \ln[1.25\ f_2\ x]\pi a_o^2 \qquad (19)$$

This formulation includes two arbitrary constants, f_1 and f_2, which may be independently adjusted to fit a variety of atomic systems. If no preliminary information about the ionization process is available then Drawin suggests setting both constants equal to unity.[69,70]

Numerous other empirical formulations have been developed in an attempt to predict unknown cross sections with a minimum of computational difficulty. Lotz, for instance, has devised a mathematical expression which claims to display the variations in the cross sections as a function of the quantum numbers characterizing the initial state.[38,60] Interestingly enough, the Lotz relation is the result of curve fitting to a combination of measured cross sections and Coulomb-Born calculations

for selected targets.[38] Unfortunately, the empirical approaches which have been devised to date all employ varying amounts of input data whose a priori applicability is difficult to assess. As a result, it appears that the most appropriate application of such empirical techniques is the retrospective evaluation of independently determined cross sections.

Extension to Multiple Ionization of Ionic Targets

Previous sections have discussed a number of techniques which can be used to theoretically predict the magnitude and functional form of selected electron impact ionization cross sections. It is important to note however, that nearly all of these models have been developed to examine single ionization of neutral targets. The more interesting case of multiple ionization has been essentially neglected, largely because the assumptions inherent in most of the theoretical approaches necessarily limit their direct applicability to the simpler, single ionization events. Furthermore, these models do not rigorously consider the problem of an energetic electron incident upon a positively charged target. The resulting ionization process is likely however to display a larger cross section than a similar collision involving a neutral species. Such an effect presumably arises from the Coulombic focusing action of the electron beam by the ionic target and hence, the atomic ionization models tend to underestimate the corresponding cross sections. Consequently, a number of modifications must be made to the various theoretical approaches before they can be used to calculate the desired multiple ionization cross sections for ionic targets.

The Problem of Multiple Ionization

Nearly all of the theoretical ionization calculations performed to date have restricted themselves to the direct single ionization of neutral atoms. Unfortunately, only a few of these theories can be modified to handle multiple ionization and, in any event, the resulting cross sections are likely to be suspect for complicated electronic configurations.[4,6] At present, an extension of the Gryzinski collision model is the sole procedure by which one can calculate multiple ionization cross sections for a fairly comprehensive set of atomic systems.[65] To date however, the double ionization event is the only process to which the Gryzinski extension has been applied. For this special case, it is assumed that the neutral target becomes doubly ionized as a result of only two of the many possible ionization chronologies. One possibility is for each of the two atomic electrons to be ionized by an individual binary encounter with the incident particle. Alternatively, the incident electron may ionize one atomic electron which, upon escaping from the target, impact ionizes the second electron. None of the other possible double ionization mechanisms are considered in this calculation.

It is apparent from the Gryzinski derivation that similar techniques can be developed for triple, quadruple and higher order ionization events. Such extensions are yet to be reported however, although their formulation would constitute a substantial contribution to the theoretical regime of atomic collision physics.

The Problem of Ionic Targets

Most of the ionization theories discussed earlier have been derived for the specific case of an energetic electron incident upon a neutral atom. In general, the corresponding cross sections are smaller than those displayed by the isoelectronic ionic target. This phenomenon apparently arises as a result of the Coulombic attraction between the projectile electron and the positive ion. Consequently, several empirical "focusing factors" have been developed which attempt to compensate for this effect and hence, facilitate application of the atomic theories to ionic targets. A representative focusing factor applicable to the double ionization of a charged target is given by

$$f = 1 + \left(\frac{Q_o \, (I_1 + I_2)^{\frac{1}{2}}}{E} \right) \qquad (20)$$

where Q_o is the initial charge on the target, I_1 and I_2 are the binding energies for the two electrons being ionized and E is the collision energy.[60,71] Note that for positive ions, the appropriate focusing factor is always greater than unity and hence, its multiplicative effect tends to inflate the neutral target cross section towards the presumed ionic analog. Several previous workers have employed such a focusing factor in a Gryzinski calculation of the double ionization event for selected, positively charged targets. Tripathi and Rai, for instance, have attempted to compute σ_{13} for Li^+, Na^+ and K^+ ions.[71] Unfortunately, some obvious technical blunders in their paper encourage suspicion of the resulting cross sections.

In summary, numerous difficulties hinder the development of a procedure which can calculate electron impact multiple ionization cross sections for a fairly comprehensive set of ionic targets. Even the Gryzinski model only allows consideration of the double ionization of neutral atoms and a focusing factor must be employed to extend these calculations to positive ions. No theories have yet been developed for the interesting triple, quadruple or higher order ionization events.

Comparison of Present Results with Available Theoretical Estimates

During the course of the present research, cross section estimates for the electron impact double ionization of Rb^+ ions were obtained using the classical method of Gryzinski.[72] The results of this series of theoretical calculations are presented graphically in Figure 21. Note that the individual contributions from the 3p, 3d, 4s and 4p shells have been combined to generate the total double ionization cross sections. Figure 22 then compares the measured and calculated results and reveals that the simplistic Gryzinski procedure is only moderately successful in predicting the cross sections for the double ionization of Rb^+ ions by electron impact. Note in particular that the Gryzinski calculation significantly underestimates the cross sections for collision energies greater than about 500 eV. This underestimation is presumed to be a consequence of the incomplete theoretical evaluation of inner shell contributions to the total ionization cross sections.

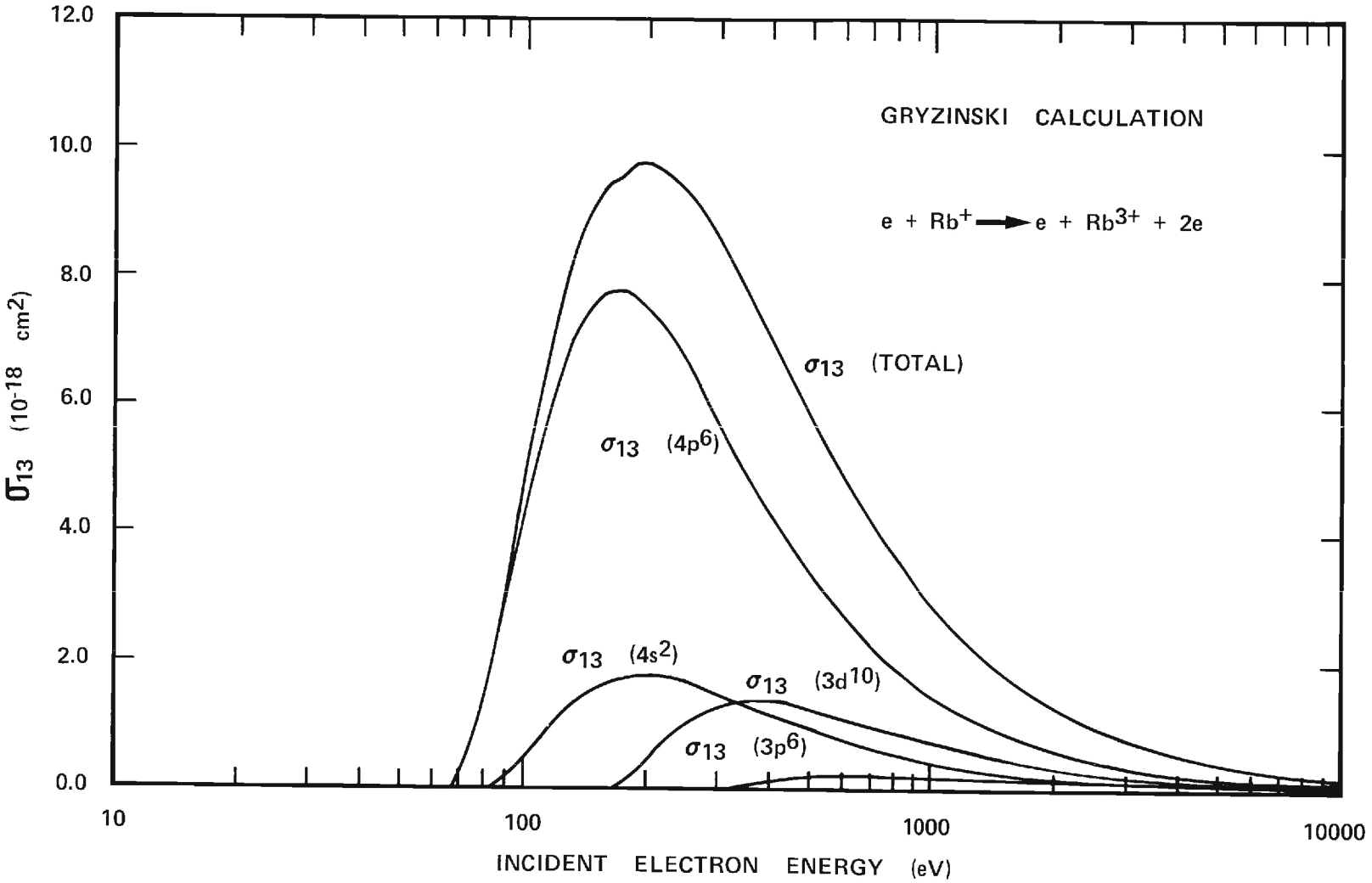

Figure 21. Cross Sections for the Double Ionization of Rb^+ Ions Calculated Using the Method of Gryzinski.

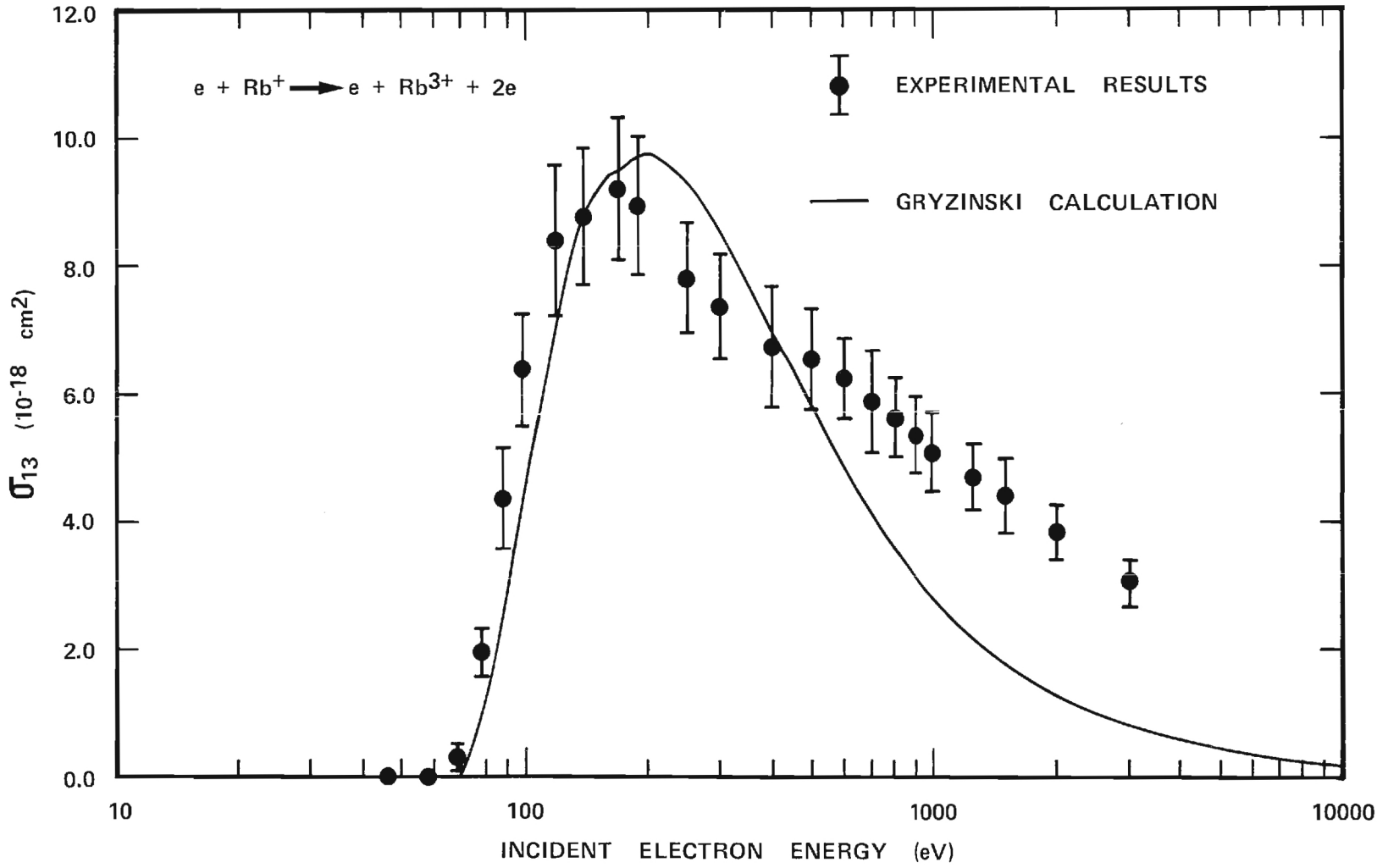

Figure 22. Comparison of the Measured Double Ionization Cross Sections with Estimates Obtained Using the Method of Gryzinski.

CHAPTER IV

CONCLUSIONS

The absolute cross sections for the double, triple and quadruple ionization of Rb^+ ions by electron impact have been measured from below their respective thresholds to approximately 3000 eV. This determination has been accomplished using a crossed beam facility operating under both continuous and pulsed beam conditions. Numerous consistency checks have been performed to evaluate possible sources of experimental error. The present research represents the first double ionization measurement for Rb^+ ions and also the first absolute triple and quadruple determination for any atomic or ionic target.

The cross sections resulting from this series of experiments are summarized in Tables 1 through 3 and presented graphically in Figures 17 through 20, respectively. Examination of the measured double ionization cross sections reveals some apparent structure for several energy regimes near the peak of the curve. Unfortunately, the relative magnitude of these variations is of the order of the total probable error and thus, can not conclusively be regarded as present. It should be remarked however, that these error limits are felt to be conservative and, in any event, the experimental procedures employed presumably prevent the introduction of artificial variations in the measured cross sections. If such structure is indeed present, its existence is probably the result of inner shell effects.

The measured double ionization cross sections have been compared with theoretical results obtained using a classical method developed by Gryzinski. Examination of Figure 22 reveals that the Gryzinski technique is only moderately successful in predicting the cross sections for the double ionization of Rb^+ ions by electron impact. No theoretical calculations are available for the triple and quadruple ionization events. The qualitative shape of the cross section curves however, appears to suggest the tentative conclusion that inner shell effects are of significant importance in the electron impact multiple ionization of singly charged rubidium ions.

APPENDIX A

DERIVATION OF σ_{1N} IN TERMS OF EXPERIMENTAL PARAMETERS

In this appendix an expression for the electron impact multiple ionization cross section for the singly charged ionic targets will be derived. The resulting equation allows the determination of the desired absolute cross sections in terms of experimentally observable quantities. This important relation will be obtained using a procedure differing only slightly from that employed by previous workers.[55,68]

Consider a collimated beam of monoenergetic electrons incident upon an array of singly charged ionic targets. Let the ion and electron beams have particle number densities of n_i and n_e and velocities of v_i and v_e, respectively. It is further required that the ion beam be sufficiently tenuous such that no target is shielded by its neighbors and no projectile electron interacts with more than one target. Under these conditions, the number of $1 \rightarrow N$ ionizing events, R'_{1N}, per unit volume per second is given by

$$R'_{1N} = n_i \, n_e \, v_r \, \sigma_{1N} \tag{A-1}$$

where v_r is the relative velocity of the colliding particles and σ_{1N} is the cross section for the ionization process. Note that σ_{1N} has the dimensions of area and is a measure of the likelihood of the $1 \rightarrow N$ ionization event taking place.

Now, if the electrons and ions move in mutually perpendicular, well-collimated beams parallel to the X and Y axes, respectively, their number densities and relative velocity can be obtained from

$$n_e\ (y,z) = \frac{S_e\ (y,z)}{e\ v_e} \tag{A-2}$$

$$n_i\ (x,z) = \frac{S_i\ (x,z)}{e\ v_i} \tag{A-3}$$

$$v_r = (v_i^2 + v_e^2)^{\frac{1}{2}} \tag{A-4}$$

where S_e and S_i are the electronic and ionic current densities and e is the electronic charge. Substitution of these quantities into Equation (A-1) with subsequent multiplication by the differential volume element yields the following expression for the number of ionizing events per second.

$$R'_{1N}\ (x,y,z)\ dx\,dy\,dz = \frac{(v_i^2 + v_e^2)^{\frac{1}{2}}}{e^2\ v_i\ v_e}\ \sigma_{1N}\ S_i\ (x,z)\ S_e\ (y,z)\ dx\,dy\,dz \tag{A-5}$$

Note that the equations involving S_e and S_i indicate that these current densities depend upon several position coordinates. In practice however, the electron motion in the x-direction will average out any ion density variations in the x-direction. Similarly, the ions traveling in the y-direction average out possible electron density variations in the y-direction. Thus, the only density variations that need be considered are those in the z-direction. Equation (A-5) may now be written as

$$R'_{1N}(z)\,dz = \frac{(v_i^2 + v_e^2)^{\frac{1}{2}}}{e^2\, v_i\, v_e}\ \sigma_{1N}\ i(z)\ j(z)\ dz \qquad \text{(A-6)}$$

where i(z) and j(z) are the one dimensional ion and electron current densities, respectively. Upon integration, the expression for the number of ionizing events per second becomes

$$R_{1N} = \frac{(v_i^2 + v_e^2)^{\frac{1}{2}}}{e^2\, v_i\, v_e}\ \sigma_{1N} \int_{-\infty}^{\infty} i(z)\ j(z)\ dz \qquad \text{(A-7)}$$

In the present experiment the number of ionizing events per second is not observed but is obtained indirectly from the measured $I_{SIG}^{N+}(I,J)$ current as shown by Equation (A-8).

$$R_{1N} = \frac{I_{SIG}^{N+}(I,J)}{e\ N} \qquad \text{(A-8)}$$

Substitution of this result into Equation (A-7) and solving for σ_{1N} yields

$$\sigma_{1N} = \frac{e\ v_i\ v_e}{N(v_i^2 + v_e^2)^{\frac{1}{2}}} \cdot \frac{I_{SIG}^{N+}(I,J)}{\int_{-\infty}^{\infty} i(z)\ j(z)\ dz} \qquad \text{(A-9)}$$

Note that Equation (A-9) is an expression for the desired cross section in terms of the various experimental parameters and is identical to Equation (4) in the text.

Normally, the electron velocity is much greater than the ion velocity and so it is very nearly correct and quite convenient to write Equation (A-9) in the following form:

$$\sigma_{1N} = \frac{e\, v_i}{N} \cdot \frac{I^{N+}_{SIG}(I,J)}{I\ J} \cdot F \qquad \text{(A-10)}$$

where

$$F \triangleq \frac{I\ J}{\int_{-\infty}^{\infty} i(z)\ j(z)\ dz} \equiv \frac{\int_{-\infty}^{\infty} i(z)\ dz \int_{-\infty}^{\infty} j(z)\ dz}{\int_{-\infty}^{\infty} i(z)\ j(z)\ dz} \qquad \text{(A-11)}$$

and I and J are the total target ion and total incident electron currents, respectively.

Note that with the exception of F, Equation (A-10) involves only known or directly measurable experimental quantities. The form factor, F, however, involves an overlap integral which depends upon the current density distributions of both the ion and electron beams. Fortunately, an accurate numerical approximation for the form factor may be obtained by using the movable slit scanner diagramed in Figure 4. This determination is made by first observing that the integrands in Equation (A-11) will, in practice, be zero outside some finite interval. Let this range of integration be uniformly partitioned into segments of length Δz. Under these conditions F may be approximated by

$$F \simeq \frac{\Delta z \sum_k i_k \sum_k j_k}{\sum_k i_k\ j_k} \qquad \text{(A-12)}$$

where i_k and j_k are the average ion and electron current densities respectively in the k^{th} partition.

If a movable slit scanner having an ion slit height h_i and an electron slit height h_e is positioned such that the slits are centered

on the k^{th} partition, then

$$i_k \cong \frac{I_k}{h_i} \tag{A-13}$$

and

$$j_k \cong \frac{J_k}{h_e} \tag{A-14}$$

where I_k and J_k are the ion and electron currents passing through their respective slits when the scanner is occupying the k^{th} position. Substitution of these relations into Equation (A-12) yields the following expression for the approximate form factor.

$$F = \frac{\Delta z \sum_k I_k \sum_k J_k}{\sum_k I_k J_k} \tag{A-15}$$

Thus, if the scanner is moved across the beams in uniform steps of length Δz, the resulting incremental currents allow the calculation of an approximate form factor. It should be emphasized that this expression for the form factor is independent of the slit heights and is a function of only the Δz spacing between slit positions.

APPENDIX B

TYPICAL EXPERIMENTAL PARAMETERS AND DATA

Typical experimental parameters and data are presented in Tables 4 through 8. Table 4 summarizes selected experimental operating parameters and the results of several preliminary adjustments observed just prior to run number 167-53. Form factor data appropriate to this particular determination and the corresponding double ionization measurement data appear in Tables 5 and 6, respectively. Similarly, Table 7 presents typical triple ionization measurement data while Table 8 displays experimental parameters characteristic of the quadruple ionization configuration.

TABLE 4. Typical Experimental Operating Parameters

RUN: 167-53	ELECTRON ENERGY: 300 eV	ION: Rb^+
DATE: 11-27-78	ION ENERGY: 1500 eV	PROCESS: σ_{13}
APERTURE CURRENT: 0μA	ELECTRON CURRENT: 1800μA	ION CURRENT: 33.3nA
PRESSURE: 7×10^{-9}t	DUTY CYCLES: J-100%, I-100%	ELECTROMETER SCALE: 30mV

ADJUST FOCUSING

I in 1^+ Cup: 32.7nA	First Analyzer Voltage:	980 ± 30V
I in 3^+ Cup: 32.5nA	First Analyzer Voltage:	2940 ± 40V
	Second Analyzer Voltage:	1600 ± 100V

1^+ to 3^+ loss: 0.62%

TABLE 5. Typical Form Factor Data Sheet

DIFFERENTIAL FORM FACTOR

σ_{1N} For Rb^+ (N = 3)	DATE: 11-27-78
TAKEN: BEFORE RUN # 167-53	SLOW ELECTRON CORRECTION:
ELECTRON ENERGY = 300 eV	SEC = 1833/1810 = 1.013

QUANTITY	INITIAL	FINAL
I	33.1×10^{-9} A	32.8×10^{-9} A
J	1833 μA	1829 μA

INDEX	I_k(nA)	J_k(μA)	$I_k J_k (10^{-15} A^2)$
1228	0	0	0
1207	0.05	0	0
1186	0.31	0	0
1164	0.86	0	0
1144	1.41	0	0
1123	1.57	0	0
1103	1.63	0	0
1082	1.72	0	0
1061	1.64	0	0
1040	1.63	1	1.63

TABLE 5. Typical Form Factor Data Sheet (Continued)

INDEX	I_k(nA)	J_k(μA)	$I_kJ_k(10^{-15}A^2)$
1020	1.65	3	4.95
999	1.68	43	72.24
978	1.71	268	458.28
957	1.74	479	833.46
936	1.78	416	740.48
916	1.86	300	558.00
894	1.94	185	358.90
874	2.09	89	186.01
853	1.95	18	35.10
832	1.37	5	6.85
812	1.75	2	3.50
790	1.74	0	0
770	0.73	0	0
749	0.14	0	0
728	0	0	0

Δz	ΣI_k	ΣJ_k	ΣI_kJ_k
0.015 in	32.95 nA	1809 A	3259.4×10^{-15} A^2

$$F = (2.54 \text{ cm/in})(\Delta z \text{ in}) \frac{(\Sigma I_k)(\Sigma J_k)}{\Sigma(I_kJ_k)} = 0.697 \text{ cm}$$

TABLE 6. Typical DC Mode Measurement Data For σ_{13} Configuration

RUN: 167-53	ELECTRON ENERGY: 300 eV	ION: Rb^+
DATE: 11-27-78	APERTURE CURRENT: 0 μA	PROCESS: σ_{13}

MEASURED SIGNALS

$I^{N+}(I,J)$	$I^{N+}(I,O)$	$I^{N+}(O,J)$	$I^{N+}(O,O)$
$+ 2.084 \times 10^{-15}$A	0.000×10^{-15}A	0.000×10^{-15}A	0.000×10^{-15}A
$+ 2.084 \times 10^{-15}$A	0.000×10^{-15}A	0.000×10^{-15}A	0.000×10^{-15}A
$+ 2.064 \times 10^{-15}$A	0.000×10^{-15}A	0.000×10^{-15}A	0.000×10^{-15}A
AVERAGE			
$+ 2.077 \times 10^{-15}$A	0.000×10^{-15}A	0.000×10^{-15}A	0.000×10^{-15}A

$$I_{SIG}^{N+}(I,J) = [I^{N+}(I,J) - I^{N+}(I,O)] - [I^{N+}(O,J) - I^{N+}(O,O)]$$

$$I_{SIG}^{N+}(I,J) = 2.077 \times 10^{-15}\text{A}$$

ION ENERGY = 1500 eV	$\frac{e\ v_i}{N} = 3.1026 \times 10^{-13}$ (N = 3)
ION CURRENT: $I = 3.33 \times 10^{-8}$A	ELECTRON CURRENT: $J = 18.00 \times 10^{-4}$A
FORM FACTOR: F = 0.697 cm	SLOW ELECTRON CORRECTION: SEC = 1.013

$$\sigma_{1N} = \frac{e\ v_i}{N} \cdot \frac{I_{SIG}^{N+}(I,J)}{I \quad J} \cdot F \cdot SEC$$

$$\sigma_{1N} = 7.59 \times 10^{-18}\text{cm}^2 \quad (300\text{ eV, N=3})$$

TABLE 7. Typical Pulsed Mode Measurement Data

For σ_{14} Configuration

RUN: 176-98	ELECTRON ENERGY: 800 eV	ION: Rb^+
DATE: 7-12-79	APERTURE CURRENT: 0 μA	PROCESS: σ_{14}

MEASURED SIGNALS

COINCIDENCE	ANTICOINCIDENCE	$I^{N+}_{SIG}(I,J) = \frac{I^{N+}_C - I^{N+}_A}{2}$
$+ 5.8820 \times 10^{-16}$ A	$+ 0.5042 \times 10^{-16}$ A	$+ 2.6889 \times 10^{-16}$ A
$+ 5.6468 \times 10^{-16}$ A	$+ 0.6386 \times 10^{-16}$ A	$+ 2.5041 \times 10^{-16}$ A
$+ 5.9157 \times 10^{-16}$ A	$+ 0.6050 \times 10^{-16}$ A	$+ 2.6553 \times 10^{-16}$ A
	AVERAGE SIGNAL	$+ 2.6161 \times 10^{-16}$ A

ION ENERGY = 1500 eV	$\frac{e\ v_i}{N} = 2.327 \times 10^{-13}$ (N = 4)
ION CURRENT: $I = 2.76 \times 10^{-8}$ A	ELECTRON CURRENT: $J = 7.27 \times 10^{-4}$ A
FORM FACTOR: F = 0.666 cm	SLOW ELECTRON CORRECTION: SEC = 1.011

$$\sigma_{1N} = \frac{e\ v_i}{N} \cdot \frac{I^{N+}_{SIG}(I,J)}{I\ \ J} \cdot F \cdot SEC$$

$$\sigma_{1N} = 2.04 \times 10^{-18}\ cm^2 \quad (800\ eV,\ N = 4)$$

TABLE 8. Typical Pulsed Mode Measurement Data

For σ_{i5} Configuration

RUN NUMBER:	177-4
DATE:	7-23-79
ELECTRON ENERGY:	400 eV
N:	5
ION ENERGY:	1500 eV
e:	1.602×10^{-19} Coulombs
v_i:	5.82×10^{6} cm/sec
$I^{N+}_{SIG}(I,J)$:	5.294×10^{-17} A
I:	3.00×10^{-8} A
J:	7.17×10^{-4} A
F:	0.509 cm
SEC:	1.011

$$\sigma_{1N} = \frac{e\ v_i}{N} \cdot \frac{I^{N+}_{SIG}(I,J)}{I \quad J} \cdot F \cdot SEC$$

$$\sigma_{1N} = 2.36 \times 10^{-19} cm^2 \quad (400\ eV,\ N=5)$$

REFERENCES†

1. J. J. Thomson, Philos. Mag. 23, 449 (1912).

2. G. H. Dunn, IEEE Trans. Nucl. Sci. NS-23, 929 (1976).

3. D. H. Crandall, R. A. Phaneuf, and P. O. Taylor, Phys. Rev. A 18, 1911 (1978).

4. M. H. Mittleman, Phys. Rev. Lett. 16, 498 (1966).

5. A. van der Woude, IEEE Trans. Nucl. Sci. NS-19, 187 (1972).

6. R. J. Tweed, J. Phys. B, 6, 270 (1973).

7. M. Gryzinski, Phys. Rev. 138, A336 (1965).

8. J. N. Bardsley and M. A. Biondi, Adv. At. Mol. Phys. 6, 1 (1970).

9. R. U. Datla, M. Blaha, and H. J. Kunze, Phys. Rev. A 12, 1076 (1975).

10. F. L. Walls and G. H. Dunn, Phys. Today 27, 30 (1974).

11. C. J. Cook and C. M. Ablow, AFCRC-TN-59-472 (1959).

12. S. M. Trujillo, R. H. Neynaber, and E. W. Rothe, Rev. Sci. Instrum. 37, 1655 (1966).

13. J. Wm. McGowan, R. Caudano, and J. Keyser, Phys. Rev. Lett. 36, 1447 (1976).

14. D. Auerbach, R. Cacak, R. Caudano, T. D. Gaily, C. J. Keyser, J. Wm. McGowan, J. B. A. Mitchell, and S. F. J. Wilk, J. Phys. B 10, 3797 (1977).

15. V. A. Belyaev, B. G. Brezhnev, and E. M. Erastov, JETP Lett. 3, 207 (1966).

16. R. D. Rundel, K. L. Aitken, and M. F. A. Harrison, J. Phys. B 2, 954 (1969).

---

† The abbreviations appearing herein conform to those suggested by the American Institute of Physics Style Manual (1978).

17. H. D. Smyth, Proc. R. Soc., London 102, 283 (1923).

18. A. Von Hippel, Ann. Phys. 87, 1035 (1928).

19. R. W. Ditchburn, Proc. R. Soc., London 123, 516 (1929).

20. H. Funk, Ann. Phys. 4, 149 (1930).

21. R. L. F. Boyd and G. W. Green, Proc. R. Soc., London 71, 351 (1958).

22. W. L. Fite and R. T. Brackmann, Phys. Rev. 112, 1141 (1958).

23. K. T. Dolder, M. F. A. Harrison, and P. C. Thonemann, Proc. R. Soc., London A-264, 367 (1961).

24. K. T. Dolder, M. F. A. Harrison, and P. C. Thonemann, Proc. R. Soc., London A-274, 546 (1963).

25. M. F. A. Harrison, K. T. Dolder, and P. C. Thonemann, Proc. Phys. Soc., London 82, 368 (1963).

26. W. C. Lineberger, J. W. Hooper, and E. W. McDaniel, Phys. Rev. 141, 151 (1966).

27. J. W. Hooper, W. C. Lineberger, and F. M. Bacon, Phys. Rev. 141, 165 (1966).

28. J. B. Wareing and K. T. Dolder, Proc. Phys. Soc., London 91, 887 (1967).

29. B. Peart and K. T. Dolder, J. Phys. B 1, 240 (1968).

30. B. Peart and K. T. Dolder, J. Phys. B 1, 872 (1968).

31. R. K. Feeney, J. W. Hooper, and M. T. Elford, Phys. Rev. A 6, 1469 (1972).

32. W. E. Sayle, II, R. K. Feeney, and T. F. Divine, Abstracts of Papers of the IXth International Conference on the Physics of Electronic and Atomic Collisions, edited by J. S. Risley and R. Geballe, (University of Washington Press, Seattle, 1975), pp. 895.

33. T. F. Divine, R. K. Feeney, W. E. Sayle, II, and J. W. Hooper, Phys. Rev. A 13, 54 (1976).

34. R. K. Feeney, W. E. Sayle, II, and T. F. Divine, Phys. Rev. A 18, 82 (1978).

35. K. L. Aitken and M. F. A. Harrison, J. Phys. B 4, 1176 (1971).

36. K. L. Aitken, M. F. A. Harrison, and R. D. Rundel, J. Phys. B 4, 1189 (1971).

37. J. N. Bradbury, T. E. Sharp, B. Mass, and R. N. Varney, Nucl. Instrum. Methods 110, 75 (1973).

38. W. D. Barfield, IEEE Trans. Plasma Sci. PS-6, 71 (1978).

39. B. L. Schram, F. J. DeHeer, M. J. Van Der Wiel, and J. Kistemaker, Physica 31, 94 (1965).

40. B. L. Schram, J. H. Boerboom, and J. Kistemaker, Physica 32, 185 (1966).

41. B. L. Schram, Physica 32, 197 (1966).

42. M. J. Van Der Wiel, TH. M. El-Sherbini, and L. Vriens, Physica 42, 411 (1969).

43. TH. M. El-Sherbini, M. J. Van Der Wiel, and F. J. DeHeer, Physica 48, 157 (1970).

44. R. K. Feeney, D. W. Baggett, D. W. Hughes, G. W. Rivers, and W. E. Sayle, ORO-3027-38 (1977).

45. R. K. Feeney, D. W. Hughes, G. B. Hoak, D. C. Priester, and W. E. Sayle, ORO-3027-43 (1978).

46. R. K. Feeney, D. W. Hughes, G. B. Hoak, and D. C. Priester, ORO-3027-48 (1979).

47. B. Peart and K. T. Dolder, J. Phys. B 2, 1169 (1969).

48. W. L. Fite, in Atomic and Molecular Processes, edited by D. R. Bates, (Academic Press Inc., New York, 1962), Chapter 12.

49. L. J. Kieffer and G. H. Dunn, Rev. Mod. Phys. 38, 1 (1966).

50. M. F. A. Harrison, Brit. J. Appl. Phys. 17, 371 (1966).

51. M. F. A. Harrison, in Methods of Experimental Physics, edited by B. Bederson and W. L. Fite, (Academic Press Inc., New York, 1968), pp. 95-115.

52. K. T. Dolder, in Case Studies in Atomic Collision Physics, Vol. I, edited by E. W. McDaniel and M. R. C. McDowell, (North-Holland Publishing Company, Amsterdam, 1969), Chapter 5.

53. G. H. Dunn, in Proceedings of the First International Conference on Atomic Physics, edited by B. Bederson, V. W. Cohen, and F. M. J. Pichanick, (Plenum Press, New York, 1969), pp. 417-433.

54. K. T. Dolder and B. Peart, Rep. Prog. Phys. 39, 693 (1976).

55. R. K. Feeney, Absolute Experimental Cross Sections for the Ionization of Singly Charged Barium Ions by Electron Impact, Ph.D. thesis Georgia Institute of Technology, Atlanta, Georgia, 1970.

56. R. K. Feeney, W. E. Sayle, II, and J. W. Hooper, Rev. Sci. Instrum. 47, 964 (1976).

57. J. R. Pierce, Theory and Design of Electron Beams, (D. Van Nostrand Company, Inc., Princeton, New Jersey, 1954), second edition, Chapter 10.

58. F. M. Bacon, The Excitation of Barium Ions by Electron Impact, Ph.D. thesis, Georgia Institute of Technology, Atlanta, Georgia, 1968.

59. A. L. Edwards, Statistical Analysis (Holt, Rinehart and Winston, Inc., New York, 1969), third edition, Chapter 11.

60. M. R. H. Rudge, Rev. Mod. Phys. 40, 564 (1968).

61. O. Bely and H. Van Regemorter, Ann. Rev. Astron. Astrophys. 8, 329, (1970).

62. M. J. Seaton, Planet. Space Sci. 12, 55 (1964).

63. M. Gryzinski, Phys. Rev. 115, 374 (1959).

64. M. Gryzinski, Phys. Rev. 138, A305 (1965).

65. M. Gryzinski, Phys. Rev. 138, A322 (1965).

66. L. Vriens, in Case Studies in Atomic Collision Physics, Vol. I, edited by E. W. McDaniel and M. R. C. McDowell, (North-Holland Publishing Company, Amsterdam, 1969), Chapter 6.

67. G. Elwert, Z. Naturforsch. 7a, 432 (1952).

68. W. C. Lineberger, The Ionization of Lithium Ions by Electron Impact, Ph.D. thesis, Georgia Institute of Technology, Atlanta, Georgia, 1965.

69. H. W. Drawin, Z. Phys. 164, 513 (1961).

70. H. W. Drawin, Z. Phys. 168, 238 (1962).

71. D. N. Tripathi and D. K. Rai, J. Chem. Phys. 55, 1268 (1971).

72. R. K. Feeney, private communication, October 1979.

REPORT NO. ORO–3027–53

Final Technical Report

Covering the Period
September 1, 1969 to March 31, 1980

THE EXCITATION AND IONIZATION OF IONS BY ELECTRON IMPACT

By:

R. K. Feeney
D. W. Hughes
J. W. Hooper

Contract No. EY–76–S–05–3027

U. S. Department of Energy
Oak Ridge, Tennessee

31 March

GEORGIA INSTITUTE OF TECHNOLOGY
SCHOOL OF ELECTRICAL ENGINEERING
ATLANTA, GEORGIA 30332

1980

FINAL REPORT

THE EXCITATION AND IONIZATION OF IONS BY ELECTRON IMPACT

REPORT NO. ORO-3027-53

by

R. K. Feeney
D. W. Hughes
J. W. Hooper

Covering the Period

September 1, 1969 to March 31, 1980

CONTRACT NO. EY-76-S-05-3027

Oak Ridge, Tennessee

U. S. Department of Energy

Georgia Institute of Technology
School of Electrical Engineering
Atlanta, Georgia 30332

March 31, 1980

TABLE OF CONTENTS

		Page
ABSTRACT		i
SECTION		
I.	INTRODUCTION	1
II.	SUMMARY OF TECHNICAL ACCOMPLISHMENTS	3
III.	PUBLICATIONS AND PRESENTATIONS	5
V.	GRADUATE STUDENT PARTICIPATION	11
APPENDIX	SUMMARY OF PROGRESS IN ELECTRON IMPACT IONIZATION MEASUREMENTS OF IONS	12
REFERENCES		17

ABSTRACT

This report presents a brief summary of the technical accomplishments of a research program active from September 1, 1969, through March 31, 1980. All of the work was related to the atomic collision process of importance in magnetic confinement fusion. A chronological tabulation of technical accomplishments, a list of publications, and a summary of progress in the measurement of electron impact ionization cross sections are given.

INTRODUCTION

This Final Report presents a brief summary of the accomplishments of a research program that was active over more than a decade. All of the work was related to the atomic collision process of importance in magnetic confinement fusion. The time period specified by the current contract to be covered by this report is September 1, 1969 through March 31, 1980. However, for completeness, work done in preceding periods from December 1, 1962 through August 31, 1969, which was completed under earlier revisions of the same contract, is also included.

The initial accomplishment under this research program was the first successful continuous beam measurement of the electron impact cross sections of a positive ion. This work was followed by important relative and absolute measurements of electron impact excitation cross sections of positive ions. Although most subsequent work was devoted to electron-ion collisions, thin film energy loss and electron neutral scattering measurements were also accomplished. In the final work of the program, the first triple and quadruple electron impact ionization cross sections were measured.

Since all of the work completed under this research program has been or will be reported in journal articles and major technical reports, technical results will not be presented in this Final Report. However, a chronological tabulation of the major technical accomplishments and a list of publications and presentations will be given. In addition student contribution to the research effort will be

reviewed. Because the research program covers such a long period of time and a wide variety of topics, it is impossible to present well-grounded summaries of progress in the present report. However, technical progress in the measurement of electron impact ionization cross sections, to which the majority of recent scientific effort has been devoted, is discussed in the Appendix.

SUMMARY OF TECHNICAL ACCOMPLISHMENTS

The significant technical accomplishments of the research program are listed below in approximate chronological order.

1965 First continuous beam measurement of the electron impact ionization cross section of a positive ion; the measurement of the electron impact ionization cross sections of Li^+ ions.

1965 Measurement of the electron impact ionization cross sections of Na^+ and K^+ ions.

1968 First relative measurement of an electron impact excitation cross section of a positive ion excited to an ordinary state; relative measurement of the electron impact excitation cross sections of the Ba^+ resonance lines.

1970 First absolute measurement of any electron impact excita-tion cross section of an ion; absolute measurement of the electron impact excitation cross sections of the Ba^+ resonance lines.

1970 Developed a small, surface-ionization-type source of positive ions.

1971 First measurement of an energy distribution of ions transiting a thin film as a function of incident energy and angle.

1975 First definitive microwave transient response measurement of electron-atom collision frequency.

1975 Measurement of the electron impact ionization cross sections of Tl^+ ions.

1976 Developed and characterized a family of aluminosilicate-type ion sources.

1978 Measurement of the electron impact single ionization cross sections of Rb^+ ions.

1979 Developed a class of aluminosilicate-metal-matrix-type ion sources.

1979 First measurement of the electron impact triple and quadruple ionization cross sections of an ion; measured the double, triple and quadruple electron impact ionization cross sections of Rb^+ ions.

PUBLICATIONS AND PRESENTATIONS

Listed below are the refereed publications, technical reports, and conference presentations that were partially supported by the contracting agency.

Refereed Publications

1. "Absolute Cross Sections for Single Ionization of Alkali Ions by Electron Impact. I. Description of Apparatus and Li^+ Results," W. C. Lineberger, J. W. Hooper, and E. W. McDaniel, Physical Review, Vol. 141, pp. 151-164, January 1966.

2. "Absolute Cross Sections for Single Ionization of Alkali Ions by Electron Impact. II. Na^+ and K^+ Results and Comparisons with Theory," J. W. Hooper, W. C. Lineberger, and F. M. Bacon, Physical Review, Vol. 141, pp. 165-173, January 1966.

3. "Relative Experimental Cross Sections for Excitation of Ba^+ Ions by Electron Impact (8.0-98eV)," F. M. Bacon and J. W. Hooper, Physical Review, Vol. 178, pp. 182-197, February 1969.

4. "Surface Ionization Type Ion Source of Ba^+ Ions for Use in Collision Experiments," R. K. Feeney, F. M. Bacon, M. T. Elford, and J. W. Hooper, Review of Scientific Instruments, Vol. 43, pp. 549-550, 1972.

5. "Absolute Experimental Cross Sections for the Ionization of Singly Charged Barium Ions by Electron Impact," R. K. Feeney, J. W. Hooper, and M. T. Elford, Physical Review A, Vol. 6, pp. 1469-1478, October 1972.

6. "Absolute Experimental Cross Sections for the Excitation of Barium Ions by Electron Impact," M. O. Pace and J. W. Hooper, Physical Review A, Vol. 7, pp. 2033-2055, June 1973.

7. "Absolute Experimental Cross Sections for the Ionization of Tl^+ Ions by Electron Impact," T. F. Divine, R. K. Feeney, William E. Sayle II, and J. W. Hooper, Physical Review A, Vol. 13, pp. 54-57, January 1976.

8. "Microwave Transient Response Measurements of Elastic Momentum Transfer Collison Frequency in Argon," D. A. McPherson, R. K. Feeney, and J. W. Hooper, Physical Review A, Vol. 13, pp. 167-179, January 1976.

9. "Aluminosilicate Sources of Positive Ions for Use in Collision Experiments," R. K. Feeney, William E. Sayle II, and J. W. Hooper, Review of Scientific Instruments, Vol. 46, pp. 964-967, August 1976.

10. "Absolute Experimental Cross Sections for the Electron Impact Ionization of Rb^+ Ions," R. K. Feeney, W. E. Sayle, and T. F. Divine, Physical Review A, Vol. 18, pp. 82-84, July 1978.

11. Multiple Ionization of Rb^+ Ions," D. W. Hughes and R. K. Feeney, to be submitted to Physical Review A.

12. "An Aluminosilicate-Composite Type Ion Source of Alkali Ions," D. W. Hughes and R. K. Feeney, to be submitted to Review of Scientific Instruments.

Technical Reports

1. The Ionization of Alkali Ions by Electron Impact, W. C. Lineberger, J. W. Hooper, and E. W. McDaniel, Technical Progress Report No. 8 (Summary Report), Report No. ORO-3027-8, U. S. Atomic Energy Commission, Georgia Institute of Technology, May 1965.

2. The Excitation and Ionization of Ions by Electron Impact, J. W. Hooper and F. M. Bacon, Technical Progress Report No. ORO-3027-10, U. S. Atomic Energy Commission, Georgia Institute of Technology, February 1967.

3. The Excitation of Barium Ions by Electron Impact, F. M. Bacon and J. W. Hooper, Technical Summary Report, Report No. ORO-3027-12, U. S. Atomic Energy Commission, Georgia Institute of Technology, February 1968.

4. The Excitation and Ionization of Ions by Electron Impact, J. W. Hooper, Technical Progress Report, Report No. ORO-3027-13, U. S. Atomic Energy Commission, Georgia Institute of Technology, May 1968.

5. The Excitation and Ionization of Ions by Electron Impact, J. W. Hooper, J. C. Majure, D. McPherson, and M. O. Pace, Technical Progress Report, Report No. ORO-3027-15, U. S. Atomic Energy Commission, Georgia Institute of Technology, May 1969.

6. The Excitation and Ionization of Ions by Electron Impact, J. W. Hooper, R. K. Feeney, J. C. Majure, D. McPherson, and M. O. Pace, Technical Progress Report, Report No. ORO-3027-16, U.S. Atomic Energy Commission, Georgia Institute of Technology, May 1970.

7. Absolute Experimental Cross Sections for the Ionization of Singly Charged Barium Ions by Electron Impact, R. K. Feeney and J. W. Hooper, Technical Summary Report, Report No. ORO-3027-18, U.S. Atomic Energy Commission, Georgia Institute of Technology, January 1971.

8. The Excitation and Ionization of Ions by Electron Impact, J. W. Hooper, R. K. Feeney, J. C. Majure, and D. McPherson, Technical Progress Report, Report No. ORO-3027-19, U.S. Atomic Energy Commission, May 1971.

9. The Excitation and Ionization of Ions by Electron Impact, J. W. Hooper, R. K. Feeney, W. E. Sayle, D. McPherson, and P. Schlthess, Technical Progress Report, Report No. ORO-3027-21, U.S. Atomic Energy Commission, Georgia Institute of Technology, May 1972.

10. The Excitation and Ionization of Ions by Electron Impact, R. K. Feeney, T. F. Divine, J. W. Hooper, D. McPherson, and W. E. Sayle, Technical Progress Report, Report No. ORO-3027-22, U.S. Atomic Energy Commission, Georgia Institute of Technology, May 1973.

11. The Excitation and Ionization of Ions by Electron Impact, R. K. Feeney, T. F. Divine, J. W. Hooper, R. M. Kovac, D. McPherson, and W. E. Sayle, Technical Progress Report, Report No. ORO-3027-23, U.S. Atomic Energy Commission, Georgia Institute of Technology, May 1974.

12. Microwave Transient Response Measurements of Elastic Momentum Transfer Collision Frequency, D. A. McPherson, R. K. Feeney, and J. W. Hooper, Technical Summary Report, Report No. ORO-3027-26, U.S. Atomic Energy Commission, Georgia Institute of Technology, December 1974.

13. The Excitation and Ionization of Ions by Electron Impact, R. K. Feeney, T. F. Divine, R. M. Kovac, D. McPherson, and W. E. Sayle, Technical Progress Report, Report No. ORO-3027-30, U.S. Energy Research and Development Administration, Georgia Institute of Technology, May 1975.

14. The Excitation and Ionization of Ions by Electron Impact, R. K. Feeney, D. W. Baggett, D. W. Hughes, G. W. Rivers, and W. E. Sayle, Technical Progress Report, Report No. ORO-3027-33, U.S. Energy Research and Development Administration, Georgia Institute of Technology, May 1976.

15. The Excitation and Ionization of Ions by Electron Impact, R. K. Feeney, D. W. Baggett, D. W. Hughes, G. W. Rivers, and W. E. Sayle, Technical Progress Report, Report No. ORO-3027-38, U.S. Energy Research and Development Administration, Georgia Institute of Technology, May 1977.

16. The Excitation and Ionization of Ions by Electron Impact, R. K. Feeney, D. W. Hughes, G. B. Hoak, D. C. Priester, and W. E. Sayle, Technical Progress Report, Report No. ORO-3027-43, U.S. Department of Energy, Georgia Institute of Technology, May 1978.

17. The Excitation and Ionization of Ions by Electron Impact, R. K. Feeney, D. W. Hughes, G. B. Hoak, and D. C. Priester, Technical Progress Report, Report No. ORO-3027-48, U.S. Department of Energy, Georgia Institute of Technology, May 1979.

18. The Electron Impact Ionization of Rubidium Ions, D. W. Hughes and R. K. Feeney, Technical Summary Report, Report No. ORO-3027-52, U. S. Department of Energy, Georgia Institute of Technology, March 1980.

19. The Excitation and Ionization of Ions by Electron Impact, R. K. Feeney, D. W. Hughes and J. W. Hooper, Final Report, No. ORO-3027-53, U. S. Department of Energy, Georgia Institute of Technology, March 1980.

Presentations

1. "Absolute Experimental Cross Sections for Single Ionization of Na^+ and K^+ Ions by Electron Impact," J. W. Hooper, W. C. Lineberger, and F. M. Bacon, IVth International Conference on the Physics of Electronic and Atomic Collisions, Quebec, Canada, August 1965.

2. "Relative Experimental Cross Sections for Excitation of Ba^+ Ions by Electron Impact," F. M. Bacon and J. W. Hooper, Vth International Conference on the Physics of Electronic and Atomic Collisions, NAUKA, Leningrad, USSR, July 1967.

3. "Absolute Experimental Cross Sections for Excitation of Ba^+ Ions by Electron Impact," M. O. Pace and J. W. Hooper, VIth International Conference on the Physics of Electronic and Atomic Collisions, MIT, Boston, MA, July 1969.

4. "Absolute Experimental Cross Sections for the Single Ionization of Ba^+ Ions by Electron Impact," J. W. Hooper and R. K. Feeney, VIth International Conference on the Physics of Electronic and Atomic Collisions, MIT, Boston, MA, July 1969.

5. "Status of Electron Impact Ionization Cross Section Measurements," Symposium on Electron-Ion Collision, R. K. Feeney, Joint Institute for Laboratory Astrophysics, University of Colorado, Boulder, CO, July 1974, (invited paper).

6. "Absolute Experimental Cross Sections for the Ionization of Tl^+ Ions by Electron Impact," T. F. Divine, R. K. Feeney, J. W. Hooper, and W. E. Sayle II, XXVIIth Annual Gaseous Electronics Conference, Houston, TX, October 1974.

7. "Microwave Transient Response Measurements of Elastic Momentum Transfer Collision Frequency," D. W. McPherson, R. K. Feeney, and J. W. Hooper, XXVII Annual Gaseous Electronics Conference, Houston, TX, October 1974.

8. "Aluminosilicate Sources of Positive Ions," R. K. Feeney, W. E. Sayle, and J. W. Hooper, Second International Conference on Plasma Science, Ann Arbor, MI, May 1975.

9. "Absolute Experimental Cross Sections for the Ionization of Cs^+ Ions by Electron Impact," W. E. Sayle, R. K. Feeney, and T. F. Divine, IXth International Conference on the Physics of Electronic and Atomic Collisions, Seattle, WA, July 1975.

10. "Measurements of the Electron Impact Ionization Cross Sections of Rb^+ Ions," R. K. Feeney, W. E. Sayle II, and T. F. Divine, XXVIIIth Annual Gaseous Electronics Conference, Rolla, MO, October 1975.

11. "Electron Impact Double Ionization Cross Sections for Use in Beam-Probe Calibration," R. K. Feeney and W. E. Sayle, IEEE International Conference on Plasma Science, Austin, TX, May 1976.

12. "Electron Impact Double Ionization Cross Sections of Cs^+ Ions," R. K. Feeney and W. E. Sayle, XXIXth Annual Gaseous Electronics Conference, Cleveland, OH, October 1976.

13. "Electron Impact Double Ionization Cross Sections of Tl^+ Ions," R. K. Feeney and W. E. Sayle II, Conference on Atomic Processes in High Temperature Plasmas, Knoxville, TN, February 1977.

14. "A Penning-Type Ion Source for Collision Experiments," D. W. Hughes, R. K. Feeney, and W. E. Sayle, IEEE International Conference on Plasma Science, Troy, NY, May 1977.

15. "Absolute Cross Sections of Electron Impact Double Ionization of Na^+ Ions," W. E. Sayle and R. K. Feeney, Xth International Conference on the Physics of Electronic and Atomic Collisions," Paris, France, July 1977.

16. "Absolute Experimental Cross Sections for the Electron Impact Ionization of Rb^+ Ions for Use in Ion Beam Probe Calibration," D. W. Hughes, R. K. Feeney, and W. E. Sayle II, IEEE International Conference on Plasma Science, Monterey, CA, May 1978.

17. "Electron Impact Double Ionization Cross Sections of K^+ Ions," R. K. Feeney and W. E. Sayle II, XXXIst Annual Gaseous Electronics Conference, Buffalo, NY, October 1978.

18. "Electron Impact Multiple Ionization of Alkali Ions," R. K. Feeney, D. W. Hughes, and W. E. Sayle, Conference on Atomic Processes in High Temperature Plasmas, Boulder, CO, January 1979.

19. "A Thermionic Ion Source for Use in Collision Experiments," D. W. Hughes, R. K. Feeney, and A. T. Chapman, IEEE International Conference on Plasma Science, Montreal, Quebec, Canada, June 1979.

GRADUATE STUDENT PARTICIPATION

Many outstanding students were associated with the research program over its long history. Six Ph.D. degrees and four M.S. degrees were awarded to students active in the work. A summary of student participation is given below in Table I.

TABLE I. STUDENT RESEARCH

Student Name	Research Topic	Degree	Date Graduated	Current Area of Specialization
W. C. Lineberger	Ionization of Li^+, Na^+ and K^+	Ph.D.	1965	Physical Chemistry
F. M. Bacon	Excitation of Ba^+ (relative)	Ph.D.	1967	Ion and Neutron Source Development
M. O. Pace	Excitation of Ba^+ (absolute)	Ph.D.	1970	Gas Breakdown
R. K. Feeney	Ionization of Ba^+	Ph.D.	1970	Atomic Collisions and Materials
J. C. Majure	Energy Loss In Thin Films	Ph.D.	1971	Electromagnetics
D. A. McPherson	Momentum Transfer Collision Frequency	Ph.D.	1974	Simulation of Electromagnetic Systems
T. F. Divine	Ionization of Tl^+, Rb^+ and Cs^+	M.S.	1974	Antennas and Computers
R. M. Kovac	Ion Source Development	M.S.	1975	Electronics
D. W. Baggett	Excitation	M.S.	1977	Systems
D. W. Priester	Ion Source Development	M.S.	1979	Power Engineering
D. W. Hughes	Multiple Ionization of Rb^+	Ph.D.	1980	Semiconductor Fabrication

APPENDIX

SUMMARY OF PROGRESS IN ELECTRON IMPACT IONIZATION MEASUREMENTS OF IONS

The twenty years from about 1960 to 1980 have seen immense progress in electron impact ionization measurements. The beginning of this period coincided with the development of the crossed beam techniques for collision experiments. This method has now been applied to a wide variety of ionization processes involving many different ionic species. At the present time it appears that the factor limiting the extension to this technique to many processes of current interest is the inability to produce the desired ion in a known quantum state. It is therefore likely that indirect measurements of ionization cross sections will become increasingly important in the future.

The following material briefly summarizes the possible experimental techniques and discusses the status of crossed beam measurements.

Experimental Techniques

Historically, a considerable effort has been devoted to the development of techniques for the experimental investigation of collisions between interacting particles. Although quite diverse in their individual characteristics, nearly all of these procedures can be grouped into one of four general categories of experiments. Selected techniques from a particular category then allow either

the direct measurement or the indirect inference of the desired absolute atomic cross sections.

In plasma afterglow experiments, for instance, a target gas is initially heated by means of a shock wave or an electrical discharge. Observation of the resulting afterglow then allows the experimenter to infer relative cross sections about the processes of interest.[1] Unfortunately, such a technique is not inherently absolute, and thus it is necessary to calibrate the apparatus on a plasma whose characteristics have been independently determined.

An alternative approach attempts to deduce reaction rates from spectroscopic observations of plasmas with known characteristics.[2] This procedure suffers from a host of interpretive difficulties but appears to hold promise for the very highly charged ions whose cross sections are inaccessible by other methods.

The third technique involves trapping target particles by means of a static electric or magnetic field and subsequently bombarding them with projectiles of known energy.[3] This procedure has yielded relative atomic cross sections for several processes of interest but must be absolutely calibrated by comparison with events having independently determined cross sections.

Finally, the most frequently employed method, and the only technique which is inherently absolute, involves a direct collision between the two beams of particles. Subsequent measurement of the rate at which the resulting products are formed then allows the determination of the desired atomic cross sections. In principle, the two colliding beams may intersect at any angle between zero and ninety degrees. In the particular case when the intersection

angle is zero degrees, the technique is known as "merging beams." Formal suggestion of the merged beam concept has been in existence since at least 1959 when it was recognized that the interaction energy may be made arbitrarily small with this technique.[4,5] There is, in fact, little doubt that the merged beam procedure has allowed investigation of the previously inaccessible energy range from thermal energies to a few electron volts. Unfortunately, important difficulties with the method still exist and, in particular, it remains a formidable undertaking for experimentalists to determine the intersection geometry of the colliding particles with satisfactory accuracy in a merged beam configuration.[6,7]

In contrast, adjustment of the intersection angle to a value between zero and ninety degrees to conduct an "inclined beam" experiment was suggested in the 1960's.[8,9] This concept was introduced in an attempt to trade-off the low interaction energy inherent in the merged beam technique for a more accurate knowledge of the intersection geometry of the colliding beams. In principle, the most advantageous feature of inclined beams at different angles is the variety of interaction energies accessible. However, remaining difficulties with the collison geometry have encouraged manipulation of the intersection angle to the limiting value of ninety degrees. In fact, this special case of perpendicular intersection is of such importance that the term "crossed beams" has been reserved for its description.

Status of Crossed Beam Experiments

Experimental realizations of the crossed beam concept have been in existence since the 1920's. Early measurements concentrated on the bombardment of neutral atoms with beams of electrons to infer ionization potentials and, hence, binding energies for mercury, potassium and sodium.[10-13] These pioneering experiments demonstrated the fundamentals of the technique but frequently yielded excessive values for the resulting atomic cross sections. The universal difficulty with these early experiments involved the interaction of the atomic beam with the background gas. In particular, the target beam was often charged stripped on the residual gas in the system and, hence, gave rise to an erroneously high product collection rate. Shortcomings of this nature were largely circumvented in 1958 when experimentalists began using modulated beams and synchronous detection to separate legitimate signal from the charge stripping background.[14,15] Numerous measurements of electron impact ionization cross sections for neutral atoms soon followed, and in the early 1960's the crossed beam technique was successfully applied to the study of charged particle--charged particle collisions. Of particular importance was the work performed at Culham Laboratory in England resulting in single ionization cross sections for He^+, Ne^+ and N^+ ions.[16-18] Since that time many other cross sections of interest have been determined using the crossed beam technique, and much of the earlier work has been critically evaluated.[19-25] Much of the subsequent activity has been motivated by the data needs of the Controlled Thermonuclear Research program. As a result, single

ionization cross sections for Ba^+, Tl^+ and all the singly charged alkali ions have been determined.[26-34] Similarly, some effort has been devoted to the single ionization of multiply charged atmospheric ions in an attempt to extrapolate existing theory to more complex electronic structures.[35-39] Comparatively little attention has, however, been given to the interesting single collision, multiple ionization events. Scientists in the Netherlands have, however, attempted some relative abundance measurements for the production of multiply charged noble gases by electron impact.[40-42] Unfortunately, these experiments apparently suffer from metastable contamination of the primary beam and, in any event, the results do not agree with independent determinations of the relevant cross sections.[43,44] Similarly, the Georgia Tech group has recently done some preliminary work on the double ionization of alkali ions for use in ion beam probe calibration.[45-47] To date, however, Peart and Dolder's double ionization cross section for Li^+ is the only reliable multiple ionization measurement reported in the literature.[48]

The research, summarized in the last Technical Summary Report (ORO-3027-52) of the present contract, is expected to contribute substantially to the higher order ionization data base by reporting the first successful measurement of the absolute cross sections for the electron impact double, triple and quadruple ionization of singly charged rubidium ions.

REFERENCES

1. J. N. Bardsley and M. A. Biondi, Adv. At. Mol. Phys. 6, 1 (1970).

2. R. U. Datla, M. Blaha, and H. J. Kunze, Phys. Rev. A 12, 1076 (1975).

3. F. L. Walls and G. H. Dunn, Phys. Today 27, 30 (1974).

4. C. J. Cook and C. M. Ablow, AFCRC-TN-59-472 (1959).

5. S. M. Trujillo, R. H. Neynaber, and E. W. Rothe, Rev. Sci. Instrum. 37, 1655 (1966).

6. J. Wm. McGowan, R. Caudano, and J. Keyser, Phys. Rev. Lett. 36, 1447 (1976).

7. D. Auerbach, R. Cacak, R. Caudano, T. D. Gaily, C. J. Keyser, J. Wm. McGowan, J. B. A. Mitchell, and S. F. J. Wilk, J. Phys. B. 10, 3797 (1977).

8. V. A. Belyaev, B. G. Brezhnev, and E. M. Erastov, JETP Lett. 3, 207 (1966).

9. R. D. Rundel, K. L. Aitken, and M. F. A. Harrison, J. Phys. B. 2, 954 (1969).

10. H. D. Smyth, Proc. R. Soc., London 102, 283 (1923).

11. A. Von Hippel, Ann. Phys. 87, 1035 (1928).

12. R. W. Ditchburn, Proc. R. Soc., London 123, 516 (1929).

13. H. Funk, Ann. Physik 4, 149 (1930).

14. R. L. F. Boyd and G. W. Green, Proc. R. Soc., London 71, 351 (1958).

15. W. L. Fite and R. T. Brackmann, Phys. Rev. 112, 1141 (1958).

16. K. T. Dolder, M. F. A. Harrison, and P. C. Thonemann, Proc. R. Soc., London A-264, 367 (1961).

17. K. T. Dolder, M. F. A. Harrison, and P. C. Thonemann, Proc. R. Soc., (London) A-274, 546 (1963).

18. M. F. A. Harrison, K. T. Dolder, and P. C. Thonemann, Proc. Phys. Soc., London 82, 368 (1963).

19. W. L. Fite, in Atomic and Molecular Processes, edited by D. R. Bates, (Academic Press Inc., New York, 1962), Chapter 12.

20. L. J. Kieffer and G. H. Dunn, Rev. Mod. Phys. 38, 1 (1966).

21. M. F. A. Harrison, Brit. J. Appl. Phys. 17, 371 (1966).

22. M. F. A. Harrison, in Methods of Experimental Physics, edited by B. Bederson and W. L. Fite, (Academic Press Inc., New York, 1968), pp. 95-115.

23. K. T. Dolder, in Case Studies in Atomic Collision Physics, Vol. I, edited by E. W. McDaniel and M. R. C. McDowell, (North-Holland Publishing Company, Amsterdam, 1969), Chapter 5.

24. G. H. Dunn, in Proceedings of the First International Conference on Atomic Physics, edited by B. Bederson, V. M. Cohen, and F. M. J. Pichanick, (Plenum Press, New York, 1969), pp. 417-433.

25. K. T. Dolder and B. Peart, Rep. Prog. Phys. 39, 693 (1976).

26. W. C. Lineberger, J. W. Hooper, and E. W. McDaniel, Phys. Rev. 141, 151 (1966).

27. J. W. Hooper, W. C. Lineberger, and F. M. Bacon, Phys. Rev. 141, 165 (1966).

28. J. B. Wareing and K. T. Dolder, Proc. Phys. Soc., London 91, 887 (1967).

29. B. Peart and K. T. Dolder, J. Phys. B 1, 240 (1968).

30. B. Peart and K. T. Dolder, J. Phys. B 1, 872 (1968).

31. R. K. Feeney, J. W. Hooper, and M. T. Elford, Phys. Rev. A 6, 1469 (1972).

32. W. E. Sayle II, R. K. Feeney, and T. F. Divine, Abstracts of Papers of the IXth International Conference on the Physics of Electronic and Atomic Collisions, edited by J. S. Risley and R. Geballe, (University of Washington Press, Seattle, 1975), pp. 895.

33. T. F. Divine, R. K. Feeney, W. E. Sayle II, and J. W. Hooper, Phys. Rev. A 13, 54 (1976).

34. R. K. Feeney, W. E. Sayle II, and T. F. Divine, Phys. Rev. A 18, 82 (1978).

35. D. H. Crandall, R. A. Phaneuf, and P. O. Taylor, Phys. Rev. A 18, 1911 (1978).

36. K. L. Aitken and M. F. A. Harrison, J. Phys. B 4, 1176 (1971).

37. K. L. Aitken, M. F. A. Harrison, and R. D. Rundel, J. Phys. B 4, 1189 (1971).

38. J. N. Bradbury, T. E. Sharp, B. Mass, and R. N. Varney, Nucl. Instrum. Methods 110, 75 (1973).

39. W. D. Barfield, IEEE Trans. Plasma Sci. PS-6, 71 (1978).

40. B. L. Schram, F. J. DeHeer, M. J. Van Der Wiel, and J. Kistemaker, Physica 31, 94 (1965).

41. B. L. Schram, J. H. Boerboom, and J. Kistemaker, Physica 32, 185 (1966).

42. B. L. Schram, Physica 32, 197 (1966).

43. M. J. Van Der Wiel, TH. M. El-Sherbini, and L. Vriens, Physica 42, 411 (1969).

44. TH. M. El-Sherbini, M. J. Van Der Wiel, and F. J. DeHeer, Physica 48, 157 (1970).

45. R. K. Feeney, D. W. Baggett, D. W. Hughes, G. W. Rivers, and W. E. Sayle, ORO-3027-38 (1977).

46. R. K. Feeney, D. W. Hughes, G. B. Hoak, D. C. Priester, and W. E. Sayle, ORO-3027-43 (1978).

47. R. K. Feeney, D. W. Hughes, G. B. Hoak, and D. C. Priester, ORO-3027-48 (1979).

48. B. Peart and K. T. Dolder, J. Phys. B 2, 1169 (1969).